DTIC FILE COPY

①

AD-A196 873

REPORT DOCUMENTATION PAGE		READ INSTRUCTIONS BEFORE COMPLETING FORM
1. REPORT NUMBER AFIT/CI/NR 88-19	2. GOVT ACCESSION NO.	3. RECIPIENT'S CATALOG NUMBER
4. TITLE (and Subtitle) STRUCTURAL OPTIMIZATION INCLUDING CENTRIFUGAL AND CORIOLIS EFFECTS		5. TYPE OF REPORT & PERIOD COVERED MS THESIS
		6. PERFORMING ORG. REPORT NUMBER
7. AUTHOR(s) HOWARD DWIGHT GANS		8. CONTRACT OR GRANT NUMBER(s)
9. PERFORMING ORGANIZATION NAME AND ADDRESS AFIT STUDENT AT: UNIVERSITY OF MICHIGAN		10. PROGRAM ELEMENT, PROJECT, TASK AREA & WORK UNIT NUMBERS
11. CONTROLLING OFFICE NAME AND ADDRESS		12. REPORT DATE 1988
		13. NUMBER OF PAGES 120
14. MONITORING AGENCY NAME & ADDRESS(if different from Controlling Office) AFIT/NR Wright-Patterson AFB OH 45433-6583		15. SECURITY CLASS. (of this report) UNCLASSIFIED
		15a. DECLASSIFICATION/DOWNGRADING SCHEDULE

16. DISTRIBUTION STATEMENT (of this Report)

DISTRIBUTED UNLIMITED: APPROVED FOR PUBLIC RELEASE

DTIC
ELECTE
AUG 0 3 1988
H

17. DISTRIBUTION STATEMENT (of the abstract entered in Block 20, if different from Report)

SAME AS REPORT

18. SUPPLEMENTARY NOTES
Approved for Public Release: IAW AFR 190-1
LYNN E. WOLAVER
Dean for Research and Professional Development 12 July 88
Air Force Institute of Technology
Wright-Patterson AFB OH 45433-6583

19. KEY WORDS (Continue on reverse side if necessary and identify by block number)

20. ABSTRACT (Continue on reverse side if necessary and identify by block number)
ATTACHED

88

DD FORM 1473 EDITION OF 1 NOV 65 IS OBSOLETE
1 JAN 73

ABSTRACT

STRUCTURAL OPTIMIZATION INCLUDING
CENTRIFUGAL AND CORIOLIS EFFECTS

by
Howard Dwight Gans

Chairman: William J. Anderson

This dissertation investigates the effects of centrifugal and Coriolis forces on the mode shapes and frequencies of a rotating system. Optimal redesign is then done to favorably alter the modes. The rotational effects have a profound influence on the eigenfrequencies; this is important in optimal structural redesign where the frequencies must be adjusted.

The structural matrices for the rotating system were obtained by examining the expression for the total system energy. This provides a differential stiffness matrix that models centrifugal force and a provides velocity-dependent Coriolis matrix. By using a high-level programming language (Direct Matrix Abstraction Programming) a modal analysis solution sequence was modified to account for rotational effects in free vibration. Finite element models were then created for a typical compressor blade in a modern jet engine and for a cantilever beam rotating about the vertical axis. Using these models, the effects of rotation as simulated by the finite element method were verified against theoretical results.

The optimal redesign was done by deriving complex nonlinear inverse perturbation equations for the problem involving both magnitude and phase components. The perturbation problem is solved by using nonlinear mathematical programming. In order to optimally redesign, one uses an underdetermined system, i.e., the feasible design must not be unique. This allows the application of an objective function, such as minimum structural weight or minimum change from the baseline design. Constraints, such as those

1

on frequency, are applied. Using this method, optimal stuctural changes are obtained that

meet the frequency goals to within three percent. Examples were carried out using the

general purpose software package MSC/NASTRAN and ADS (Automated Design

Synthesis).

DTIC
COPY
INSPECTED
6

Accession For		
NTIS GRA&I	✓	
DTIC TAB	☐	
Unannounced	☐	
Justification		
By		
Distribution/		
Availability Codes		
Dist	Avail and/or Special	
A-1		

STRUCTURAL OPTIMIZATION INCLUDING CENTRIFUGAL AND CORIOLIS EFFECTS

by

Howard Dwight Gans

A dissertation submitted in partial fulfillment
of the requirements for the degree of
Doctor of Philosophy
(Aerospace Engineering)
in The University of Michigan
1988

Doctoral Committee:

Professor William J. Anderson, Chairman
Professor Joe G. Eisley
Assistant Professor Pierre T. Kabamba
Assistant Professor Christophe Pierre
Professor John E. Taylor

To my father, Henry J Gans
in memoriam

ACKNOWLEDGEMENTS

TABLE OF CONTENTS

LIST OF TABLES

LIST OF FIGURES

LIST OF APPENDICES

ix

CHAPTER 1

INTRODUCTION

The desire to minimize weight while meeting design requirements is a key concept in optimal structural design. When a particular stuctural component is being examined. the engineer must consider many aspects of structural behavior, such as dynamic response. These parameters must be bounded in the design phase while still meeting the overall goal of minimizing weight.

There are numerous occasions where the design of an existing structure is found wanting and this creates the need for structural *redesign*. For example, the mission of a particular aircraft that has been used for many years may change. This happened with the T-38 trainer when it was adapted for use in lead-in fighter training. The aircraft structure may then be subjected to loads that could not be forseen in the original design. Fatigue cracks may develop due to changes in the load spectrum. Dynamic effects may result due to excitation of modal frequencies that would have remained stable under the prior usage.

In any structural redesign problem, there are several possible candidate designs that would meet the new criteria. Structural optimization can be used in the redesign problem to find the best possible configuration. The objective function for redesign, however, may be quite different from the objective function in the original design of a part. It may not be suitable to concern oneself only with weight. If the dimensions of an existing part are altered too much, it may r⁻ longer fit in the aircraft. Existing fastener locations may no longer be suitable. The balance of the entire aircraft may be thrown off. Therefore, it may be necessary to obtain the optimal design that requires the least possible change from

1

the original design in terms of some dimension, such as thickness. This is a minimum design change criterion for optimization.

For given values of design parameters, analytical methods may be used to uniquely determine the response. The response values can be compared against the desired response. A search in the design space can be undertaken for a new design, and the response and constraints can be reanalyzed. This approach is the simplest conceptually, and if the number of design variables and constraints is small, is the most advantageous. However, most problems in structural design involve a large number of design variables and/or a large number of constraints. This makes a random search approach unfeasible. In addition, a closed form analytical solution usually cannot be obtained for a large problem. Large, general purpose finite element programs are used to determine the structural response. Since these programs are expensive to run on a computer, it is desirable to avoid large numbers of trial solutions. Therefore, some form of optimization procedure coupled with finite element analysis must be used.

Some structures, because of their application, are subject to body forces in addition to the loadings caused by boundary forces. Rotating bodies experience centrifugal effects. These effects are not forces at all if viewed from a nonrotating frame of reference. However, in the rotating frame, the centrifugal effects may be viewed as a reverse-effective pseudo-force. If the rotational speed is small enough, these forces can be neglected. In high speed applications, however, the body forces must be taken into account. Centrifugal force in particular can result in stiffening. This stiffening is particularly obvious for rotating helicopter blades. When the blades are at rest, they sag under their own weight. As the blades speed up, they stiffen, to the point where they can bear not only their own weight, but the weight of the entire aircraft. A similar effect occurs in aircraft gas turbine engines. The rotating blades in the high speed compressor and turbine are subject to body forces. With the advent of higher speed blading, it is necessary to include the effect of these body forces in design. This introduces a

nonlinearity in the finite element analysis and optimization scheme.

Coriolis force is another body "force" that a rotating body may experience when viewed in a rotating coordinate system but is not a force at all if viewed in an absolute frame of reference. This force, also known as gyroscopic force, couples motion in one plane with motion in another plane. Gyroscopic effects are velocity dependent; that is, the greater the velocity in one plane, the greater the effect will be in the other plane. In systems which permit large amounts of out-of-plane motion, such as in pretwisted blades, the Coriolis forces will become great at high speeds, and thus will affect optimal redesgin. In many other systems, Coriolis forces may be ignored. The effect of the Coriolis terms on structural dynamics is documented by Greenwood (1977) and Meirovitch (1980).

The effect of rotation on the dynamic characteristics of a body has been well-documented by Washizu (1982). Simplified methods for the solution of the problem of the rotating beam have been presented by White and Malatino (1975), McDaniel and Murthy (1977), and Giurgiutiu and Stafford (1977). Isakson and Eisley (1964) related the centrifugal effect to a stiffening parameter, the Southwell coefficient. Hodges and Rutkowski (1981) derived a finite element solution to the problem of a rotating beam by creating variable order shape functions. Queau and Trompette (1981) used parameter optimization in a beam analysis of a blade. Cross-sectional properties were found under a least weight objective and with frequency and stress constraints. Kim, Anderson, and Sandtröm (1983) presented a nonlinear inverse perturbation scheme for automated redesign of modal characteristics. Hoff, et. all (1984) used the perturbation technique to develop a predictor-corrector approach, which is useful in the present study.

The advance of numerical techniques of structural optimization has been one of the most important developments in the field of engineering design. These methods have permitted the engineer to select the best possible configuration from several candidate designs. Structural optimization can also be used to modify an existing design in order to adapt existing aircraft to new requirements. One critical area where optimal structural

redesign will be of great importance is in the reanalysis of aircraft gas turbine blading. As the demand for increased performance continues, blades may have to be redesigned to counteract the effect of loading changes. New procedures will have to be created to do this efficiently.

The objective of this study is to first create a finite element solution for the stiffening effect of centrifugal force in order to calculate the mode shapes and frequencies of a structure composed of several different types of elements. Then, nonlinear inverse perturbation will be used to account for the changing nature of the stiffening effect as the design process progresses. This scheme measures design changes as perturbations of the original structure. The method will be applied to a problem involving a typical curved compressor blade. Finally, the effects of Coriolis forces on the optimal redesign process will be studied.

This dissertation begins with a review of rotating systems, structural optimization, and the optimization of rotating systems. The effect of rotation on frequencies and mode shapes is discussed in Chapter 3. A finite element procedure to account for static loads in dynamic response is also described in detail. The effect of Coriolis forces is also considered.

In Chapter 4, the rotational characteristics of rotating systems are examined. The stiffening effect of centrifugal forces is examined both by a finite element approach and by a classical theoretical formulation.

In Chapter 5, a nonlinear inverse perturbation scheme including centrifugal and Coriolis effects is developed. The application of Sequential Unconstrained Minimization Technique (SUMT) to the problem in optimization is described.

The predictor-corrector technique for the optimization of rotating systems is derived in Chapter 6. The method is applied to several simple examples.

Chapter 7 applies the procedure to a large problem. A flat compressor blade is used as an example to check the method. The effect of Coriolis forces on the optimization

problem is examined in a rotating beam.

Chapter 8 concludes the dissertation. The original contribution of this work is examined. Suggestions for future work are made.

CHAPTER 2

LITERATURE REVIEW

Literature Survey on Rotation

The characteristics of vibrating systems were treated mathematically first by Rayleigh (1898). The basic equations of motion of a rotating beam of constant section with axis of rotation perpendicular to the length of the beam were updated by Boyce, Di Prima, and Handelman (1954). Nagaraj and Shanthakumar (1975) solved the problem with Galerkin's method. Tomar and Dhole (1976) expanded the solution to encompass pretwisted beams, solving the equations by a conventional Rayleigh-Ritz approach. Putter and Manor (1978) devised a finite element model of a rotating tapered beam that incorporated centrifugal effects. Hoa (1979) added a tip mass to the finite element procedure.

The basic equations of motion for a rotating cantilever blade have been extensively investigated. Lo and Renbarger (1951) analyzed rotating beams. Houbolt and Brooks (1958) showed that centrifugal force increases the first bending frequency for a rotating blade. Carnegie (1959) and Carnegie (1967), using energy methods, expanded this work. Isakson and Eisley (1964) determined the natural frequencies of twisted blades for both rotating and nonrotating systems. This subject was also studied by Carnegie and Dawson for straight blades (1969) and for pretwisted blades (1971). Various solution methods for these equations have been proposed. Wadsworth and Wilde (1967) solved the problem using a pair of simultaneous differential equations and a Runge-Kutta approach. Rao and Carnegie (1970) used a Ritz approach. A transfer matrix approach was outlined by McDaniel and Murthy (1977). A mixed variational approach was outlined by Lang and

6

Nemat-Nasser (1979). An integrating matrix finite difference procedure was described by Hunter (1970). An improved method for the analysis of pretwisted airfoil blades was presented by Sybrahmanyam and Kaza (1984).

Coriolis effects have also been discussed by several authors. Hunter (1970) dismisses these effects as being insignificant in comparison with centrifugal forces; however, Subrahmanyam and Kaza (1985) determined that Coriolis forces are an important influence at high rotational speeds and for thick beams, They also stated that Coriolis forces may be important even at low speeds under certain geometries. This analysis was expanded by Subrahmanyam et al (1987) to include pretwisted blades. Anarsi (1986) also includes the effects of shear deformation and rotary inertia. Sisto et al (1983) analyzes the stability of a rotating blade by the use of Floquet theory.

Finite element solutions to the problem of free vibration of rotating beams was examined by Hodges and Rutkowski (1981). Thomas and Subuncu (1979), using a finite element method, solved the vibrational characteristics of rotating pretwisted asymmetric cross-sectional blading. Subuncu (1985) produced a finite element solution for blades with a nonlinear angular pretwist; however his method did not involve rotational effects. Dokainish and Rawtani (1971) obtained a finite element solution for a rotating cantilever plate. They included centrifugal forces but neglected Coriolis effects. A textbook on the topic was published by MacNeal (1973).

Literature Survey in Optimization

The problem of optimal structural design has been studied for many years. At first, a trial-and-error approach was used, with initial choice based on experience (Sheu and Praeger, 1968). However, methods of optimization now exist that obtain the desired structural configuration more efficiently. These approaches may be categorized as either direct or indirect methods (Kiusalaas, 1972). In indirect methods, an optimality criteria is used. Direct methods are based on mathematical programming.

The use of optimality criteria lies at the heart of the indirect approach to structural

optimization. Important developments in this procedure have been made by Prager and Taylor (1967) and Taylor (1968). These methods involve the establishment of a criterion that defines the optimum, such as uniform strain energy density, and the creation of an iterative procedure for obtaining the design (Venkayya, Khot, and Berke, 1973). The Kuhn-Tucker conditions are the first order necessary conditions for obtaining an acceptable design (Luenberger, 1984).

The direct, or mathematical programming, methods use numerical search techniques to solve the problem of optimal structural design. Moses (1964) presented a method for finding the optimum design by using sequential linear programming. A more general approach is to minimize the objective function as an unconstrained function, but to impose a penalty in order to limit constraint violations. This requires that several unconstrained minimization problems be solved. One such method, called the Sequential Unconstrained Minimization Technique (SUMT) was extensively described by Fiacco and McCormick (1968).

Derivatives of structural response with respect to the design variables can be obtained and used in gradient projection methods (Fletcher and Reeves, 1964). These derivatives can be calculated by a design space method (Fox, 1965). Kavanaugh (1972) used dynamic relaxation to devise an approximate algorithm for uncoupling the optimization problem.

The application of structural redesign to dynamic problems has been extensively investigated. Rayleigh (1898) provided the first solution for designing a dynamic system to meet specific frequency requirements. Turner (1967) used the equations of motion for a large deflection vibration problem as equality constraints and employed a Lagrange multiplier method. He used a finite element idealization and an iterative scheme to solve the nonlinear equations. Taylor (1967) proposed an alternate method. He developed a functional that related the system energy to the eigenvalue problem, and used this functional to obtain the optimum design. Taylor (1968) added a condition that the cross-

sectional area not be reduced below a specified minimum during the redesign process. This was accomplished by an inequality constraint and Lagrange multipliers. Sheu (1968) applied the approach of Turner and Taylor to a one-dimensional structure and added segment boundaries and specific stiffnesses as design requirements. Taylor (1969) applied an energy formulation to the problem of truss design. Sippel and Warner (1973) devised a mimimum mass optimality criterion and compared the results of continuous optimum design to piecewise uniform optimum design.

McCart, Haug, and Streeter (1970) used a steepest descent approach to obtain the optimal design for a three-bar frame. Rubin (1970) satisfied a frequency constraint and found the minimum structural weight through a step-wise procedure that defined two "modes of travel". The first mode changed the frequency to obtain a desired value. The second one minimized structural weight while keeping the frequency constant. The problem with this approach is that while it may obtain a design it may not necessarily find the *best* design. Armand (1971) used methods from optimal control theory to present a different approach to the optimal design of two-dimensional structures.

Taylor (1977) obtained a procedure that upgrades a computer model of a structure so that the calculated normal mode frequencies more nearly match those determined from experiment. This method was based on a Taylor series type expansion. Only first order terms were retained.

If a baseline structure exists but it is found that the response of the structure is unacceptible and modification is necessary, perturbation techniques may be employed to obtain the desired values. Stetson (1975) introduced small changes in mass and in the stiffness moduli of a structure. He then obtained a first order perturbation method that obtained the mode shapes for the perturbed structure. He introduced the concept of "admixture coefficients" that expressed the mode shapes of the perturbed structure in terms of combinations of the baseline mode shapes. Stetson and Palma (1976), Stetson et al (1978), and Stetson and Harrison (1981) expanded this technique to encompass a finite

element structural formulation and applied it to several problems. Sandstrom and Anderson (1982) related Stetson's admixture coefficients to physical changes in the finite element model. Kim et al (1983) obtained a complete nonlinear inverse perturbation technique using the equations of dynamic equilibrium. A SUMT penalty function method was used where the objective function was minimum weight and the penalty term involved a normalized set of residual force vectors.

One major problem of the nonlinear inverse perturbation method is that for a large problem, the number of calculations required become excessive. For that reason, Kim and Anderson (1984) and Kim (1985) used generalized dynamic reduction to transform the problem into a small sized subspace. Hoff et al (1984) overcame the difficulties in applying the nonlinear inverse perturbation method by using an incremental predictor-corrector technique. In the predictor phase, element changes necessary to enforce the desired mode shape and frequency changes are obtained through a first order solution of the dynamic equations. In the corrector, approximate eigenvectors are obtained for the objective system, which are then used to correct the elemental changes. This method was later expanded by Hoff (1985).

Literature Survey in the Optimization of Rotating Systems

Olhoff and Parbery (1982) analyzed the design of vibrating beams and rotating shafts with lumped mass at the tip and at midspan. Their method incorporated centrifugal, but not Coriolis, effects. Kengtung and Gu (1984) also studied the problem of rotating blades without Coriolis effects for small (ten element) problems using beam elements. Kounadis (1985) analyzed the effect of axial inertia on the bending frequencies of a frame structure.

Bennett (1983) examined the the application of optimization methods to problems in the design of helicopter rotors. His optimization scheme involved a linear design sensitivity approach. His method did not account for changes in blade weight and inertia properties since these affect centrifugal forces in a nonlinear manner. Therefore, he

required that blade weight and inertia remain fixed during the process of optimal design.

Queau and Trompette (1981) applied changes in inertia properties during the redesign process to determine changes in centrifugal stiffening affecting optimization. Their method also involved linear design sensitivites. It also did not update the eigenvectors during the optimization process, requiring a large number of calculations. Only beam elements were used. Their method of optimization can lead to a local minimum. Their procedure cannot be used on a general class of problems, particularly plate-like bodies.

CHAPTER 3

BACKROUND OF ROTATIONAL EFFECTS

In this chapter, the equations of motion are discussed for small motions of a rotating discrete system. The terms in the equations that represent rotational effects are shown in a structural mechanics representation. The corresponding eigenvalue problem and its methods of solution are shown. Finally, a physical example will be used to derive the Coriolis matrix for a rotating bar.

Equations of Motion of a Rotating Discrete Structure

A system consisting of n degrees of freedom has its motion fully described by n generalized coordinates $q_i(t)$, where $i = 1,2,...,n$. The kinetic energy of the system, T, may be defined as (Meirovitch, 1980):

$$T = T_0 + T_1 + T_2 \tag{3.1}$$

where

$$T_2 = \frac{1}{2} \sum_{i=1}^{n} \sum_{j=1}^{n} m_{ij} \dot{q}_i \dot{q}_j \tag{3.2}$$

is a quadratic function of the generalized velocities $\dot{q}_i(t)$.

and

$$T_1 = \sum_{i=1}^{n} f_i \dot{q}_i \tag{3.3}$$

is a linear function of the generalized velocities. The term T_0 contains no generalized velocities; however, the function T_0 and the coefficients m_{ij} and f_i will depend on the generalized coordinates q_i. The term T_0 gives rise to terms involving centrifugal force and behaves as a potential energy. The T_1 term produces Coriolis forces.

In addition to centrifugal and Coriolis forces, there may be other forces that act on the system. These include forces from a potential energy function written as a function of the generalized coordinates alone, with no time derivatives:

$$V = V(q_i) \tag{3.4}$$

Such forces can be elastic forces or gravitational forces. These elastic forces generate the conventional small-displacement system stiffness.

The final set of forces are those that fall into no particular set, and shall be represented by Q_i, the generalized forces. These forces may depend on time but not on displacement or velocities. Friction forces are an example of generalized forces.

The equations of motion of the system may be found through the use of the classic differential form of the Lagrange equation:

$$\frac{d}{dt}\left(\frac{\partial L}{\partial \dot{q}_i}\right) - \frac{\partial L}{\partial q_i} = Q_i \tag{3.5}$$

where the Langrangian L is defined by:

$$L = T - V \tag{3.6}$$

The system of equations represented by Equation (3.5) comprises a set of n nonhomogeneous nonlinear ordinary differential equations of second order. General solutions of this type of equations do not exist. Under certain conditions it is possible to make simplifying assumptions that will permit the linearization of the equations. One such assumption is that motion will be restricted to small motions in the neighborhood of the static equilibrium condition. $\dot{q}_{i0} = 0$, for $i = 1,2,...,n$. A coordinate transformation can be done to translate the origin so as to make it coincide with the static equilibrium point. Thus, only motions in the neighborhood of the trivial solution $\dot{q}_{i0} = q_{i0} = 0$ ($i = 1,2,...,n$) will be considered.

Using these assumptions, it can be shown (Meirovitch, 1980) that:

$$m_{ij} = m_{ji} = \frac{\partial^2 T_2}{\partial \dot{q}_i \, \partial \dot{q}_j}$$
$$= \frac{\partial^2 T_2}{\partial \dot{q}_j \partial \dot{q}_i} \qquad (3.7)$$

where the terms m_{ij} are called the mass or inertia coefficients.

It can also be shown that:

$$f_{ij} = \frac{\partial f_i}{\partial q_j} \qquad (3.8)$$

where the terms f_{ij} are constant coefficients. This implies that:

$$T_1 = \sum_{i=1}^{n} \sum_{j=1}^{n} f_{ij} q_i \dot{q}_j \qquad (3.9)$$

Let U be defined by:

$$U = V - T_0 \qquad (3.10)$$

where U represents a dynamic potential. Furthermore, the stiffness coefficients k_{ij} can be shown to be:

$$k_{ij} = k_{ji} = \frac{\partial^2 U}{\partial q_i \partial q_j}$$
$$= \frac{\partial^2 U}{\partial q_j \partial q_i} \qquad (3.11)$$

As discussed below, the centrifugal effects can be treated as a static preload on the system. This implies that centrifugal forces will be included in the strain energy component V of the potential energy U, rather than as T_0 kinetic energy. A full derivation of the tangent stiffness matrix including centrifugal effects is shown in Chapter 4.

The explicit equations of motion can be derived and expressed as:

$$\sum_{j=1}^{n} [m_{ij} \ddot{q}_j + b_{ij} \dot{q}_j + k_{ij} q_j] = Q_i \quad (i = 1, 2, \dots n) \qquad (3.12)$$

Note that the mass and stiffness coefficients are symmetric while the Coriolis coefficients, b_{ij}, are skew symmetric such that:

$$b_{ij} = f_{ji} - f_{ij} \quad (i,j = 1,2,\dots,n) \tag{3.13}$$

In matrix form, Equation (3.12) may be written as:

$$[M]\{\ddot{q}\} + [B]\{\dot{q}\} + [K]\{q\} = \{Q\} \tag{3.14}$$

The symmetry of the coefficients m_{ij} and k_{ij} implies that:

$$[M] = [M]^T \tag{3.15}$$

and

$$[K] = [K]^T \tag{3.16}$$

while the skew symmetry of the coefficients b_{ij} implies that:

$$[B] = -[B]^T \tag{3.17}$$

Another way to deal with the differences between centrifugal forces and Coriolis effects is as follows. In structural analysis, centrifugal force, which is dependent only on mass, position, and rotational speed, can be considered as a static preload on the system. As such, its effects can be included in the initial stress, or differential stiffness, matrix. Coriolis effects, however, are dependent on velocity, which makes them dependent on the first derivative of the eigenvector. Coriolis terms, unlike structural damping, are energy conserving. Just as the structural matrix derived from centrifugal forces can be absorbed into the stiffness matrix, the matrix derived from Coriolis effects could be absorbed into the system damping matrix if there is one.

Eigenvalue Problem for Conservative Coriolis Systems

For the free vibration problem, the damping and the generalized forces Q_i are taken to be zero. Therefore, Equation (3.12) may be written by:

$$[M]\{\ddot{q}\} + [B]\{\dot{q}\} + [K]\{q\} = \{0\} \tag{3.18}$$

MacNeal (1973) showed that the system described in Equation (3.18) is energy conserving if the mass and stiffness matrices are real, symmetric, positive definite and if the Coriolis matrix is real and skew symmetric. The solution to Equation (3.18) will be of the form:

$$\{q(t)\} = e^{pt}\{q\} \tag{3.19}$$

where p is a constant complex scalar and {q} is a constant complex vector. Equation (3.19) is introduced into Equation (3.17) and e^{pt} is canceled to obtain the eigenvalue problem:

$$(p^2[M]+p[B]+[K])\{q\} = 0 \tag{3.20}$$

The characteristic equation for this system is obtained by setting the determinant of the coefficients equal to zero:

$$|p^2[M]+p[B]+[K]| = 0 \tag{3.21}$$

This equation gives a polynomial of degree 2n in p. Greenwood (1977) states that due to the symmetry of the mass and stiffness matrices and the skew symmetry of the Coriolis matrix, all of the odd powers of p are absent from the characteristic equation. Therefore, a polynomial of nth degree in p^2 is generated. This would also be the case if the Coriolis terms were absent. Therefore, the eigenvalues will consist of n pure imaginary conjugate pairs, $p_r = \pm i\omega_r$, where $r = 1,2,...,n$. The eigenvectors will also occur in complex conjugate pairs, $\{q\}_r = \{y\}_r + i\{z\}$, $\{\bar{q}\}_r = \{y\}_r - i\{z\}_r$, where $\{y\}_r$ is the real part and $i\{z\}_r$ is the imaginary part of the eigenvector $\{q\}_r$. This implies that as a result of the Coriolis effects, the amplitude ratios will not, in general, be real. Therefore, the components of an eigenvector pair for a given eigenvalue pair will oscillate at the same frequency but not in phase.

Meirovitch (1974) provides an alternate solution to the system of Equation (3.18) that reduces it to a standard form that is similar to the system without Coriolis forces. If the matrices in Equation (3.18) are of order n, then one can introduce a 2n-dimensional state vector:

$$\{x\}^T = \left[\{\dot{q}\} \mid \{q\}\right] \tag{3.22}$$

Therefore, Equation (3.18) can be rewritten as:

$$[M^*]\{\ddot{x}\} + [B^*]\{x\} = \{0\} \tag{3.23}$$

where

$$[M^*] = \begin{bmatrix} [M] & [0] \\ [0] & [K] \end{bmatrix}$$

$$[B^*] = \begin{bmatrix} [B] & [K] \\ [-K] & [0] \end{bmatrix}$$

are real nonsingular matrices of order 2n.

Though this method reduces the system of equations involving Coriolis components to a more conventional form, the arrays created are twice as large. This will force a heavy penalty in storage requirements in numerical implementation. In actual application, the direct solution of the complex problem posed in Equation (3.18) is more efficient than the solution of the modified system of Equation (3.23). Therefore, this method posed by Meirovitch will not be used.

Derivation of Coriolis Matrix for a Bar Element

The Coriolis matrix for a rotating bar element will now be derived, using a lumped mass approach. Figure 1 shows a typical rotating bar. The entire mass of the bar will be divided into two equal lumped masses at each of the two nodes. Each mass m will have one-half of the mass of the total mass of the bar. The bar rotates around the global z-axis at a rotational speed of Ω hz.

The position vector to the mass at the first node, $\{r_1\}$, is given by:

$$\{r_1\} = x_1 \bar{i} + y_1 \bar{j} + z_1 \bar{k} \tag{3.24}$$

where x_1, y_1, and z_1 are the coordinates of node 1 in the global system and $\bar{i}$, $\bar{j}$, and $\bar{k}$ are the unit direction vectors for the x, y, and z axis respectively. Similarly, the position vector to the mass at the second node $\{r_2\}$ is given by:

$$\{r_2\} = x_2 \bar{i} + y_2 \bar{j} + z_2 \bar{k} \tag{3.25}$$

The absolute time derivative of a vector, $\{A\}$, in a rotating system is given by:
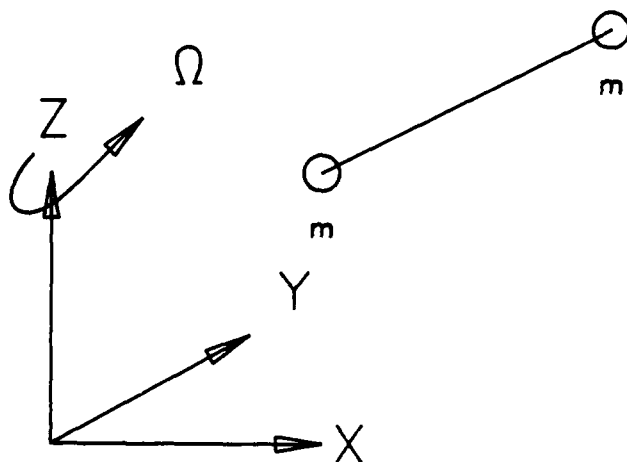
Figure 1. Rotating Bar — Lumped Mass

$$\{\dot{A}\}_0 = \{\dot{A}\}_r + \{\Omega\} \times \{A\} \tag{3.26}$$

where $\{\dot{A}\}_0$ is the absolute time derivative of $\{A\}$, $\{\dot{A}\}_r$ is the time derivative of $\{A\}$ with respect to the rotating system, and $\{\Omega\}$ is the rotation vector.

It is assumed that the rotation will be purely about the z axis. Thus the rotation vector is given by $\Omega \bar{k}$. Therefore, the absolute time derivative of the position vector to node i, also called the velocity $\{v\}_i$:

$$\tag{3.27}$$
$$\{v\}_i = (\dot{x}_i - \Omega y_i)\bar{i} + (\dot{y}_i + \Omega x_i)\bar{j} + \dot{z}_i \bar{k}$$

To find the acceleration of the mass at node i, Equation (3.26) is applied to Equation

(3.27) to obtain:

$$\{a\}_i = (\ddot{x}_i - 2\Omega\dot{y}_i - \Omega^2 x_i)\bar{i} + (\ddot{y}_i + 2\Omega\dot{x}_i - \Omega^2 y_i)\bar{j} + \ddot{z}_i\bar{k} \tag{3.28}$$

The second time derivitive terms in the above equation represent the acceleration of the mass i relative to the rotating frame. The terms dependent on Ω^2 are the centrifugal acceleration components. Notice that they are dependent only on the position of the mass, with x-displacement giving the dependency of centrifugal acceleration in the x-direction and y-displacement giving the dependency of centrifugal acceleration in the y-direction. The components of Equation (3.26) dependent on Ω are the Coriolis terms. It is important to note that Coriolis acceleration in the x-direction depends on the velocity of the mass i in the y-direction and that Coriolis acceleation in the y-direction depends on velocity in the x-direction.

Relative, centrifugal, and Coriolis acceleration can each be considered to be reversed-effective forces or D'Alembert forces. As shown above, the reversed-effective forces due to relative acceleration and centrifugal acceleration in the x-direction will be dependent upon acceleration or displacement in the x-direction, respectively, with similar forces in the y-direction. However, the reversed-effective Coriolis force that points in the x-direction depends on y-direction velocity, and vice-versa.

The kinetic energy of the mass at the *i*th node is given by:

$$T^i = \frac{1}{2}m_i\{\dot{v}\}_i \cdot \{\dot{v}\}_i \tag{3.29}$$

or

$$T^i = \frac{1}{2}m[(\dot{x}_i - \Omega y_i)^2 + (\dot{y}_i + \Omega x_i)^2 + \dot{z}^2] \tag{3.30}$$

Equation (3.30) can be broken down into its components, T_0 through T_2, to provide the desired structural matrices. The kinetic energy components are:

$$T_2^i = \frac{1}{2}\{\dot{q}\}^T[M]\{\dot{q}\} \tag{3.31}$$

$$T_1^i = \frac{1}{2}\{q\}^T[F]\{\dot{q}\} \tag{3.32}$$

$$T_0^i = \frac{1}{2} \{q\}^T [S]\{q\} \tag{3.33}$$

where

$$[M] = \begin{bmatrix} m_i & 0 & 0 \\ 0 & m_i & 0 \\ 0 & 0 & m_i \end{bmatrix}$$

$$[F] = \begin{bmatrix} 0 & -m_i\Omega & 0 \\ m_i\Omega & 0 & 0 \\ 0 & 0 & 0 \end{bmatrix}$$

$$[S] = \begin{bmatrix} m_i\Omega^2 & 0 & 0 \\ 0 & m_i\Omega^2 & 0 \\ 0 & 0 & 0 \end{bmatrix}$$

To form the Coriolis matrix from [F], one remembers from Equation (3.13) that:

$$[B] = [F]^T - [F] \tag{3.34}$$

where [F] is the matrix of the f_{ij} factors.

In order for one to form element matrices from the matrices given in Equations (3.31) through (3.34), the components from the other node must be added in. Thus [M] will become the element mass matrix, [B] will become the element Coriolis matrix, and [S] will become the element stiffness matrix from the applied load due to the rotation. This last matrix, however, differs from the differential stiffness matrix. Differential stiffness results from examining small nonlinear terms in the derivation of stiffness to form the tangential stiffness matrix for the element. These nonlinearities result from applied loading, such as centrifugal force.

The matrix derived from the T_0 component of kinetic energy has been previously used to model the effect of centrifugal loading on the eigenfrequencies of rotating structures (Trompette and Lalanne, 1974, Olhoff and Parbery, 1982, Subrahmanyam and Kaza, 1984, Queu and Trompette, 1981). In the current analysis, however, this approach will not be used. Instead, the forces generated by the centrifugal effect will be considered

as an applied load (Hoa, 1978). Optimization can then be done in the presence of the applied loads (Garstecki, 1984). A potential energy expression will then be derived from these forces (MacNeal, 1972). This puts the expression of centrifugal effects in the same format as the effects due to internal strain energy. In other words, both become structural stiffness terms. The internal strain energy components are represented as conventional infinitesimal small-displacement elastic stiffness. The components due to centrifugal potential are called differential stiffness. The total of the elastic and differential stiffnesses is called the tangential stiffness. The proof that this method accurately represents the stiffening effect of centrifugal force is in the next chapter in the examination of the Southwell effect.

The Coriolis terms, being a function of velocity, cannot be represented as a potential. Instead, the kinetic energy formulation must be used. The centrifugal and Coriolis effects therefore are formulated separately in this analysis. This is permissible because the Coriolis acceleration terms and the centripetal acceleration terms (those that generate centrifugal forces) add linearly (Greenwood, 1965). Therefore, each effect will be considered separately and then combined to produce the total desired effect.

For the generalized beam element, each node has three translational degrees of freedom and three rotational degrees of freedom. For the nodal displacement vector $\{q\}$ given by:

$$\{q\}^T = \begin{pmatrix} x_1 \ y_1 \ z_1 \ \theta_{x_1} \ \theta_{y_1} \ \theta_{z_1} \ x_2 \ y_2 \ z_2 \ \theta_{x_2} \ \theta_{y_2} \ \theta_{z_2} \end{pmatrix} \qquad (3.35)$$

where θ is the rotation degree of freedom for the indicated direction, the element matrices will have dimension 12. Therefore, the element Coriolis matrix will be a 12×12 with all terms equal to zero except for the following nonzero components b_{ij}:

$$b_{1,2} = 2m\Omega$$

$$b_{2,1} = -2m\Omega$$

$$b_{7,8} = 2m\Omega$$

$$b_{8,7} = -2m\Omega$$

Once again, it is noted that the element Coriolis matrix is skew symmetric.

It is important at this time to note the effect that the form of each matrix; [M], [B], and [K], on system stability. The kinetic energy term T_2 by definition is a positive definite or positive semidefinite function of the generalized velocities. Therefore, the mass matrix must always be positive definite or positive semidefinite (Meirovitch, 1980). Generalizations about the matrix [K] revolve around the nature of the eigensolutions. A positive definite stiffness matrix will result in real, positive eigenvalues for the system solution. A positive semidefinite stiffness matrix will also give some zero eigenvalues with the rest of the eigenvalues being real and positive. Real, nonnegative eigenvalues imply a stable system; therefore a positive definite or positive semidefinite stiffness matrix will result in a stable system. The semidefinite case will admit the existence of rigid body modes. If the stiffness matrix is negative definite, negative semidefinite, or indefinite, negative eigenvalues will result. This will generate a divergent eigensolution and an unstable system.

The Coriolis matrix [B] results from the kinetic energy term T_1. By the definition of T_1, the Coriolis matrix is always skew symmetric. However, Coriolis forces, also known as gyroscopic forces, do no work on the system. Therefore, a system with Coriolis effects not considered that is stable and energy conserving will remain so with the effects included. If, however, a system has damping, the structural matrix resulting from these effects will be positive definite or positive semidefinite. These forces serve to dissipate energy from the system and therefore the system will no longer be energy conserving. However, it will still be stable.

Summary

We have seen that the problem of the free vibration of a rotating system that encorporates both centrifugal and Coriolis effects will involve complex modal analysis. The eigenvalues will be pure imaginary; therefore the frequencies will be real. However, the eigenvectors will be complex with complex amplitude ratios. This implies that for a given

eigenvector, the eigenvector components will oscillate out of phase but at the same frequency, i.e., the motion will not be synchronous.

The element matrices can be derived by examining the system energy. The Coriolis matrix results from the expression of kinetic energy that incorporates the mixed product of nodal displacement and nodal velocities. In the expression for the free vibration of the rotating system subject to centrifugal and Coriolis effects, the Coriolis matrix has terms that multiply the unknown velocity components. Since the Coriolis matrix is skew symmetric, unlike a symmetric damping matrix, the Coriolis matrix is energy conserving.

CHAPTER 4

CENTRIFUGAL EFFECTS ON VIBRATION OF ROTATING BEAMS AND BLADES

The effect of centrifugal forces on the behavior of a rotating structure may be analytically modeled by examining in detail the centrifugal terms in the energy expression. One approach is to place these terms in the kinetic energy expression and obtain a centrifugal effects matrix. This has been done by Subrahmanyam and Kaza, Olhoff and Parbery, and others. Another approach is to create a potential energy expression that generates the centrifugal effect and use this expression to obtain a new stiffness matrix called differential stiffness. This approach is taken by Hoa and by MacNeal. The purpose *of this chapter is to prove the validity of* this approach. This will be done by comparing the analytical results using differential stiffness to the empirical Southwell approach. The method will also be compared to results obtained by Isakson and Eisley using the kinetic energy approach to centrifugal effects.

General Problem Statement

In the total optimization approach, the forward problem encompasses the modal analysis of the rotating blade. This can be thought of as a free vibration problem, with a centrifugal force applied to the blade acting as a stiffening effect. This stiffening effect can be quantified by examining the nonlinear components of the structural stiffness matrix (Appendix B).

In nonlinear analysis, $[K_T]$ is the tangent matrix:

$$[K_T] = [K_0] + [K_D] + [K_L] \tag{4.1}$$

where

$[K_T]$ is the tangent stiffness matrix,

$[K_0]$ is the small displacement stiffness matrix,

$[K_D]$ is the differential stiffness matrix

(often called geometric stiffness or initial stress matrix),

and

$[K_L]$ is the large displacement matrix.

In solving the rotating blade problem, it is assumed that the displacements are small; therefore, $[K_L]$ is neglected. The differential stiffness matrix, which is retained, does not explicitly contain displacements, but is dependent on the stress level (Zienkiewicz, 1977). Dropping the large deflection effects:

$$[K_{TOT}] = [K_0] + [K_D] \qquad (4.2)$$

This total stiffness matrix incorporates the load dependent terms and can now be used in the free vibration problem to find frequencies and mode shapes.

The matrix $[K_0]$ is given by:

$$[K_0] = \int_V [B]_0^T [D] [B_0] dV \qquad (4.3)$$

where

$[B_0]$ is the strain shape function matrix,

$[D]$ is the elastic strain-displacement matrix,

and dV is the incremental volume.

Furthermore. it can be shown (Appendix B) that:

$$[K_D]\{\Delta u\} = \int_V [\Delta B^t]^T \{\sigma\} dV \qquad (4.4)$$

where

$[\Delta B^t]$ is the incremental change of the tangent strain matrix due to a small increment in the displacements and forces

and $\{\sigma\}$ is the stress vector.

Let us consider the vibration of a simple model for a first-stage turbine blade on a

circular hub in a typical aircraft engine, such as the General Electric CF6 (Figure 2). The blade outer radius is about 787.4 mm, the inner radius is 393.7 mm, the blade width is 556.8 mm, and the blade thickness is 87.38 mm. The structure is made of Inconel 718, with E (Young's modulus) equal to 202696 MPa, ρ (density) equal to 8.2121E-9 Mg/mm^3, and ν (Poisson's ratio) equal to 0.29. The blade is rotated at a constant speed, Ω.

Several rotational speeds were applied, and the first flexural mode was examined. A log-log plot of $\dfrac{\lambda_1 - \lambda_1^0}{\lambda_1^0}$ vs. Ω was made, where λ_1 and λ_1^0 are the fundamental (first) eigenvalues of the rotating and nonrotating structures, respectively (Figure 3). The valid portion of the curve is for Ω above 40.0 sec^{-1}. For Ω less than 40.0 sec^{-1}, numerical errors give erroneously high values for $\dfrac{\lambda_1 - \lambda_1^0}{\lambda_1^0}$. A conventional Cartesian plot (Figure 4) helps put these errors in perspective.

Southwell Coefficient

The Rayleigh-Southwell approximation is an analytical method of calculating and simply representing the effect of centrifugal stiffening on modal frequency (Isakson and Eisley, 1960). Using this method, the natural frequency under rotation may be expressed as:

$$\omega_{R_n}^2 = \omega_{N_n}^2 + K_n \Omega^2 \tag{4.5}$$

where

ω_{R_n} = natural frequency under rotation for the nth mode.

ω_{N_n} = natural frequency with no rotation for the nth mode. and

K_n = the Southwell coefficient for the nth mode.

For plate-like bodies, an analysis of the syst.. n kinetic energy (Isakson and Eisley, 1960) demonstrates that the Southwell coefficient can be shown to be:

$$K_n = \frac{\int_0^R \left\{ T_1 \left[(\Phi'_{y_n})^2 + (\Phi'_{z_n})^2 \right] - \rho \Phi_{y_n}^2 \right\} dx}{\int_0^R \rho \left[\Phi_{y_n}^2 + \Phi_{z_n}^2 \right] dx} \tag{4.6}$$
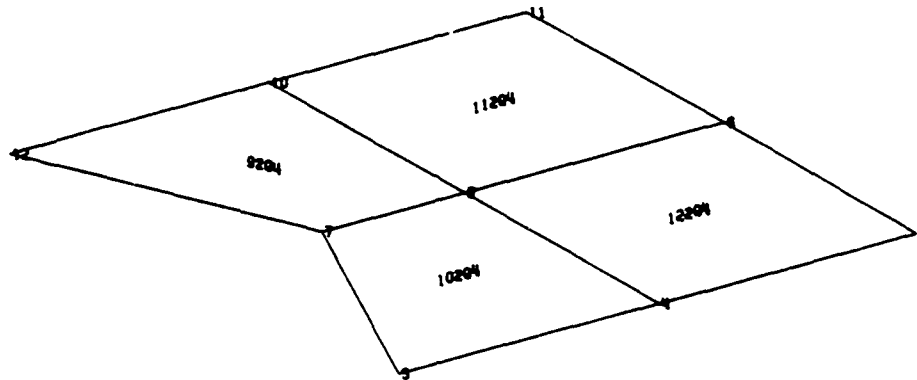
Figure 2. Rotating Blade Model

where

$$T_1 = \int_x^R \rho x dx$$

and Φ_{y_n}, Φ_{z_n} are displacements in the y- and z-directions describing the shape of the nth natural mode of the nonrotating blade, and R = rotor radius.

Isakson and Eisley in 1960 and in 1964 computed the Southwell coefficient for various blade configurations, using analytical and experimental techniques. However, a careful interpretation of Figure 3 will provide a more straightforward method for determining the Southwell coefficient for a particular mode.
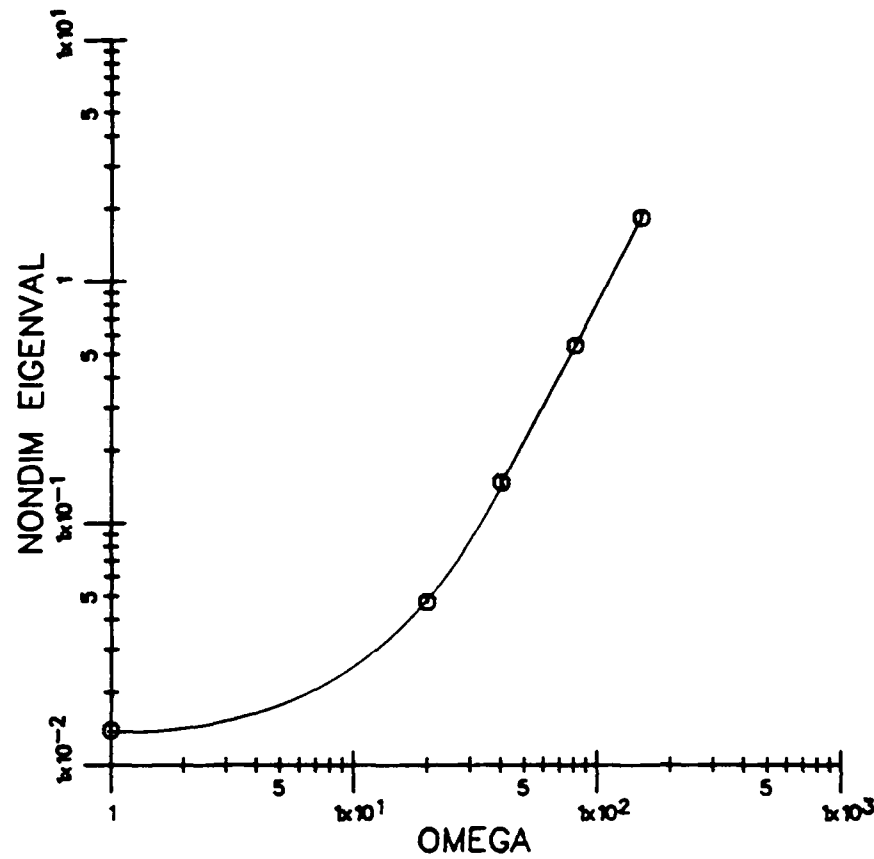
Figure 3. Effect of Rotation on
System Fundamental Eigenvalue
$(\lambda_1 - \lambda_1^0)/\lambda_1^0$

The eigenvalue λ is related to the frequency ω by:

$$\lambda = \omega^2 \qquad (4.7)$$

Therefore, equation (4.5) may be rewritten as:

$$\lambda_n = \omega_{N_n}^2 + K_n \Omega^2 \qquad (4.8)$$

where λ_n = eigenvalue of the rotating structure.

Rewriting and applying to the fundamental mode $(n = 1)$ results in:
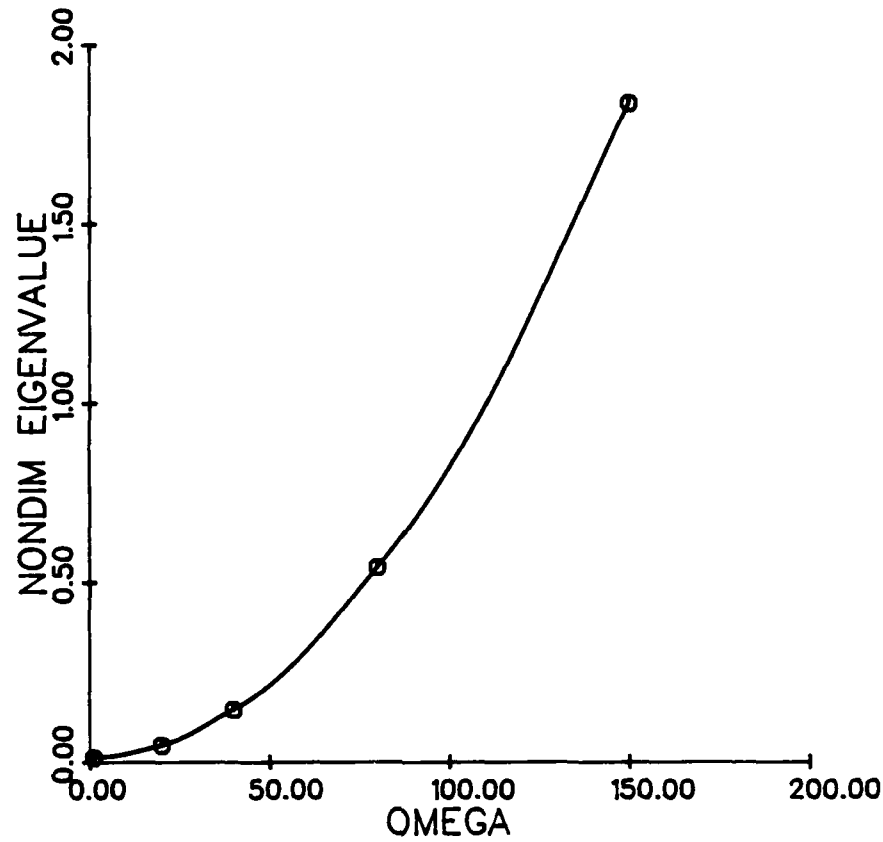
Figure 4. Cartesian Plot of Rotational Effect
on Nondimensionalized frequency, $(\lambda_1 - \lambda_1^0)/\lambda_1^0$

$$\left[\frac{\lambda_1 - \lambda_1^0}{\lambda_1^0}\right] = \left[\frac{K_1}{\lambda_1^0}\right]\Omega^2 \tag{4.9}$$

Equation (4.9) shows that the plot of $\dfrac{\lambda_1 - \lambda_1^0}{\lambda_1^0}$ vs. Ω should pass through the origin. This is demonstrated in Figure 4, with only a small numerical error evident. Thus it is seen that the deviation of Figure 3 from a straight line at low values of Ω is indeed caused by small numerical errors.

Taking the log of Equation (4.9) gives:

$$\ln\left[\frac{\lambda_1 - \lambda_1^0}{\lambda_1^0}\right] = \ln\left[\frac{K_1}{\lambda_1^0}\right] + \ln \Omega^2 \tag{4.10}$$

The numerical curve in Figure 3 may be approximated by:

$$\ln\left[\frac{\lambda_1 - \lambda_1^0}{\lambda_1^0}\right] = \ln\beta + \alpha\ln\Omega \tag{4.11}$$

where α and β are unknown parameters. The slope α of the log-log curve is given in Equation (4.11) and it is the power to which Ω is raised. Comparing Equation (4.11) to Equation (4.10) one sees the theoretical value of α equals 2. The numerical curve in Figure 3 has a slope of 1.91. This indicates an error in the finite element approximation of 4.5% for the experiment.

Figure 5 illustrates that α may be approximated by 2. Therefore, Equation (4.10) may be rewritten:

$$\ln\left[\frac{\lambda_1 - \lambda_1^0}{\lambda_1^0}\right] = \ln\beta + \ln\Omega^2 \tag{4.12}$$

Comparing Equation (4.12) to Equation (4.10), one obtains:

$$\beta = \frac{K_1}{\lambda_1^0} \tag{4.13}$$

Therefore, Equation (4.10) may be rewritten:

$$\frac{\lambda_1 - \lambda_1^0}{\lambda_1^0} = \beta\Omega^2 \tag{4.14}$$

This implies that β is the slope of a plot of $\dfrac{\lambda_1 - \lambda_1^0}{\lambda_1^0}$ vs Ω^2 (Figure 5). For this example, β equals 8.0761E-5.

K_1 is given from Equation (4.13):

$$K_1 = \beta\lambda_1^0 \tag{4.15}$$

For this problem, $K_1 = 46.45$.
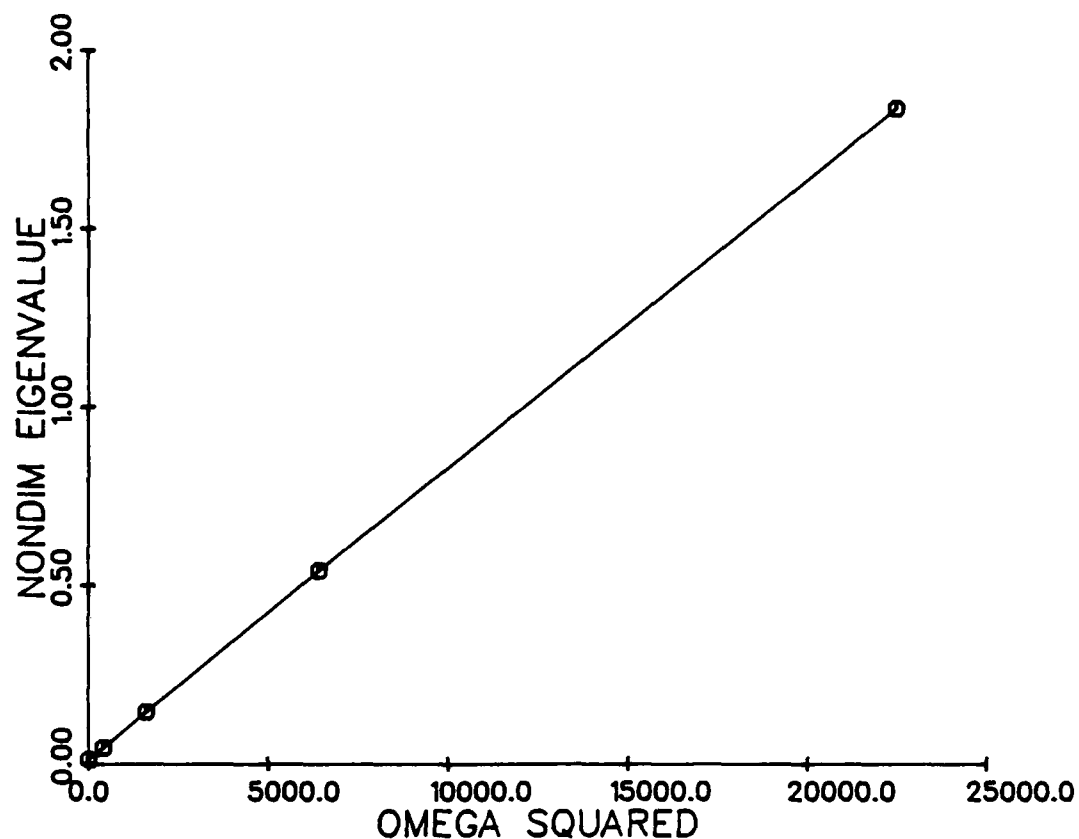
Figure 5. Effect of Rotation on Eigenvalue

The above results can be generalized to all modes:

$$K_n = \beta_n \lambda_n^0 \tag{4.16}$$

where λ_n^0 is the nonrotating eigenvalue for mode n and β_n is the slope of the plot of the quantity $\dfrac{\lambda_n - \lambda_n^0}{\lambda_n^0}$ vs. Ω^2.

As an illustration, let us examine a simple rotating bar (Figure 6). Consider a concentrated mass m at the end of a massless bar of length L, moment of inertia I, and Young's modulus E. The bar rotates about the z-axis with a frequency Ω. The left end (x = 0) is clamped and the right end (x = L) is constrained to allow only x-displacements and

z-displacements (no y-rotations).
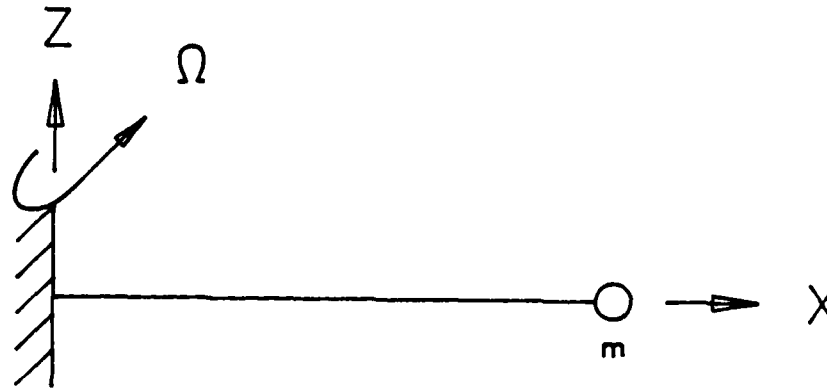
Figure 6. Rotating Beam with End Mass

The extensional (x-direction) displacements are needed to generate internal loads (were these displacements not permitted, the load P would be totally absorbed by the constraint). There is no differential stiffness in the extensional direction (Appendix B). The extensional components of the stiffness matrix are not affected and the eigenvalue in this direction remains unchanged. Therefore, for the purpose of this demonstration. we will concern ourselves only with masses, stiffnesses, and eigenvalues involving only transverse (z-direction) displacements. This can be done because the stiffness and mass terms for the x- and z-directions are completely uncoupled.

We now reduce the small displacement stiffness matrix $[K_0]$ to one term:

$$[K_0] = \frac{12EI}{L^3} \tag{4.17}$$

The differential stiffness matrix $[K_D]$ has nonzero components of only one term and is:

$$[K_D] = \frac{6P}{5L} \qquad (4.18)$$

where P is the load applied to the beam. In this case, P is the centrifugal force and is given by:

$$P = 4\pi^2\Omega^2 mL \qquad (4.19)$$

Substituting Equation (4.19) into Equation (4.16) and using Equation (4.2), one obtains:

$$[K_{TOT}] = \frac{12EI}{L^3} + \frac{24\pi^2\Omega^2 m}{5} \qquad (4.20)$$

The general form of the eigenvalue problem in finite element analysis is:

$$[K_{TOT}]\{\phi\}_i = \lambda_i[M]\{\phi\}_i \qquad (4.21)$$

where $[M]$ is mass matrix, $\{\phi\}_i$ the eigenvector, and λ_i the eigenvalue.

The eigenvalues λ_i are found from solving the characteristic equation:

$$\left| [K_{TOT}] - \lambda_i[M] \right| = 0 \qquad (4.22)$$

This particular problem considers only one degree of freedom; therefore, only one eigenvalue λ_1 exists. It is found from Equation (4.20) to be:

$$\lambda_1 = \frac{12EI}{mL^3} + \frac{24\pi^2\Omega^2}{5} \qquad (4.23)$$

The eigenvalue in the z-direction for the nonrotating problem λ_1^0 can be found by using the stiffness matrix given in Equation (4.17):

$$\lambda_1^0 = \frac{12EI}{mL^3} \qquad (4.24)$$

(Note that the above result could also be derived from Equation (4.23) with $\Omega = 0$.)

Equations (4.23) and (4.24) can be manipulated to obtain:

$$\ln\left[\frac{\lambda_1 - \lambda_1^0}{\lambda_1^0}\right] = \ln\left[\frac{\frac{2}{5}\pi^2 mL^3}{EI}\right] + \ln\Omega^2 \qquad (4.25)$$

Comparison of Equation (4.25) to Equation (4.11) obtains:

$$\beta = \frac{\frac{2}{5}\pi^2 mL^3}{EI} \qquad (4.26)$$

Therefore, Equation (4.13) gives:

$$K_1 = \frac{24}{5}\pi^2 \simeq 47.3741 \qquad (4.27)$$

This is the theoretical value of the Southwell coefficient for the mass with one degree of freedom at the end of a massless rotating beam.

Let us now try a numerical experiment. Let E equal 73.77E3 MPa, L equal 250 mm, I equal 3.2552E4 mm^4, A (cross section area of the beam) equal 625 mm^2, and m equal 5.0E-4 Mg. Figure 7 is a log-log plot of $\dfrac{\lambda_1 - \lambda_1^0}{\lambda_1^0}$ vs. Ω and Figure 8 is a conventional Cartesian plot of the same variables. Figure 9 is a plot of $\dfrac{\lambda_1 - \lambda_1^0}{\lambda_1^0}$ vs Ω^2. The finite element data agree exactly with the theoretical results given by Equation (4.25). Figure 7 shows that α = 2.000. β, derived from Figure 9, = 1.2844E-5. Equation (4.15) gives K_1 = 47.374. This agrees exactly with the theoretical result of Equation (4.27). Therefore, for this problem, there is no error between the finite element approximation and the theoretical result.

Thus we see that finite elements and graphical analysis can provide a simpler method for calculating the Southwell Coefficient. This technique is more general than that of Isakson and Eisley in that they were restricted to blade shapes that could provide a closed form solution. The finite element method can provide Southwell type of information for a rotating blade of any geometry.

It is also seen that the potential energy approach that leads to the development of differential stiffness can be used to accurately determine the stiffening effect of rotation on the eigenvalues of the structure. Results obtained from this method compare favorably with those obtained from a theoretical examination of the change in the characteristic
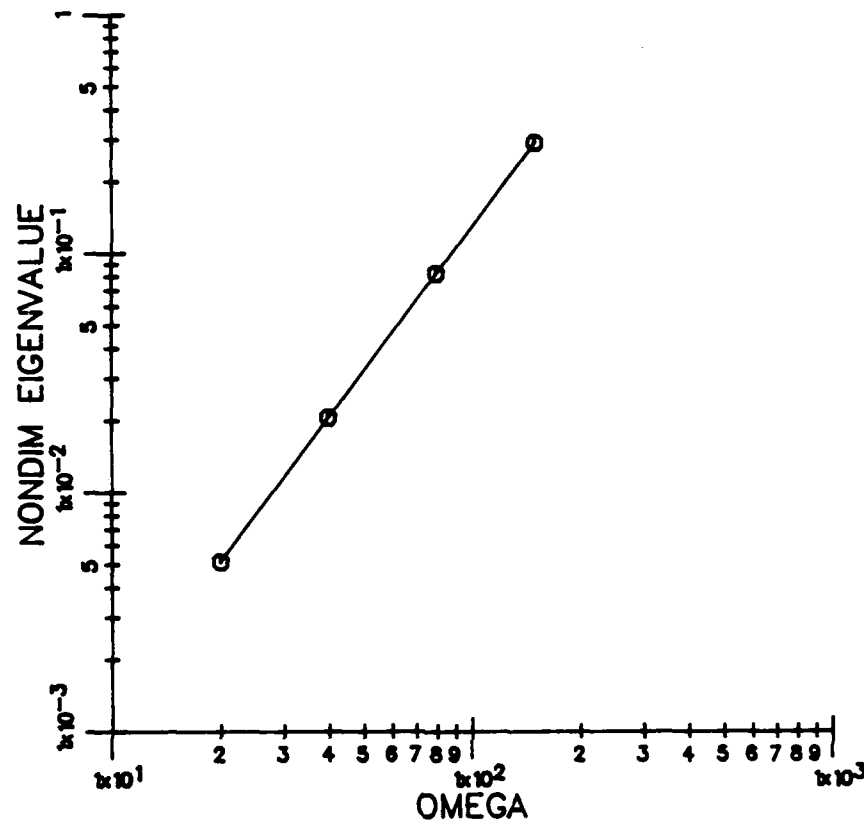
Figure 7. Effect of Rotation on Frequency
for Bar

frequencies due to rotation. Therefore, the potential energy approach and differential stiffness can be used to model the centrifugal effect in rotating bodies.
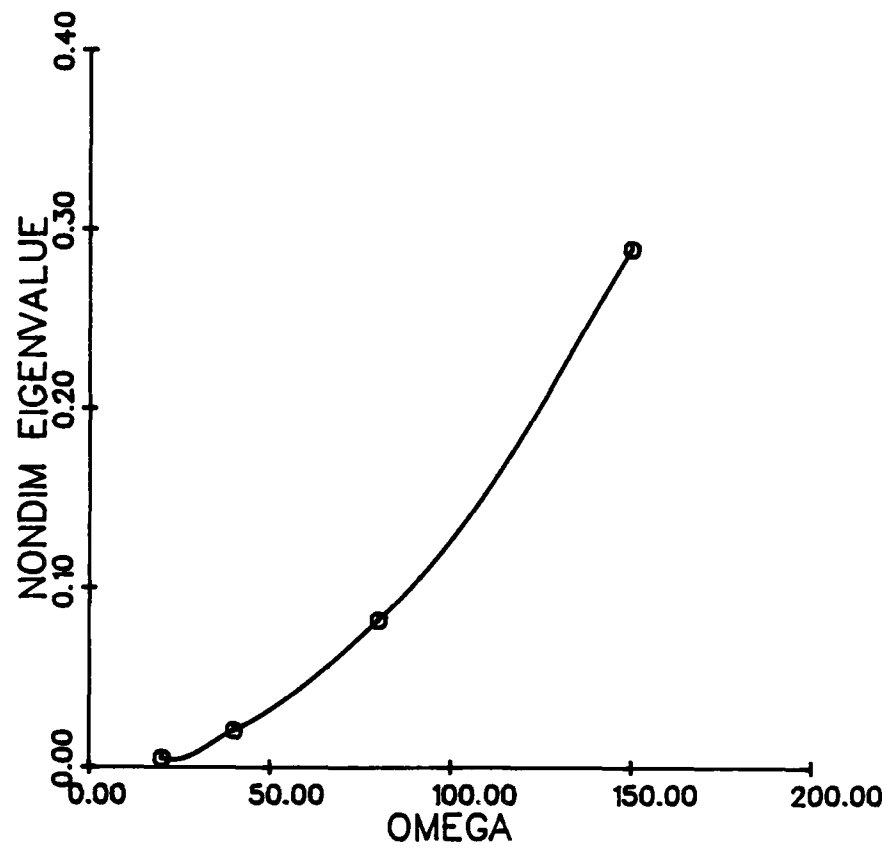
Figure 8. Cartesian Plot of Rotational Effect, Bar
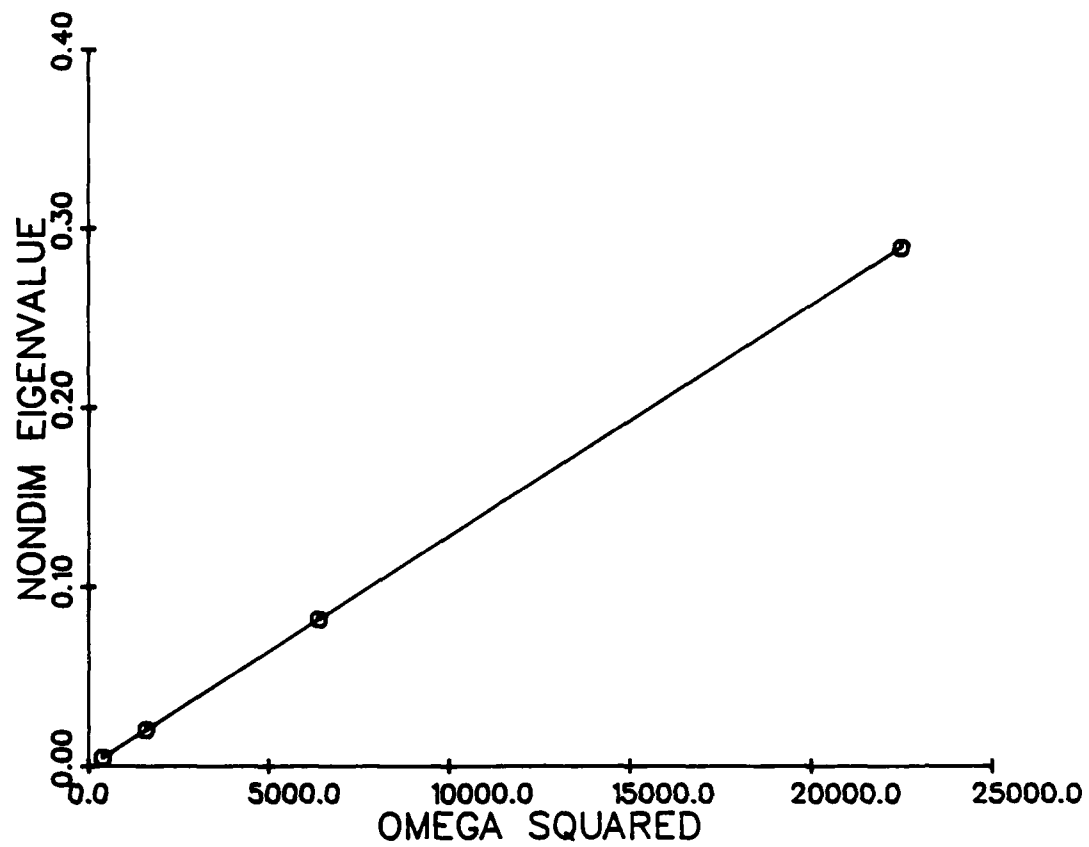
Figure 9. Rotational Effect on Frequency
Bar Model

CHAPTER 5

PERTURBATION METHODS IN OPTIMAL DESIGN

This chapter will discuss the theory and applications of the perturbation method as it relates to the problem of redesign in the presence of rotational effects. The theory of nonlinear inverse perturbation will be presented. The linear perturbation equations as derived by Stetson will be modified to include centrifugal effects. Then, new equations for nonlinear inverse perturbation will be derived from first principles that include complex components. These equations will be applicable for Coriolis effects. An overview of the optimization techniques used will also be presented.

Definition of Basic Terms in Optimization

The *baseline system* is the original system configuration. The starting values of the system parameters and system performance are first determined for the baseline system.

The *objective system* is the system that exhibits the desired system performance. This system is the goal of the redesign process.

The *system parameters* are those independent factors that each influence the system performance. One such parameter, and the one that will be the primary subject of this analysis, is element thickness. This parameter influences both mass and stiffness. One goal of the first part of the analysis is to determine how changes in thickness actually alter the mass and stiffness matrices.

The *system performance* is, simply, the behavior of the system. System performance can be measured in terms of statics, such as stress and displacement, or in terms of dynamics, such as eigenvalues and eigenvectors.

Optimal redesign is the process by which the desired change in performance is

obtained by altering the parameters in the most advantageous manner so as to minimize (or maximize) the system objective function. This *objective function* is a measure of a desired quantity. Two of the more common system objective functions are minimimum weight and minimum change from the baseline system.

Perturbation Methods

The first task is to determine the effect of the system parameters on system performance. This involves analyzing the structural matrices to see what the effect of a change in one basic parameter, thickness for example, would have on each matrix. This having been done, the effect of changes to the baseline system can be tracked throught the redesign process as one works toward the objective system.

We first wish to determine the influence of element thickness upon the differential stiffness matrix of beam and plate elements. This matrix may be defined by (Cook, 1974):

$$[K_D^e] = \int_V [N']^T \begin{bmatrix} [s] & [0] & [0] \\ [0] & [s] & [0] \\ [0] & [0] & [s] \end{bmatrix} [N']dV \tag{5.1}$$

where

$[K_D^e]$ = elemental differential stiffness matrix,

$[N']$ = derivative of the shape function matrix, and

$[s]$ = matrix of applied stresses

$$[s] = \begin{bmatrix} \sigma_{x0} & \tau_{xy0} & \tau_{xz0} \\ \tau_{xy0} & \sigma_{y0} & \tau_{yz0} \\ \tau_{xz0} & \tau_{yz0} & \sigma_{z0} \end{bmatrix}$$

Figure 2 from Chapter 4 illustrates a typical rotating structure. Let Ω be the rotational frequency of the structure about the z-axis in hz. Let us now suppose that there exists an element of the structure with the centroid at a radial distance r_0 from the origin, length b, mass m, thickness t, cordwise distance a, and density ρ. The centrifugal force F

applied to this structure is given by:

$$F = 4\pi^2\Omega^2 r_0 m \tag{5.2}$$

where m may be expressed by:

$$m = \rho abt \tag{5.3}$$

Therefore,

$$F = 4\pi^2\Omega^2 r_0 \rho abt \tag{5.4}$$

This illustrates that the centrifugal force is linearly dependent on thickness. The differential stiffness matrix is linearly dependent on the centrifugal force, though the constant of proportionality may be dependent on geometry. Therefore, we can say:

$$[K_D^e] \propto t \tag{5.5}$$

This implies that a change in thickness will effect the differential stiffness matrix linearly.

One can relate the baseline and objective systems through perturbations of the baseline system quantities. The stiffness and mass matrices are perturbed by:

$$[k'] = [k] + [\Delta k] \tag{5.6}$$

and

$$[m'] = [m] + [\Delta m] \tag{5.7}$$

where $[\Delta k]$ and $[\Delta m]$ are the perturbations to the baseline stiffness and mass matrices, respectively. These perturbations will cause perturbations in the dynamic response. Let the matrix of eigenvectors be given by $[\phi]$ and the diagonal matrix of eigenvectors be given by $[\omega^2]$. The perturbations in the eigenvalue and eigenvector matrices are given by:

$$[\omega'^2] = [\omega^2] + [\Delta(\omega^2)] \tag{5.8}$$

$$[\phi'] = [\phi] + [\Delta\phi] \tag{5.9}$$

where $[\Delta(\omega^2)]$ and $[\Delta\phi]$ are the changes to the baseline system eigenvalues and eignevectors, respectively.

The structural changes described in Equations (5.6) and (5.7) can be decomposed into p element change properties where a group of elements may be allowed to change. Thus

$$[\Delta k] = \sum_{e=1}^{p} [\Delta k_e] \tag{5.10}$$

$$[\Delta m] = \sum_{e=1}^{p} [\Delta m_e] \tag{5.11}$$

where $[\Delta k_e]$ and $[\Delta m_e]$ are changes to the stiffness and mass matrices of element e, respectively. Furthermore, each element change can be expressed as a fractional change α_e from the baseline system. The change α_e may represent a change in element thickness. In general, α_e can be expressed by:

$$[\Delta k_e] = [k_e]\alpha_e \tag{5.12}$$

$$[\Delta m_e] = [m_e]\alpha_e \tag{5.13}$$

Hoff (1985) used the linear relationships given in Equations (5.12) and (5.13) in his work on optimal redesign; however, he pointed out that nonlinear relations may be required for certain applications. In the case of plates, membrane components of the stiffness matrix and also the differential stiffness matrix vary linearly with the plate thickness. The bending component of the stiffness matrix, however, varies as the cube of the plate thickness. Therefore, for plates, Equation (5.12) is replaced by:

$$[\Delta k_e] = [k_{e_{memb}}]\alpha_e + [k_{e_{diff}}]\alpha_e + [k_{e_{bend}}](3\alpha_e + 3\alpha_e^2 + \alpha_e^3) \tag{5.14}$$

where $[k_{e_{memb}}]$ contains the membrane components, $[k_{e_{diff}}]$ contains the differential stiffness components, and $[k_{e_{bend}}]$ contains the bending components of $[k_e]$.

Equation (5.14) also holds for beams, with the exception that the element stiffness matrix containing only extensional properties, $[k_{e_{ext}}]$, replaces $[k_{e_{memb}}]$. Therefore, for beams:

$$[\Delta k_e] = [k_{e_{ext}}]\alpha_e + [k_{e_{diff}}]\alpha_e + [k_{e_{bend}}](3\alpha_e + 3\alpha_e^2 + \alpha_e^3) \tag{5.15}$$

The first matrix eigenvalue and eigenvector redesign method using perturbation was developed by Stetson (1975). This procedure involves the linearization of the uncoupled

energy equations of the objective structure:

$$[K'] = [M'][\omega'^2] \tag{5.16}$$

Additional work on this method was done by Stetson and Palma (1976), Stetson et al. (1978), Sandstrom and Anderson (1981), and Hoff, Bernitsas, and Anderson (1985).

Stetson developed the generalized form of the perturbation equation:

$$[\phi']^T[\Delta k][\phi'] - [\phi']^T[\Delta m] [\phi'][\omega'^2] = [\phi']^T[m][\phi'][\omega'^2] - [\phi]^T [k][\phi'] \tag{5.17}$$

To solve the above equations, note that Equation (5.17) is composed of n^2 scalar equations given by:

$$\{\psi'\}_j^T[\Delta k]\{\psi'\}_i - \omega_i'^2\{\psi'\}_j^T[\Delta m] \{\psi'\}_i = \{\psi'\}_j^T[m]\{\psi'\}_i\omega_i'^2 - \{\psi'\}_j^T[k]\{\psi'\}_i \tag{5.18}$$

for $i,j = 1,2,...,n$.

The changes, Δm and Δk, were defined in Equations (5.10) and (5.11). The mode shape changes $[\Delta\phi]$ were given by Stetson in his first order perturbation by:

$$[\Delta\phi] = [\phi][c]^T \tag{5.19}$$

where the admixture coefficients c_{ij}, $i, j = 1,2,...n$ are small and $c_{ii} = 0$.

Equations (5.8) and (5.9) are applied to Equation (5.17). This results in:

$$
\begin{aligned}
&[\phi]^T[\Delta k][\phi] + 2[\phi]^T[\Delta k][\Delta\phi] + [\Delta\phi]^T[\Delta k][\Delta\phi] \\
&- ([\phi]^T[\Delta m][\phi] + 2[\phi]^T[\Delta m][\Delta\phi] + [\Delta\phi]^T[\Delta m][\Delta\phi]) \, ([\omega^2] + [\Delta(\omega^2)]) \\
&= ([\phi]^T[m][\phi] + 2[\phi]^T[m][\Delta\phi] + [\Delta\phi]^T[m][\Delta\phi]) \, ([\omega^2] + [\Delta(\omega^2)]) \\
&- ([\phi]^T[k][\phi] + 2[\phi]^T[k][\Delta\phi] + [\Delta\phi]^T[k][\Delta\phi])
\end{aligned} \tag{5.20}
$$

Stetson then obtains the first order perturbation equations by neglecting terms of order Δ^2, Δ^3, and Δ^4. This yields (in scalar form):

$$
\begin{aligned}
\{\psi\}_j^T[\Delta k]\{\psi\}_i - \{\psi\}_j^T[\Delta m]\{\psi\}_i\omega_i^2 &= M_i\Delta(\omega_i^2) \quad \text{for } i = j \\
&= M_j c_{ij}(\omega_i^2 - \omega_j^2) \quad \text{for } i \neq j
\end{aligned} \tag{5.21}
$$

The solution of the above first order equations require the specification of the frequency changes $\Delta(\omega_i^2)$ and the mode shape changes $\Delta\psi_{ki}$ in terms of the admixture coefficients c_{ij} where $\Delta\psi_{ki}$ is the change in the kth degree of freedom of the ith mode.

In order to eliminate the admixture coefficients, the following algebraic manipulations are performed (Sandström and Anderson, 1982) for the case of non-

repeated eigenvalues. The change to the kth degree of freedom of the ith mode in terms of the admixture coefficients is:

$$\Delta\phi_{ki} = c_{i1}\phi_{k1} + c_{i2}\phi_{k2} + \ldots + c_{in}\phi_{in}$$
$$= \sum_{j=1,\,j\neq i}^{n} c_{ij}\phi_{kj} \tag{5.22}$$

Rearranging Equation (5.21) for $i \neq j$ obtains the following expression for the admixture coefficients:

$$c_{ij} = \frac{1}{M_j(\omega_i^2 - \omega_j^2)}(\{\psi\}_j^T[\Delta k]\{\psi\}_i - \omega_i^2\{\psi\}_j^T[\Delta m]\{\psi\}_i) \tag{5.23}$$

Applying Equation (5.23) to Equation (5.22) results in the following expression that relates the physical mode shape changes directly to the structural changes:

$$\Delta\psi_{ki} = \sum_{j=1}^{n}\left[\frac{\psi_{ki}}{M_j(\omega_i^2 - \omega_j^2)}(\{\psi\}_j^T[\Delta k]\{\psi\}_i - \omega_i^2\{\psi\}_j^T[\Delta m]\{\psi\}_i)\right] \tag{5.24}$$

for $i \neq j$.

Using the relationship for the change in the element mass matrix, Equation (5.14), and the nonlinear relationship for the change in the element stiffness matrix, Equation (5.15), results in the following expression, nonlinear in the element change property α_e, that describes the change in the natural frequency to the ith mode:

$$\Delta(\omega_i^2) = \frac{1}{M_i}\sum_{e=1}^{p}\left[\{\psi\}_i^T([k_{e_{memb}}] + [k_{e_{diff}}])\{\psi\}_i\alpha_e \right.$$
$$+ \{\psi\}_i^T[k_{e_{bend}}]\{\psi\}_i(3\alpha_e + 3\alpha_e^2 + \alpha_e^3)$$
$$\left. - \omega_i^2\{\psi\}_i^T[m_e]\{\psi\}_i\alpha_e\right] \tag{5.25}$$

Also, the nonlinear expression in terms of α_e for the physical mode shape change for the kth degree of freedom becomes:

$$\Delta\psi_{ki} = \sum_{e=1}^{p} \left\{ \sum_{j=1}^{n} \left[\frac{\psi_{kj}}{M_j(\omega_i^2 - \omega_j^2)} \left\{ \{\psi\}_j^T([k_{e_{memb}}] + [k_{e_{diff}}]\{\psi\}_i \alpha_e \right. \right. \right.$$
$$+ \{\psi\}_j^T[k_{e_{bend}}]\{\psi\}_i (3\alpha_e + 3\alpha_e^2 + \alpha_e^3) \tag{5.26}$$
$$\left. \left. \left. - \omega_i^2\{\psi\}_j^T[m_e]\{\psi\}_i \alpha_e \right\} \right] \right\} \quad \text{(for } j \neq i\text{)}$$

In applying the method described above in finite element analysis, practical considerations make it necessary to divide the quadrilateral elements in the finite element model into two elements: one with only membrane stiffness and one with only out-of-plane (bending) stiffness. These elements are then superimposed. This permits multiplication of the stiffness terms representing membrane properties by a linear element change factor while the stiffness terms containing the bending properties can be altered by a nonlinear change factor.

Derivation of Complex Perturbation Equations

Let us now determine the changes in the system eigenvalues and mode shapes for a problem exhibiting Coriolis behavior. As discussed previously, the eigenvalues for this system will be real; however, the mode shapes will have complex components.

The basic equation of motion for the descretized system is:

$$[M]\{\ddot{\phi}\}_i + [B]\{\dot{\phi}\}_i + [K]\{\phi\}_i = \{0\} \tag{5.27}$$

where [M], [B], and [K] are the system mass, Coriolis, and stiffness matrices respectively, and $\{\phi\}_i$ is the displacement vector for the ith mode.

Let us assume a solution for the system described in Equation (5.27) of the form:

$$\{\phi\}_i = \{\psi\}_i e^{i\omega_i t} \tag{5.28}$$

where $\{\psi\}_i$ is the eigenvector for the ith mode and ω_i is the eigenvalue for the ith mode. Applying Equation (5.28) to Equation (5.27) obtains:

$$-\omega_i^2[M]\{\psi\}_i e^{i\omega_i t} + i\omega_i[B]\{\psi\}_i e^{i\omega_i t} + [k]\{\psi\}_i e^{i\omega_i t} = \{0\} \tag{5.29}$$

The term $e^{\omega_i t}$ will be eliminated. In addition, the terms will be premultiplied by $\{\psi\}_i^T$, to obtain the following scalar equation:

$$-\omega_i^2\{\psi\}_i^T[M]\{\psi\}_i + i\omega_i\{\psi\}_i^T[B]\{\psi\}_i + \{\psi\}_i^T[K]\{\psi\}_i = 0 \tag{5.30}$$

Define *generalized mass* for mode i, M_i, to be:

$$M_i = \{\psi\}_i^T[M]\{\psi\}_i \tag{5.31}$$

Similarly, *generalized damping* or *generalized Coriolis*, B_i, is defined by:

$$B_i = \{\psi\}_i^T[B]\{\psi\}_i \tag{5.32}$$

Finally, *generalized stiffness* may be defined as:

$$K_i = \{\psi\}_i^T[K]\{\psi\}_i \tag{5.33}$$

Stetson (1975) applied the above definitions for generalized mass and generalized stiffness in obtaining his perturbation equations. Since the following analysis will employ both real and imaginary components, the full form of the terms in Equation (5.30) will be retained for now.

Perturbations of the System Including Complex Effects

When the original system is modified in the optimization process, it can be said to be perturbed. The perturbed system must also obey the equations of equilibrium. Let the perturbed system be distinguished from the original by primes. Equation (5.30) can be rewritten for the perturbed system by:

$$-[\psi']^T[M'][\psi'][\omega'^2] + i[\psi']^T[B'][\psi'][\omega'] + [\psi']^T[K'][\psi'] = 0 \tag{5.34}$$

where $[\psi']$ is the matrix of perturbed eigenvectors, and $[\omega']$ is the diagonal matrix of perturbed eigenfrequencies.

The perturbed system can be related to the original, unprimed system by:

$$[K'] = [K] + [\Delta K] \tag{5.35}$$

$$[M'] = [M] + [\Delta M] \tag{5.36}$$

$$[B'] = [B] + [\Delta B] \tag{5.37}$$

$$[\omega'] = [\omega] + [\Delta\omega] \tag{5.38}$$

$$[\omega'^2] = [\omega^2] + [\Delta\omega^2] \tag{5.39}$$

$$[\psi'] = [\psi] + [\Delta\psi] \tag{5.40}$$

The above perturbation equations are similar to Equations (5.7) through (5.10).

Equations (5.11) and (5.12) define the global changes in mass and stiffness in terms of element change properties and Equations (5.13) through (5.15) define the element changes. One last change that needs to be defined is that for the Coriolis matrix. This is done by:

$$[\Delta B] = \sum_{e=1}^{p} [\Delta b_e] \tag{5.41}$$

and

$$[\Delta b_e] = [b_e]\alpha_e \tag{5.42}$$

The last equation is justified because, as we have seen, the Coriolis matrix is linearly dependent on element mass. The element mass is itself linearly dependent on changes in thickness; the element change parameter.

Equations (5.35) through (5.42) are applied to (5.34). Terms in Δ of order 2 or higher are eliminated as are the baseline equilibrium terms, which essentially are order zero in Δ. In a manner similar to that used in section 4.1, the equations are expanded for all modes and an expression for the change in the eigenvalue in terms of admixture coefficients is obtained. This relates the change in the eigenvectors for all modes to the changes in element properties during the redesign process. This results in the following expression for the change in natural frequency in scalar form:

$$\{\psi\}_j^T[\Delta K]\{\psi\}_i + i\omega_i\{\psi\}_j^T[\Delta B]\{\psi\}_i - \omega_j^2\{\psi\}_j^T[\Delta M]\{\psi\}_i$$

$$= \{\psi\}_i^T[M]\{\psi\}_i\Delta(\omega_i^2) - i\{\psi\}_i^T[B]\{\psi\}_i\Delta\omega \qquad (i=j) \tag{5.43}$$

$$= (\{\psi\}_j^T[M]\{\psi\}_i(\omega_j^2 - \omega_i^2) - i\{\psi\}_j^T[B]\{\psi\}_i(\Delta\omega_j - \Delta\omega_i))c_{ij} \qquad (i \neq j)$$

Applying the definitions for the changes in the structural matrices to the above equation and setting $i=j$, the following expression is obtained for the frequency change for the ith mode due to application of the element changes α_e:

$$\{\psi\}_i^T[M]\{\psi\}_i\Delta(\omega_j^2) - i\{\psi\}_i^T[B]\{\psi\}_i\Delta\omega_i$$

$$= \sum_{e=1}^{p} (\{\psi\}_i^T[k_e^-]\{\psi\}_i + i\omega_i\{\psi\}_i^T[b_e]\{\psi\}_i - \omega_i^2\{\psi\}_i^T[m_e]\{\psi\}_i)\alpha_e \tag{5.44}$$

where $[k_e^-]$ is the approximation of the cubic expansion of the element stiffness matrix such that:

$$[k_e^{\sim}] = [k_{e_{memb}}] + [k_{e_{diff}}] + 3[k_{e_{bend}}] \tag{5.45}$$

However, it must be remembered that the eigenvector is itself a complex quantity, with both amplitude and phase components. Let us express the complex eigenvector for the ith mode, $\{\psi\}_i$ as:

$$\{\psi\}_i = \{\phi\}_i + i\{\xi\}_i \tag{5.46}$$

where $\{\phi\}_i$ denotes the real part of the ith eigenvector and $\{\xi\}_i$ denotes the imaginary part. Therefore, Equation (5.44) becomes two equations; one that equates real parts and another one that equates imaginary parts. These are, respectively,

$$\left(\{\phi\}_i^T[M]\{\phi\}_i - \{\xi\}_i^T[M]\{\xi\}_i \right) \Delta(\omega_i^2) + \{\xi\}_i^T[B]\{\xi\}_i \Delta(\omega_i)$$

$$= \sum_{e=1}^{p} \left\{ \{\phi\}_i^T[k_e^{\sim}]\{\phi\}_i - \{\xi\}_i^T[k_e^{\sim}]\{\xi\}_i - \left(\{\phi\}_i^T[m_e]\{\phi\}_i - \{\xi\}_i^T[m_e]\{\xi\}_i \right)\omega_i^2 \right\}\alpha_e \tag{5.47}$$

and

$$2\{\phi\}_i^T[M]\{\xi\}_i \Delta(\omega_i^2) - \left(\{\phi\}_i^T[B]\{\phi\} + \{\xi\}_i^T[B]\{\xi\}_i \right) \Delta\omega_i$$

$$= \sum_{e=1}^{p} \left\{ 2\{\phi\}_i^T[k_e^{\sim}]\{\xi\}_i + \left(\{\phi\}_i^T[b_e]\{\phi\}_i + \{\xi\}_i^T[b_e]\{\xi\}_i \right)\omega_i - 2\{\phi\}_i^T[m_e]\{\xi\}\omega_i^2 \right\}\alpha_e \tag{5.48}$$

Note that for the case of no Coriolis terms and purely real eigenvectors, Equation (5.47) degenerates to Equation (5.25) and Equation (5.48) becomes identically satisfied.

To determine the eigenvector change in the Coriolis system, the admixture coefficients c_{ij} previously defined in Equation (5.45) can be used. From these admixture coefficients, the eigenvectors of the perturbed system can be obtained:

$$\Delta\psi_{ki} = \sum_{e=1}^{p} \left\{ \sum_{j=1}^{n} \left[\frac{\psi_{kj}}{\{\psi\}_i^T[M]\{\psi\}_i(\omega_i^2 - \omega_j^2) - i\{\psi\}_i^T[B]\{\psi\}_i(\omega_i - \omega_j)} \right. \right.$$

$$\times \left\{ \{\psi\}_j^T[k_e^{\sim}]\{\psi\}_i\alpha_e \right.$$

$$\left. \left. \left. + i\omega\{\psi\}_j^T[b_e]\{\psi\}_i\alpha_e - \omega_i^2\{\psi\}_j^T[m_e]\{\psi\}_i\alpha_e \right\} \right] \right\} (\text{ for } j \neq i) \tag{5.49}$$

Sequential Unconstrained Minimization Techniques

The generalized form of the optimization problem subject to both equality and inequality constraints may be stated by:

$$\text{min } F(\{x\}) \tag{5.50}$$

subject to

$$g_j(\{x\}) \leq 0 \quad j = 1, 2, ..., m \tag{5.51}$$

$$h_k(\{x\}) = 0 \quad k = 1, 2, ..., l \tag{5.52}$$

In the external penalty function method, a penalty is associated with the violation of a constraint. The penalties are applied outside the region of the feasible domain. All intermediate solutions lie in the infeasible region. The solution is obtained by convergence from the outside. The solution may start from an infeasible point; therefore, an initial feasible point is not required. However, when the optimum solution is achieved, this solution also is not in the feasible region. Bellagamba and Yang (1981) applied the exterior penalty function approach to the problem of truss optimization.

The internal penalty function method, however, always keeps the solutions inside the feasible domain. The solution procedure can be stopped at any time and a permissible optimized result will be obtained. If one wishes to start the design process from inside the feasible region, one must obviously start with a feasible solution. This may not always be possible.

The Augmented Lagrange Multiplier (ALM) method produces a way to reduce the dependency of the algorithm on the choice of penalty parameters and the way they are updated. This is accomplished by combining the use of Lagrange multipliers with penalty functions. Using only Lagrange multipliers gives an optimum that is a stationary point rather than a true minimum of the Lagrangian. Using only stationary functions gives a minimum that leaves open the possibility of an ill-conditioned solution that is not feasible. Using both creates an unconstrained problem that obtains a feasible, well-conditioned solution that is a true minimum.

The minimization problem may now be stated in terms of the following augmented Lagrangian:

$$F(\{x\},\{\lambda\},r_p) = F(\{x\}) + \sum_{j=1}^{m}[\lambda_j\psi_j + r_p\psi_j^2]$$
$$+ \sum_{k=1}^{l}\left\{\lambda_{k+m}h_k(\{x\}) + r_p[h_k(\{x\})]^2\right\} \tag{5.53}$$

where

$$\psi_j = \max\left[g_j\{x\}, \frac{-\lambda_j}{2r_p}\right] \tag{5.54}$$

The update formulas for the Lagrange multipliers are:

$$\lambda_j^{p+1} = \lambda_j^p + 2rp\left\{\max\left[g_j(\{x\}), \frac{-\lambda_j^p}{2r_p}\right]\right\} \tag{5.55}$$

$$\lambda_{k+m}^{p+1} = \lambda_{k+m}^p + 2r_p h_k\{x\} \tag{5.56}$$

for $j = 1,m$ and $k = 1,l$.

Vanderplaats (1984) states that the ALM method has the following advantages:

1. The method is relatively insensitive to the value of r_p. It is not necessary to increase r_p to ∞.

2. Precise $g_j(\{x\})$ and $h_k(\{x\})$ are possible.

3. Acceleration is achieved by updating the Langrange multipliers.

4. The starting point may be either feasible or infeasble.

5. At the optimum, the value of $\lambda_j^* \neq 0$ will automatically identify the active constraint set.

Vanderplaats (1982) provides a historical overview of optimization methods. Vanderplaats (1983) introduced a computer implementation of optimization methods, ADS.

CHAPTER 6

OPTIMAL REDESIGN METHOD

In this chapter, the predictor-corrector method for optimal redesign will be developed. This development will take place in the context of simple example problems. In later chapters the method will be expanded to large problems and to the inclusion of Coriolis effects with complex eigenvectors.

Predictor-Corrector Method

Consider the first example for optimal structural redesign, the rotating beam, shown in Figure 10. Only vibration in the x-z plane will be considered; therefore, the permitted vibratory degrees of freedom will be x- and z-axis displacements and y-axis rotations. Furthermore, the left end of the beam will clamped, and the right end will be "guided" so as to permit only x- and z-axis displacements and rotations. This guided bending condition is chosen because the problem then can also be readily solved by theoretical means. The theoretical solution will be used for comparisons.

The first design change seeks a 10% increase in the fundamental flexural model frequency. In the predictor step, we will assume that the element change α_e is small; therefore, the quantity $(1+\alpha_e)^3 - 1$ may be approximated by $3\alpha_e$. This results in a 3.11% error, but is done so as to facilitate solving for α, which we shall see will be the unknown in the inverse perturbation scheme. The element change property α_e is given by:

$$\alpha_e = \frac{\Delta t_e}{t_e} \tag{6.1}$$

where t_e is the element thickness, and Δt_e is the change in element thickness. Thickness for the beam in Figure 10 is z-direction in the cross section. The scalar equation that gives
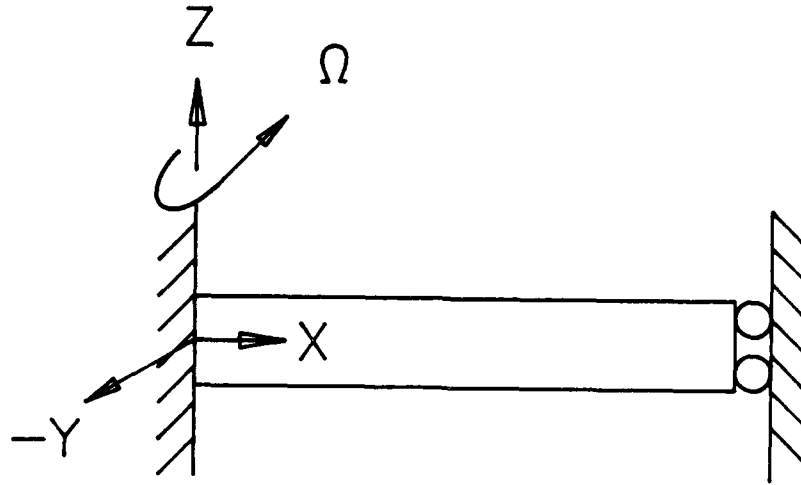
Figure 10. Rotating Beam

the relationship between α_e and the desired change in natural frequency for the ith mode $\Delta\omega_i$, neglecting Coriolis effects but including centrifugal effects, is given from Equation (5.25):

$$\Delta(\omega_i^2) = \frac{1}{M_i} \sum_{e=1}^{p} \left[\{\psi\}_i^T ([k_{e_{memb}}] + [k_{e_{diff}}] + 3[k_{e_{bend}}])\{\psi\}_i \alpha_e \right.$$
$$\left. - \omega_i^2 \{\psi\}_i^T [m_e] \{\psi\}_i \alpha_e \right] \tag{6.2}$$

where the approximation of the expansion of $(1+\alpha_e)^3$ as $3\alpha_e$ is applied.

The above equation is called the *predictor*. It relates the change in the element change properties to a prescribed change in the desired eigenfrequency. In this way the equation predicts what the system configuration should be for a given amount of frequency change. For the complex case involving Coriolis effects, Equations (5.47) and (5.48) serve

as the predictor equations. Note that in that case there are two predictor equations.

For the single element case, Equation (6.2) can be solved as one equation with one unknown. When the bar is divided up into two or more elements, the excess unknown element change properties can be found by optimizing some function, such as minimum weight or minimum structural change. Equation (6.2) then becomes an equality constraint in the optimization scheme. In the Coriolis problem, there are two equality constraints. Therefore, it is seen that the problem becomes one of parametric optimization, with thickness as the parameter to be optimized.

Using the results from the static analysis, one finds the eigenvalues and eigenvectors for the rotating system by finite element modal analysis using MSC/ NASTRAN as modified with Direct Matrix Abstraction Programming (DMAP). The restart procedure used is described in Appendix A. The eigenvectors are stored, printed out, and written to a FORTRAN file. Another FORTRAN postprocessor strips out the eigenvector for the desired mode and appropriately partitions it for each element. Once this has been accomplished, all of the quantities necessary to formulate Equation (6.2) have been obtained.

Equation (6.2) is used as an equality constraint in the Augmented Lagrange Multiplier (ALM) procedure described in Chapter 5. Inequality constraints are also formulated. The first inequality constraint requires α_e to be greater than -0.5. This ensures that the element thickness will always be positive during the redesign process and in no case will an element be reduced by more than 50%. This makes certain that unwanted secondary effects, such as static failure due to the "applied" centrifugal load will not occur. The second inequality constraint forces the α_e to be less than 1E5. This supplies an upper bound to the search procedure. The function to be minimized in the first example is the design change:

$$f(\{\alpha\}) = \sum_{e=1}^{p} (\alpha_e)^2 \tag{6.3}$$

where $\{\alpha\}$ is the vector of element change properties α_e.

Alternatively, the function to be minimized could be minimum weight. For a system of uniform density, this function is given by:

$$f(\{\alpha\}) = \sum_{e=1}^{p} A_e \alpha_e \qquad (6.4)$$

where A_e is the element planform area perpendicular to the thickness.

The element change properties determined from Equations (6.3) or (6.4) are used to recompute the cross sectional area and moments of inertia for each element. A reanalysis is then accomplished to determine the eigenvalues and eigenvectors. The perturbed eigenvectors are necessary to perform the next step in the procedure, namely the corrector.

The corrector examines the potential energy imbalance between the system output from the predictor and the desired system and corrects the imbalance through additional elemental changes. This enforces the natural frequency constraint on the ith mode. The following equation is used for the example with no Coriolis effects:

$$\sum_{e=1}^{p} (\{\psi'\}_i^T[k_e^-]\{\psi'\}_i - \omega'^2_i\{\psi'\}_i^T[m_e]\{\psi'\}_i)\alpha_e = \omega'^2_i\{\psi'\}_i^T[M]\{\psi'\}_i - \{\psi'\}_i^T[K]\{\psi'\}_i \qquad (6.5)$$

where $\{\psi'\}$ is the perturbed eigenvector, ω' is the desired eigenvalue, and $[K]$ and $[M]$ are the global stiffness and mass matrices, respectively. Note that the global stiffness matrix is the total tangential stiffness matrix that includes the differential components.

If Coriolis effects are included, then the following equation is used for the corrector:

$$\sum_{e=1}^{p} (\{\psi'\}_i^T[k_e^-]\{\psi'\}_i + i\omega'_i\{\psi'\}_i^T[b_e]\{\psi'\}_i - \omega'^2_i\{\psi'\}_i^T[m_e]\{\psi'\}_i)\alpha_e$$
$$= \omega'^2_i\{\psi'\}_i^T[M]\{\psi'\}_i - i\omega'_i\{\psi'\}_i^T[B]\{\psi'\}_i - \{\psi'\}_i^T[K]\{\psi'\}_i \qquad (6.6)$$

Notice that the above equation can be broken down into two equations; one that equates the real parts and another that equates the imaginary parts. This results in two equality constraints for the corrector step:

$$\sum_{e=1}^{p}\left[\left(\{\phi'\}_i^T[k_e^-]\{\phi'\}_i -\{\xi'\}_i^T[k_e^-]\{\xi'\}_i\right) -\left(\{\phi'\}_i^T[m_e]\{\phi'\}_i -\{\xi'\}_i^T[m_e]\{\xi'\}_i\right)\omega_i^2\right]\alpha_e \qquad (6.7)$$

$$= (\{\phi'\}_i^T[M]\{\phi'\}_i -\{\xi'\}_i^T[M]\{\xi'\}_i)\omega_i'^2 - (\{\phi'\}_i^T[K]\{\phi'\}_i -\{\xi'\}_i^T[K]\{\xi'\}_i)$$

and

$$\sum_{e=1}^{p}\left[2\{\phi'\}_i^T[k_e^-]\{\xi'\}_i +\left(\{\phi'\}_i^T[b_e]\{\phi'\}_i +\{\xi'\}_i^T[b_e]\{\xi'\}_i\right)\omega'_i -2\{\phi'\}_i^T[m_e]\{\xi'\}_i\omega_i'^2\right]\alpha_e \qquad (6.8)$$

$$= 2\{\phi'\}_i^T[M]\{\xi'\}_i\omega_i'^2 - (\{\phi'\}_i^T[B]\{\phi'\}_i +\{\xi'\}_i^T[B]\{\xi'\}_i)\omega' -2\{\phi'\}_i^T[K]\{\xi'\}_i$$

Notice that when the Coriolis effects are absent, the above equations degenerate into those used previously.

The perturbed eigenectors may be obtained in one of two ways. The first method, mentioned above, is simply rerunning the predictor. This yields the full, nonlinearly-perturbed matrix of eigenvectors and the desired mode can be easily partitioned out. The second procedure involves the application of Equation (5.26), where the change to the kth degree of freedom for the ith mode in the absence of Coriolis effects is:

$$\Delta\psi_{ki} = \sum_{e=1}^{p}\left\{\sum_{j=1}^{n}\left[\frac{\psi_{kj}}{M_j(\omega_i^2-\omega_j^2)}\left\{\{\psi\}_j^T([k_{e_{memb}}]+[k_{e_{diff}}]\{\psi\}_i\alpha_e\right.\right.\right.$$
$$\left.\left.\left.+\ \{\psi\}_j^T[k_{e_{bend}}]\{\psi\}_i(1+\alpha_e)^3 \right.\right.\right. \qquad (6.9)$$
$$\left.\left.\left.-\ \omega_i^2\{\psi\}_j^T[m_e]\{\psi\}_i\alpha_e\right\}\right]\right\} \text{ (for } j\ne i)$$

If Coriolis effects are present, then Equation (5.49) can be used to compute the perturbed complex eigenvectors.

The above equation is a linear approximation of the perturbations in the eigenvectors. Using the results of reanalysis, one obtains the full, nonlinear changes in the eigenvector. These two candidate procedures have definite trade offs. Using Equation (6.6) avoids another finite element run. However, Equation (6.6) involves many matrix multiplications and manipulations and additional programing. Doing the reanalysis involves another finite element run, but it is simple to do and provides the exact

intermediate answers. It also incorporates the changes in centrifugal force due to mass changes, which is something Equation (6.6) cannot do. As a side benefit, the intermediate result of the predictor method alone are provided.

A third approach that one can use in the corrector step is to simply use the original, unperturbed eigenvector. This should provide reasonable results provided that the change between the original and objective systems is small. The benefit of this procedure is that neither a finite element reanalysis nor a new, intricate matrix solution is required.

As shown in Figure 11, the finite element solver is first run. This is done to generate the system structural matrices and the eigenvectors. Then, using this information, the equation of constraint for the predictor is used using the frequency change equation or equations given in Equation (6.4) or (6.5) and (6.6). This constraint is used in the next step, the optimizer. Optimization is accomplished with respect to minimum weight or minimum change. Finally, a finite element analysis is done to obtain the system matrices and eigenvectors for the perturbed system produced by the predictor.

Figure 12 shows an overview of the corrector step. First, the finite element solver is run for the perturbed system resulting from the predictor. This is done to generate the system structural matrices and the eigenvectors. Then, using this information, the equation of constraint for the predictor is used using the energy balance equation or equations given in Equation (6.4) or (6.5) and (6.6). This constraint is used in the next step, the optimizer. Finally, a finite element analysis is done to obtain the system matrices and eigenvectors for the perturbed system produced by the predictor. Note that this last finite element analysis is not really required; it is done to confirm the results. Only the initial analysis and the intermediate analysis are required.

Examples

The first physical problem to which the predictor-corrector method is applied is shown in Figure 10. It is an initially uniform aluminum 2024T-6 beam of length L equal to 250 mm, with moment of inertia I equal to 3.2552E4 mm^4, cross sectional area A of
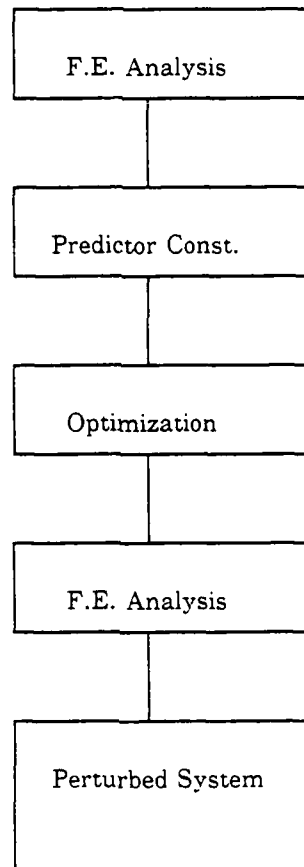
Figure 11. Predictor Overview

```
┌─────────────────────┐
│    F.E. Analysis    │
└─────────────────────┘
          │
┌─────────────────────┐
│   Corrector Const.  │
└─────────────────────┘
          │
┌─────────────────────┐
│    Optimization     │
└─────────────────────┘
          │
┌─────────────────────┐
│    F.E. Analysis    │
└─────────────────────┘
          │
┌─────────────────────┐
│                     │
│  Optimized System   │
│                     │
└─────────────────────┘
```
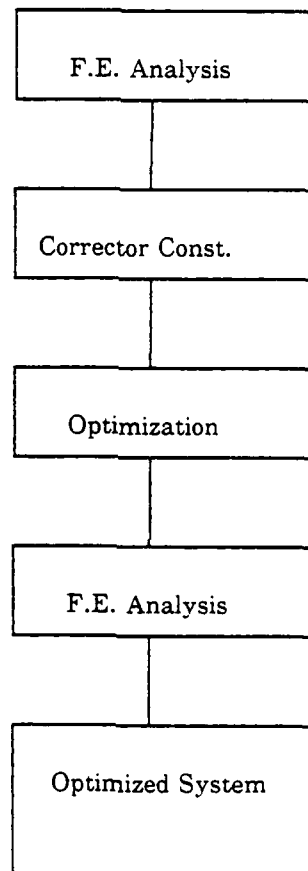
Figure 12. Corrector Overview

625 mm^2, Young's modulus E of 73.77E3 MPa, Poisson's ratio ν equal to 0.33, and density ρ of 2.774E-9 Mg/mm^3. The beam rotates at a speed Ω of 80 hz.

A preliminary step done here is to determine the fundamental flexural frequency for the problem of the nonrotating beam. This will be used to test the convergence of the finite element mesh. The exact solution for fundamental frequency is 3.5043E3 rad/sec (see Appendix B). Table 1 shows that the accuracy of the mesh improves when more elements are used.

Table 1. Mesh Convergence

No. of elements	ω_1	Percent error
1	2.917166E3	16.8
2	3.320063E3	5.3
4	3.365316E3	3.9

For the rotating beam, the bending effects of the beam are separated from the axial effects. This is done because the effect of extensional (membrane) stiffness on the predictor-corrector equations is linear in the design variable α_e while the effect of thickness on bending stiffness is cubic in α_e. The separation has been accomplished in an artificial way by splitting each element into two superimposed subelements: one with moment of inertia and no cross sectional area and another with cross sectional area and no moment of inertia. At first this sounds unmotivated, but it is consistent with the additive value of stiffness. Bending moment of inertia and cross-sectional area are indeed distinct properties. Any relationship between the two is a consequence of a specific geometry where the two quantities are related by a common parameter. For a rectangular beam, both the moment of inertia and cross sectional area are dependent on thickness. Therefore, in this case, this parameter is thickness, and optimization of this parameter will

be done.

The beam is divided into four equal-length finite elements, and each element is composed of two subelements. The mesh is shown in Figure 13.

For the given mesh, the fundamental frequency of the rotating beam is $\omega_1 = $ 3.374117E3 rad/sed. The modal frequency, ω_1^d, equals $1.1\omega_1$ and will therefore be 3.711529E3 rad/sec with a desired change of frequency $\Delta\omega_1^d$ of 3.374120E2 rad/sec. The predictor obtains a fundamental modal frequency ω_1^p of 3.722036E3 rad/sec. This is within 3.11% of the desired frequency change. The corrector step is then done, using the method that employs an updated eigenvector from the intermediate MSC/NASTRAN analysis. The fundamental frequency from the corrector, ω_1^c, is 3.713899E3 rad/sed. Thus it is seen that the predictor-corrector obtains the frequency change to within 1% of the desired change.
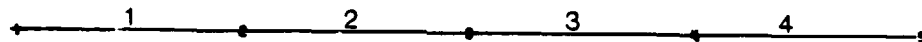
Figure 13. Finite Element Model for Rotating Beam

The next test case for optimal redesign will be the simple rotating blade from Chapter 4. The blade is made of Inconel 718 steel with Young's modulus of 202.696E3 MPa, Poisson's ratio of 0.29, and density of 8.2121E-9 Mg/mm^3. The blade outer radius is 787.4 mm as measured from a the center of a rigid hub of radius 393.70 mm, has a width of 556.78 mm, and is initially of uniform thickness 87.38 mm. The rotation speed Ω is 81.2 hz.

Figure 14 shows a finite element model for this blade, which is the same as the model in Figure 2. The rigid hub is not modeled. This finite element model consists of four quadrilateral elements, and each element is once again broken into two subelements. The first subelement has only membrane properties and the second one has only bending properties. As in the case of the beam, this is done in order to separate membrane stiffness from bending stiffness.

A difficulty presented by quadrilateral elements in many general purpose finite element programs is the that stiffness and "coupled" mass matrices output are in element coordinates. (The "coupled" mass matrix is a consistent mass matrix with the rotational terms removed.) Since the eigenvectors are always in the basic (global) coordinate system, it is necessary to transfer the stiffness and mass matrices to the basic system. The stiffness matrix can be transformed by:

$$[K_{basic}] = [T]^T [K_{element}][T] \qquad (6.10)$$

where $[K_{basic}]$ is the element stiffness matrix in the basic system, $[K_{element}]$ is the element stiffness matrix in the element system, and $[T]$ is the element-to-basic transformation matrix. The element mass matrices are similarly transformed to the basic coordinate system.

The fundamental modal frequency for the rotating blade of Figure 6.4, ω_1, is 2.478E3 rad/sec. For a 10% desired increase in ω_1, ω_1^d is 2.726E3 rad/sec and $\Delta\omega_1^d$ is 2.483E2 rad/sec. The predictor gives ω_1^p of 2.653E3 rad/sec. $\Delta\omega_1^p$ is 1.749E2 rad/sec, which is 70.42% of the desired frequency change. The corrector obtains ω_1^c of 2.705E3
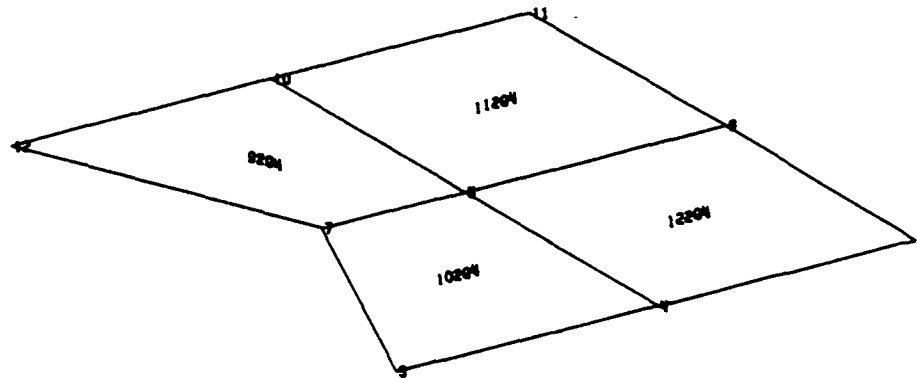
Figure 14. Finite Element Model for Rotating Blade

rad/sec. $\Delta\omega_1^c$ is 2.268E2 rad/sec which is 91.33% of the desired change.

Figure 15 shows the cross section of the optimal stuctural design of the blade. The original structure is shown in solid lines and the optimal structure is in dashed lines. Thickness differences have been exaggerated. Refined meshes will be the subject of the next section.

To summarize the results of the previous two examples, the governing equation of the predictor step, Equation (6.2), is a linear representation of a nonlinear perturbation of the mass and stiffness matrices and the matrix of eigenvectors with respect to a change in thickness. However, the higher order perturbation terms are important. The predictor achieved only 70% to 96% of the desired frequency change. Additional nonlinearities are brought back into the analysis in the corrector in the form of recalculated eigenvectors. Changes in centrifugal force due to mass changes are also incorporated in the reanalysis.

Figure 15. Optimized Shape of Rotating Blade

The predictor-corrector method outlined in this section obtained 90% to 99% of the desired frequency change in one complete cycle. The end result is an improved method for the optimal redesign of a rotating structure.

CHAPTER 7

OPTIMAL REDESIGN OF ADVANCED SYSTEMS

Review of Solution Procedure

A method has been devised to obtain the optimal stuctural redesign of a rotating system that incorporates centrifugal and Coriolis effects. This method extends the inverse perturbation scheme devised by Hoff into the nonlinear physical problem regime. We must deal with the structurally nonlinear effects of rotation and to obtain the optimal redesign with a minimum number of finite element analyses. In order to account for the effect of the static displacements due to rotation on the bending frequencies and mode shapes, a *new finite element solution sequence was created.* This involved a preliminary static solution where the displacements due to rotation were first calculated. Then, a differential stiffness matrix, $[K_D]$, was calculated. This matrix represents the effect of the displacements on the structural stiffness. A Coriolis matrix was also generated that incorporated the energy-conserving coupling effects of velocity in one plane to displacement in another plane. The differential stiffness matrix and the Coriolis matrix were then incorporated into the modal analysis and the frequencies and mode shapes were obtained.

For the rotating problem without Coriolis effects, Equation (3.2) gives the scalar relationship between the element change α_e and the desired change in natural frequency for the ith mode, $\Delta\omega_i$. This equation was used as an equality constraint for the function to be opimized, Equation (6.3). The perturbed eigenvectors for the new system were then obtained via an intermediate finite element reanalysis. These were used in Equation (6.4) to correct the energy imbalance between the predicted system and the desired system through additional structural changes. This equation was used as an equality constraint in

63

the optimization of Equation (6.3). Finally, the new eigenvalues and eigenvectors of the redesign system were obtained by finite element reanalysis.

Rotating Compressor Blade

The next step is to use the above method on more complicated problems. Figure 16 shows a finite element model for a curved rotating blade. The blade is made of Inconel 718 steel, has a radius of 254.0 mm, a length of 69.34 mm, and rotates at a speed of 200 hz. It has an angle of attack of 30 degrees and is modeled after a NACA 64 airfoil. This is a blade typically found in a jet engine high-pressure compressor.
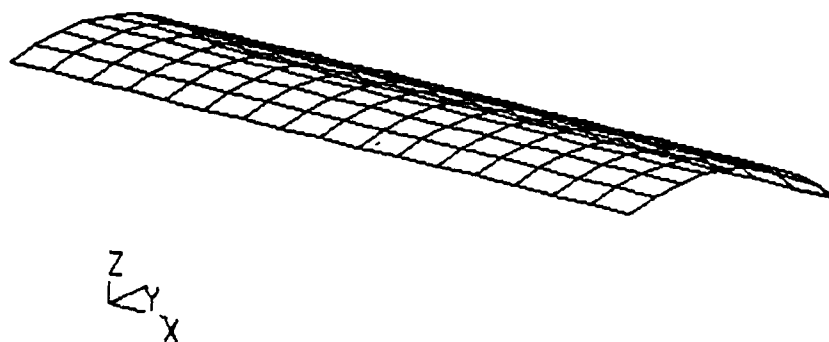
Figure 16. Rotating Blade

The finite elements are each divided into two subelements; one with membrane properties only and another superimposed element with only bending properties. This finite element model has approximately 1000 degrees of freedom. The elements are grouped (linked) into twelve regions. During the analysis, the thickness of the regions will

change, but the elements within each region will maintain a common thickness. (Each superimposed membrane and bending element region will also keep a common thickness. The twelve regions are shown in Figure 17.) Table 2 shows the initial thickness, in millimeters, of the regions.

10	7	4	1
11	8	5	2
12	9	6	3

Figure 17. Blade Regions

Let α_i be the element change property for the ith element. Using Equation (6.2) for the first mode, define the contribution of the ith element E_i to the frequency change $\Delta(\omega_1^2)$ to be:

$$E_i = \frac{1}{M_1}\left[\{\psi\}_1^T\left\{[k_{i_{memb}}] + [k_{i_{diff}}] + 3[k_{i_{bend}}]\right\}\{\psi\}_1 \right.$$

$$\left. - \omega_1^2\{\psi\}_1^T[m_i]\{\psi\}_1\right] \tag{7.1}$$

Now let α_k' be the common element change property for all of the elements in region

Table 2. Initial Region Thickness

Region Number	Thickness (mm)
1	1.734
2	1.734
3	1.734
4	2.312
5	2.312
6	2.312
7	3.005
8	3.005
9	3.005
10	3.467
11	3.467
12	3.467

k. In the corrector, the lower limit on α_k' must be changed so that no region will have a thickness less than one-half of the thickness of the region in the original geometry. Let α_{k_1}' denote this new lower bound of the element change parameter for each region. Let E_k' be the sum of the E_k factors for each element in region k. Therefore, using Equation (6.2). the optimization problem for the predictor becomes the minimization of:

$$f(\alpha_k') = \sum_{k=1}^{12} (\alpha_k')^2 \tag{7.2}$$

subject to the equality constraint:

$$\sum_{k=1}^{12} E_k' \alpha_k' = \Delta\omega_1^2 \tag{7.3}$$

and the inequality constraints:

$$\alpha_k^{'} > -0.5 \tag{7.4}$$

$$\alpha_k^{'} < 1E5 \tag{7.5}$$

For the corrector, Equation (4.4) is modified as follows. Let J_i be:

$$J_i = \{\psi'\}_1^T[k_1^-]\{\psi'\}_i - \omega_1^{'2}\{\psi'\}_1^T[m_1]\{\psi'\}_i)\alpha_1 \tag{7.6}$$

Define G to be:

$$G = \omega_1^{'2}\{\psi'\}_1^T[m]\{\psi'\}_1 - \{\psi'\}_1^T[k]\{\psi'\}_1 \tag{7.7}$$

where $\{\psi'\}$ is the perturbed *eigenvector*, ω' *is the desired eigenvalue, and* [k] and [m] are the global stiffness and mass matrices, respectively.

Now let $\alpha_k^{'}$ be the common element change property for all of the elements in region k. Let $J_k^{'}$ be the sum of the J_k factors for each element in region k. Therefore, using Equation (6.5), the optimization problem for the predictor becomes the minimization of:

$$f(\alpha_k^{'}) = \sum_{k=1}^{12} (\alpha_k^{'})^2 \tag{7.8}$$

subject to the equality constraint:

$$\sum_{k=1}^{12} J_k^{'}\alpha_k^{'} = G \tag{7.9}$$

and the inequality constraints:

$$\alpha_k^{'} > \alpha_{k_l}^{'} \tag{7.10}$$

$$\alpha_k^{'} < 1E5 \tag{7.11}$$

For this problem another FORTRAN postprocessor must be written that groups together the stiffness, mass, differential stiffness, eigenvector, and transformation matrices for each element. This is done so as to minimize matrix storage requirements and programming steps during the predictor or corrector. Rather than read in all of the matrices for all of the elements at once, they are read in per element. The matrix operations for the predictor or corrector are then performed, the results are stored, and then the program loops back to read in the matrices for the next element.

Three complete finite element static and dynamic analyses are required for each

cycle in this method. The first run gives the eigenvalues and mode shapes for the original system. The second one gives the values for the system output by the predictor. The final analysis verifies the results of the corrector.

Another possible objective function is minimum weight. In this case, the function to be minimized in the predictor comes:

$$f(\{\alpha_k'\}) = \sum_{k=1}^{12} A_k' \alpha_k' \tag{7.12}$$

subject to the inequality constraints:

$$\alpha_k' > -0.5 \tag{7.13}$$

and

$$\alpha_k' < 1E5 \tag{7.14}$$

In the corrector step for the minimum weight problem, the objective function remains minimum minimum weight. However, as in the minimum change case, the lower limit on the element change parameter must be changed so that no region will have a thickness less than one-half the thickness of the region in the original geometry.

Results of Analysis

It is first noted that for the nonrotating system, the fundamental frequency is 7.6656E3 rad/sec. For the rotating system including centrifugal effects, the fundamental frequency is 8.3802E3 rad/sec. This implies a 9.32% increase in fundamental frequency due to the centrifugal effect of rotation.

Figures 18 and 19 show the first two eigenvectors for the rotating blade when centrifugal effects are not included. The first eigenvector is a flapping, or bending, mode and the second one is a twisting, or torsional mode. The fundamental eigenvector is indeed that of out-of-plane bending. Figures 20 and 21 show the first two eigenvectors when centrifugal effects are included. Notice that the mode shapes remain unchanged. Therefore, the effect of rotation changes the eigenvalues but the eigenvectors retain their identity.
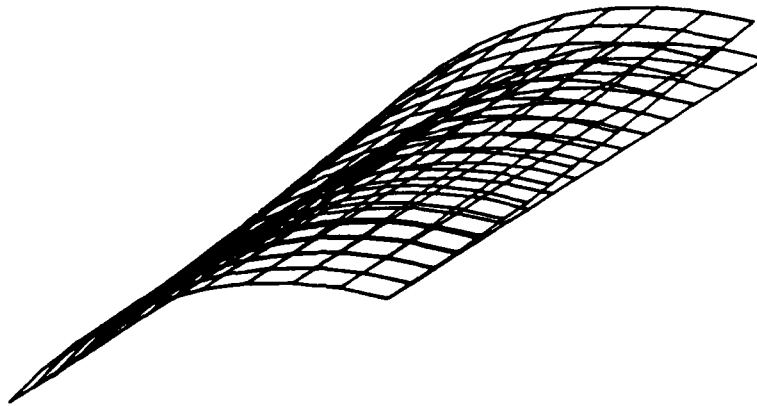
Figure 18. Mode Shape 1, Blade
No Rotational Effects

The problem of the rotating blade was analyzed for several cases and using several different methods to account for nonlinearities. In cases 1 and 2, a 10% increase in the fundamental eigenfrequency was desired, with the objective function for case 1 being minimum change and the objective function for case 2 being minimum weight. In cases 1 and 2, centrifugal effects were included in both the structural analysis and the optimization, but Coriolis effects were neglected. Results of both predictor and corrector are shown in Table 3. Note that the predictor results can be considered to be results from a linear, one-step analysis since the effect of redesign on the eigenvectors does not enter into the predictor procedure. Improvements from the predictor to corrector step show the benefit of the use of the nonlinear optimization techniques.

In Table 3, the first colum denotes the objective functions used in the predictor and
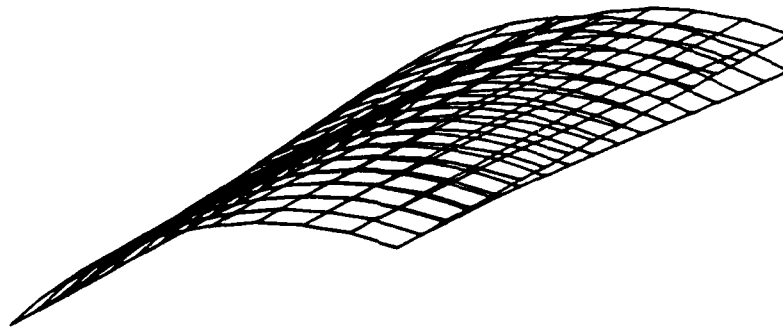
Figure 19. Mode Shape 2, Blade
No Rotational Effects

the corrector respectively. The symbol C/C denotes minimum change in both parts. If

W/W is indicated, minimum weight was used in both the predictor and corrector. The use

of W/C which symbolizes that minimum weight was used in the predictor while minimum

change was used in the corrector indicates a hybrid system (Case 3), which shall be

described later. The next column entry, ω_1, indicates the fundamental frequency for the

system. The desired frequency is denoted by ω_1^d. The fundamental frequency resulting

from the predictor geometry is indicated by ω_1^p. The percentage of the desired frequency

change accomplished by the predictor is symbolized by $\% \Delta_p$. The percent weight change

resulting from the predictor, $\% \Delta W_p$, is given in the next column. The fundamental

frequency of the corrector geometry is denoted by ω_1^c. The percentage of the desired

frequency change accomplished by the corrector is given by $\% \Delta_c$. In the final column, the
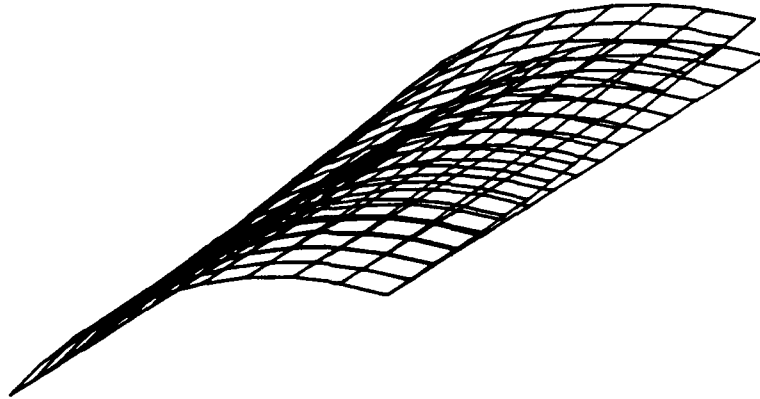
Figure 20. Mode Shape 1, Blade
Rotational Effects Included

percent weight change resulting from the corrector, $\%\Delta W_c$, is given.

Figure 22 shows the final spanwise optimized thickness of the structure for Case 1.

Figure 23 shows the final optimized shape of the structure for Case 2. Notice that in the

minimum change example, emphasis is given to adding material at the root. In the

minimum weight-minimum weight example (Case 2), all of the regions except for the root

have been reduced to the lower limit on thickness. This is the pathological case in

optimization where the system is driven to an extreme. When this is done in this example,

undesirable side effects occur, such as mode switching. The first bending mode is no longer

the fundamental frequency and the the solution to the problem in optimization is no longer

dependable. The frequency results shown for the corrector are for the bending mode:

however, this frequency is technically no longer ω_1. A way out of this quandary can be
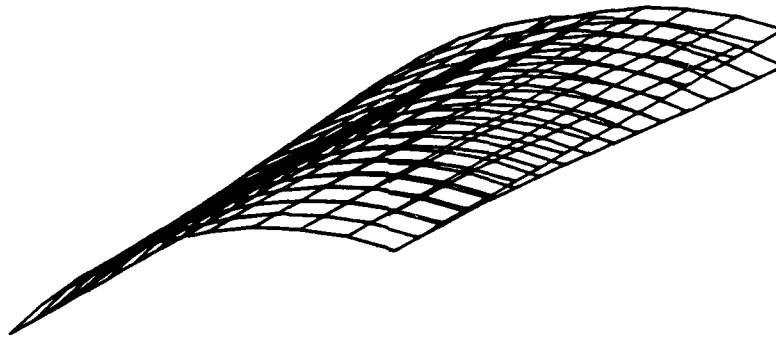
Figure 21. Mode Shape 2, Blade
Rotational Effects Included

found by a close examination of the results of the predictor. This step obtains 99% of the desired frequency change and also a weight reduction of -14%. Therefore, this solution is close to the frequency constraint, and only a small change is necessary to satisfy it. This implies that a hybrid approach involving a predictor stop with a minimum *weight* objective function and a corrector with a minimum *change* objective function could work.

The results of this hybrid step are shown in Case 3 and Figure 24. In this example, material is added at the root but proportionally less than in the minimum change-minimum change situation. Emphasis is given to removing material from the outboard regions, with most material removed from the second set of elements from the end. Since minimum weight is the objective of the predictor, it is not suprising that more material is removed in Case 3 than in the Case 1 situation.

Cases involving degradations of the solution procedure are shown in Appendix C. These were done to observe the effect of the absence of centrifugal effects on the problem in optimization.

Two other problems were studied; both involved large (30%) changes in the fundamental frequency. In Case 4, the 30% change is accomplished in one step. A second iteration is performed to obtain an improved solution (Case 5). In another situation, the 30% change is broken down into three 10% increments (Cases 6 through 8). In both of these examples, only a minimum change optimization function is used. Table 4 shows the results of the iterative procedure. The linear predictor step obtains the desired frequency change with less than 24% accuracy, but at the end of the first iteration, the desired frequency change is accomplished to within less than 1%. The second iteration is done for completeness, and gives the desired change in fundamental frequency to within $\frac{1}{100}$ of 1%.

In Table 5, each iteration obtains the desired change in frequency for that iteration to less than 1%. The final iteration, which completes the 30% change, gives the desired change to within $\frac{9}{100}$ of 1%. These two Tables show that excellent accuracy on the frequency goal is obtained, showing the feasibility of making large changes.

The use of the word "accuracy" needs some close examination. "Accuracy" has been used to describe how close the frequency change obtained by solving the problem in optimization is to the desired frequency change. This is done in terms of a discrete finite element model. An analysis was made in Appendix B of the convergence of discrete finite element models to a theoretical solution involving a nonrotating beam. This can be used to give an indication of the accuracy of the finite element model in that case. However, no such comparison to a theoretical solution is made for the rotating blade presented in this chapter. Closed-form solutions to non-abstract structural systems are difficult to obtain. Therefore, in all discussions on accuracy in this chapter, comparisons are made from one discrete model to another.

Table 3. Optimization Results for Blade, 10% Change

Case	Opt.	$\omega_1 (\times 10^3)$	$\omega_1^d (\times 10^3)$	$\omega_1^p (\times 10^3)$	$\% \Delta_p$	$\% \Delta W_p$	$\omega_1^c (\times 10^3)$	$\% \Delta_c$	$\% \Delta W_c$
1	C/C	8.38025	9.21828	9.24552	103.25	4.09	9.21976	100.18	0.025
2	W/W	8.38025	9.21828	9.21037	99.057	−14.07	8.94778	67.722	−37.31
3	W/C	8.38025	9.21828	9.21037	99.057	−14.07	9.21738	99.893	−14.03
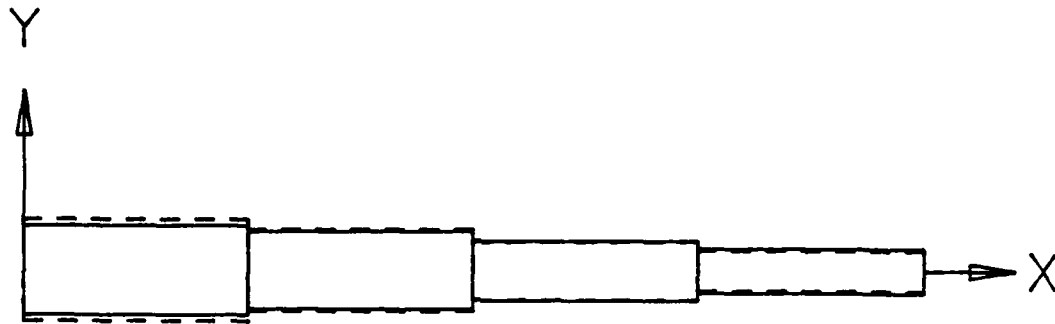
Figure 22. Optimally Redesigned Blade, Case 1
Minimum Change

Optimization Constraints

The optimizer is run iteratively, with the solution of the previous step becoming the

starting point for the succeeding step (the initial starting point is the origin). In nonlinear

mathematical programming, the approach is to minimize the objective function while

driving the equality constraint function to zero. Table 6 shows for each case the number of

iterations i required for final solution, the value of the objective function f, and the value of

the constraint λ. The solution is terminated when further iterations obtain improvements

only of less than 0.001 (Reason 1) or further iterations cause the solution to diverge, as

indicated by increasing values of objective function or constraint (Reason 2). The table also

gives the reason for termination, 1 or 2, as indicated above. Note that in no case were

more than seven iterations required.
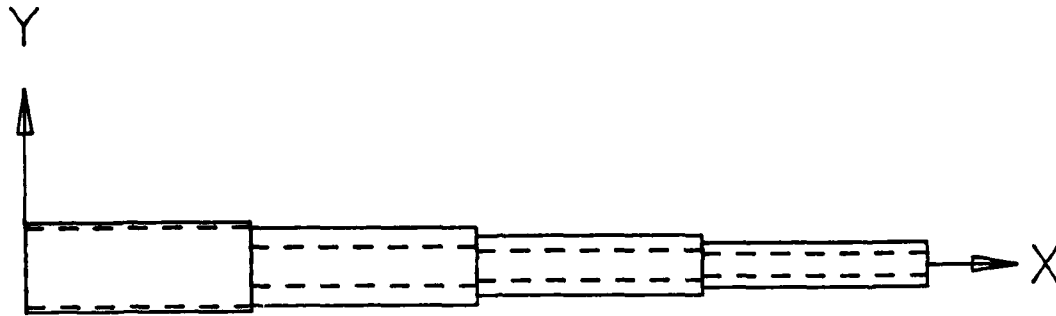
Figure 23. Optimally Redesigned Blade, Case 2
Minimum Weight

In Table 6, it is noticed that cases with a minimum *change* objective function have

the optimized value of the function λ close to zero, but cases with a minimum *weight*

objective function often have negative values. This is logical: for minimum change, low

values imply low sum of the squares of change. For minimum weight, large negative

values imply a large reduction of volume.

Rotating Beam Incorporating Coriolis Effects

The next example will consider the case of the rotating beam presented in the

prevous chapter (Figure 13) at high rotational speed. Once again, the beam will be divided

into four elements with each element composed of two subelements; one having bending

properties only and the other posessing only tension-compression properties. The rotation

speed will be 300 hz.
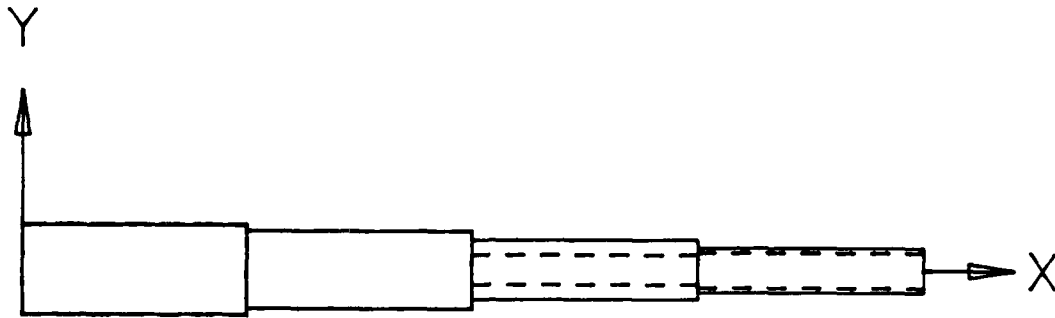
Figure 24. Optimally Redesigned Blade, Case 3
Hybrid

For this problem, the fundamental eigenfrequency without rotation is 2.093729E3

rad/sec. Figure 25 illustrates the first mode shape of the beam, a bending mode. When

centrifugal effects are included, the fundamental frequncy is 2.952001E3 rad/sec, an

increase of 40.99%. When Coriolis effects are included in addition, the fundamental

frequency drops slightly to 2.951942E3 rad/sec. The inclusion of Coriolis forces in the

rotating problem decreases the fundamental frequency by −2.00E-3% from the rotating

problem that includes centrifugal but not Coriolis effects.

Table 8 summarizes the results from the optimal redesign of the rotating beam.

The notation is the same as for the rotating blade. In Case 9, centrifugal effects are

included in both the structural analysis and in the optimization. A minimum *change*

objective was used. Case 10 was identical to case 1; however, the *hybrid* case was

**Table 4. Optimization Results for Blade, 30% Change
Iterative Procedure
Minimum Change**

Case	Opt.	ω_1 ($\times 10^3$)	ω_1^d ($\times 10^3$)	ω_1^p ($\times 10^3$)	% Δ_p	%ΔW_p	ω_1^c ($\times 10^3$)	% Δ_c	%ΔW_c
4	C/C	8.38025	10.8943	11.4736	123.04	13.72	10.9170	100.90	9.80
5	C/C	10.0170	10.8943	10.8953	100.04	9.68	10.8945	100.01	9.68

**Table 5. Optimization Results for Blade, 30% Change
Incremental Procedure
Minimum Change**

Case	Opt.	$\omega_1 (\times 10^3)$	$\omega_1^d (\times 10^3)$	$\omega_1^p (\times 10^3)$	$\% \Delta_p$	$\% \Delta W_p$	$\omega_1^c (\times 10^3)$	$\% \Delta_c$	$\% \Delta W_c$
6	C/C	8.38025	9.21828	9.24552	103.25	4.09	9.21976	100.18	0.025
7	C/C	9.21976	10.0578	10.0806	102.72	8.62	10.0687	100.11	8.46
8	C/C	10.0687	10.8967	10.9163	102.34	13.68	10.8974	100.09	13.56

Table 6. *Optimizer Parameters during Blade Solutions*

Case	i (pred.)	f (pred.)	λ (pred.)	t	i (cor.)	f (cor.)	λ (cor.)	t
1	4	1.176E0	−4.593E-1	1	4	8.725E-4	3.234E-2	1
2	4	1.176E0	−4.593E-1	1	4	−6.217E2	−1.342E-2	1
3	4	1.191E1	1.737E-1	1	4	7.732E-5	−5.828E-2	1
4	3	1.269E1	−1.815E0	2	5	2.515E-1	3.269E-3	1
5	4	5.318E-4	5.318E-4	1	3	1.162E-6	6.199E-3	1
6	4	1.176E0	−4.593E-1	1	4	8.725E-4	3.234E-2	1
7	7	9.212E-1	1.419E1	1	4	5.153E-4	1.642E-2	1
8	2	7.511E-1	−9.854E-2	1	4	3.165E-4	1.242E-2	1
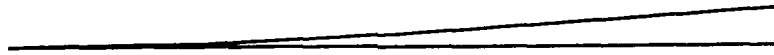
Figure 25. Mode Shape 1, Beam

analyzed incorporating a minimum *weight* objective function in the predictor and a

minimum *change* objective function in the corrector. Coriolis effects were included in Case

11 in both the structural analysis and equations of constraint. Optimization was

accomplished using a minimum *change* objective function. Figures 26 and 27 show the

final configuration of the rotating beam for Cases 9 and 10, respectively. Case 11, being a

minimum change case, shows an optimized shape similar to Figure 26.

Optimization

As in the previous section, the values for constraint functions, constraint values, and

reason for termination are given for each of the three cases in Table 8. For the cases

involving complex equations, the constraint shown is the real constraint.

Notice that the function evaluations for the minimum change objective are close to

zero, and the function evaluations for the minimum weight objective (predictor only) are

Table 7. Optimization Results for Beam, 10% Change

Case	Opt.	$\omega_1\ (\times 10^3)$	$\omega_1^d\ (\times 10^3)$	$\omega_1^p\ (\times 10^3)$	$\%\,\Delta_p$	$\%\Delta W_p$	$\omega_1^c\ (\times 10^3)$	$\%\,\Delta_c$	$\%\Delta W_c$
9	C/C	2.95200	3.24720	3.20162	84.560	2.01	3.23587	96.162	1.86
10	W/C	2.95200	3.24720	3.14233	64.476	−16.07	3.23107	94.534	−15.13
11	C/C	2.95194	3.24714	3.23506	95.910	2.63	3.24569	99.508	2.68
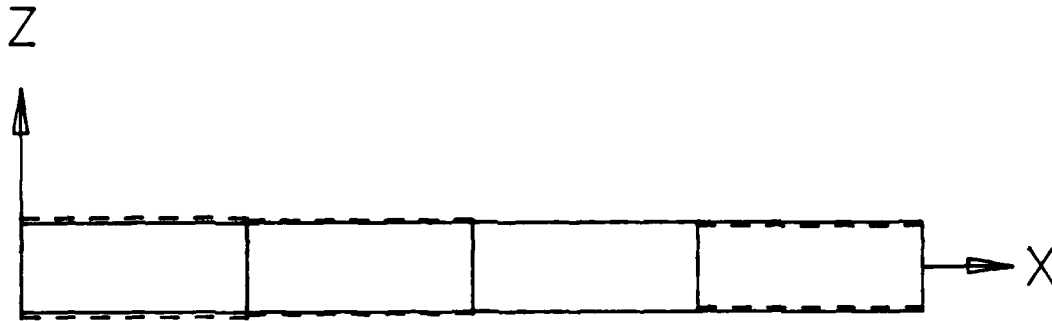
Figure 26. Optimally Redesigned Beam, Case 9

negative. They are not as big in this example as in the blade example.

Summary of Results

The predictor-corrector methods breaks the solution of the problem of nonlinear optimal redesign into two parts. The first part, the predictor, solves for the required structural changes for a given required change of frequency. In this step, the effect of structural changes on the mode shapes is not considered. Therefore, this part of the solution may be considered as a conventional linear structural analysis. In the corrector, the effect of the structural changes on the mode shapes is taken into account and the system is once again modified to obtain an improved solution.

In all of the examples involving the rotating blade, the final result of the predictor-corrector approach obtains the desired frequency change to within one percent. In the
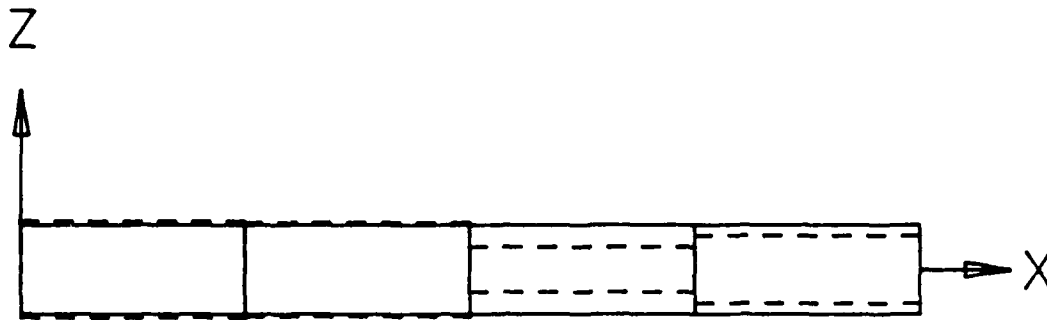
Figure 27. Optimally Redesigned Beam, Case 10

minimum change cases, the linear predictor overshoots the solution by a few percent. The corrector changes the final solution so that the eigenfrequency is at the desired value. Even for large changes, the predictor-corrector method obtains the desired solution, if suitable iteration or incrementing is done.

For the rotating beam with a *minimum weight* objective function, the linear predictor undershoots the desired frequency goal by quite a bit, as much as 35%. The corrector obtains the desired frequency to within one percent.

The rotating beam shows some other interesting results. In Case 9, the desired change is obtained to within 4%. In Case 10, there is a lot of undershoot by the predictor, but the corrector obtains the desired solution to within 6%. However, when both centrifugal and Coriolis forces are included in Case 11, the best solution is found. The linear approach gives an answer to within 5% and the corrector improves this to within 1%. The method

Table 8. Optimizer Parameters for Beam Redesign

Case	i (pred.)	f (pred.)	λ (pred.)	t	i (cor.)	f (cor.)	λ (cor.)	t
9	6	2.251E-2	−4.676E-2	1	4	4.836E-5	−1.122E-2	1
10	7	−6.242E-1	−1.094E-8	1	4	2.639E-3	1.170E-4	1
11	5	2.183E-2	−5.050E-3	1	4	2.714E-5	3.333E-4	1

used in Case 11 represents the best theoretical formulation. The equations used represent the full nonlinear structural approach with both centrifugal and Coriolis effects.

One of the reasons behind the lack of accuracy surrounding the problem of optimization with respect to minimum weight is that this optimization function in the presence of the nonlinear effects of the corrector drives most of the structure to the pathological extreme of the lower bound on thickness. This is an undesirable solution. Not only does it introduce inaccuracies that somewhat distance the frequency change from the desired value, but it also causes mode switching that results in the bending mode no longer being the fundamental mode. Since higher order modes were not tracked in this procedure, the solution to the problem in optimization is no longer valid.

Comparison with Other Methods

Queau and Trompette (1981) obtained minimum weight designs with constraints on frequency. Their method incorporated the centrifugal effects but not Coriolis. In the method implemented here, when minimum weight is employed, the second station from the free end has the minimum thickness and the end bulges out, though it remains less thick than the original design. This was also obtained by Queue and Trompette (Figure 28), with the dashed line indicating the final optimized shape.

Olhoff and Parbery (1982) examined the optimization of rotating beams with respect to frequency constraints. However, they employed lumped masses which tend to alter the optimized shape from the purely distributed mass approach. Their final shapes indicated tapering except near the region surrounding a lumped mass where bulging then occured. In work on the nonrotating beam, Karihaloo and Niordson (1973) obtained the classical tapered beam for the optimum shape of the initially uniform beam, where the first mode is of interest. This was confirmed by Olhoff and Parbery (1976) and expanded to higher order modes (Olhoff, 1977).
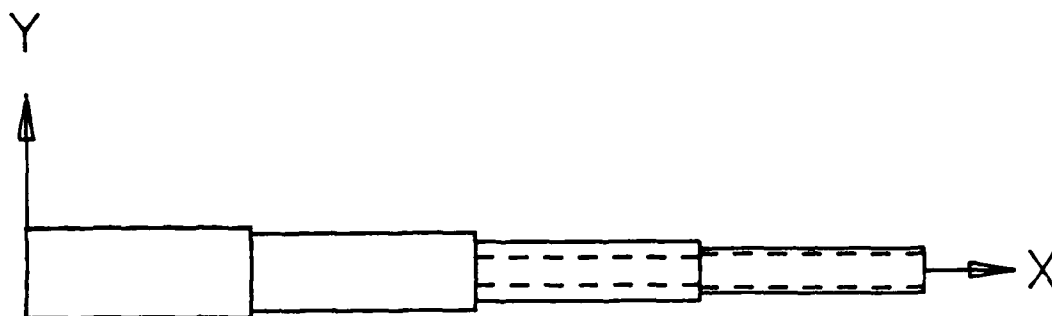
Figure 28. Rotating Blade, Optimized Shape
Queue and Trompette

CHAPTER 8

CONCLUSIONS

General Conclusions

The effect of rotation on the eigenvalues and eigenvectors of a system was successfully modeled through the use of finite element theory. Both centrifugal forces and Coriolis effects were included. The centrifugal forces in this work were treated as a static load and therefore the effect was included as a mild geometric nonlinearity in the differential stiffness matrix. The velocity-dependent Coriolis terms were formulated into a separate Coriolis matrix. These terms were found to be very small in the examples treated here. The results obtained by the finite element formulation were shown to be in close agreement to those obtained by classical means.

By far, the major rotary phenomenon affecting the fundamental eigenvalue was centrifugal force. The centrifugal effect increased the fundamental frequency of the blade and the beam by several percent. The mode shapes remained unchanged from the nonrotating system. The centrifugal forces serve to stiffen the rotating body. Coriolis forces slightly decreased the fundamental frequency. Since Coriolis forces are velocity dependent, they affected both the amplitude and phase of the eigenvector components creating a complex eigenvector problem. However, the eigenvalues remained real.

The predictor-corrector method for structural optimization using inverse perturbation was extended to incorporate centrifugal forces. To accomplish this, the element stiffness matrices were separated to isolate the effects of in-plane stiffness (membrane or extensional), bending stiffness, and differential stiffness. When the frequency constraint involved a ten percent increase in the fundamental frequency, the

linear predictor obtained the required change within two percent for the blade or five percent for the beam. The nonlinear corrector obtained a final optimized system that met the frequency constraint within one percent. Thus the predictor-corrector method for nonlinear redesign obtained excellent agreement between the desired eigenvalue and the calculated eigenvalue, when centrifugal effects were included.

When Coriolis effects were included, both the magnitude and phase of the components of the fundamental eigenvector were required to obtain the equations of constraint. This problem in complex eigenvalue analysis was also adapted to the nonlinear inverse perturbation predictor-corrector approach. The method was applied to the problem of the rotating beam. Once again, the desired frequency change was obtained to within one percent.

The problem of large frequency change (30%) was tried for the rotating blade incorporating centrifugal effects. Both an iterative and an incremental solution were accomplished. The iterative approach obtained the desired frequency almost exactly with only two iterations required. The incremental approach also achieved the desired frequency using three incremental steps. Thus it is seen that the predictor-corrector method is extraordinarily stable, obtaining even large changes with excellent correlation between the desired change in the eigenvalue and the calculated change resulting from the redesign process.

Good solutions resulting in excellent agreement between the desired frequency change and the actual frequency change always obtain when a *minimum change* objective function is used in both the predictor and the corrector. *Minimum weight* is a useful objective function for the predictor, but when it is used in the corrector, a pathological solution results with all mass concentrated at one area. This is not acceptable. Not only is this an unrealistic redesign, but the bending frequency drifts away from the desired value and mode switching may result. To correct this deficiency in the minimum weight approach, a minimum change objective function was used in the *corrector* step. This hybrid

approach combines the desired goal of minimum weight with the stability of the minimum change objective function.

The solutions calculated by the predictor-corrector method were compared to those obtained by other authors. These solutions were for minimum weight objective under a variety of frequency goals. Good correlation between the predictor-corrector method and other methods was observed.

In summary, the predictor-corrector method for optimal redesign as extended in this dissertation obtained the desired frequency changes with excellent accuracy. MSC/ NASTRAN finite element solution sequences were modified to incorporate rotary effects. DMAP and FORTRAN languages were used to implement the derived equations of constraint. Automated Design Synthesis (ADS) was used to obtain the optimum solution. The methods used were applied to several test problems, one being a curved blade with nearly one thousand degrees of freedom. In each case, the desired frequency change was obtained to within a few percent. Therefore, the approach works and can be applied to a variety of problems in optimal redesign.

Dissertation Contribution

The major contribution is the extension of the inverse perturbation method to include both centrifugal and Coriolis effects in the optimization of rotating systems under frequency constraints. Either minimum structural change or minimum weight objective functions can be employed. Excellent agreement between the desired change in the fundamental natural frequency and the actual change as determined by reanalysis was obtained in the test cases tried. Previous researchers have neglected the Coriolis effects in the optimization of rotating systems. Both magnitude and phase-dependent constraint equations were used and it was shown how the equations reduced to the conventional rotating solution in the absence of Coriolis effects.

Another original contribution is the implementation of a method for modifying an existing large scale finite element program to incorporate static stiffening loads as

observed in the rotating frame due to the centrifugal effect. In addition, a method for incorporating a global skew-symmetric Coriolis matrix in the complex modal analysis is developed. Together, these provide the eigensolution for a rotating body. The technology developed is transportable to other sites by anyone familiar with MSC/NASTRAN and DMAP.

Suggestions for Future Work

Theoretical Recommendations

Coriolis matrices for the beam element using a consistent mass approach and in a generalized coordinate system should be obtained, as should Coriolis matrices for other elements. The problem of maximizing the differences between eigenvalues, as identified by Olhoff and Parbery (1982), should be analyzed. This is important in problems where several eigenvalues are tracked in the redesign process with emphasis given to the difference between the eigenvalues.

Practical Recommendations

The finite element method employed in this work should be generalized to include more types of elements, such as higher-order plates. A general problem incorporating several different elements should be tried. This would permit the analysis of a real-world, built up structure such as a helicopter blade. An improved method of incorporating element Coriolis matrices into the global problem within the context of existing finite element programs should be devised. This should be done so that the employment of a Coriolis matrix in complex dynamic analysis would be transparent to the user and would permit the automated analysis of the dynamic problem including all rotational effects.

APPENDICES

APPENDIX A

COMPUTER IMPLEMENTATION

Implementation of the predictor-corrector method to rotational problems is accomplished by a combination of the MSC/NASTRAN program, the ADS program and FORTRAN programming. MSC/NASTRAN is used to accomplish structural analysis, both static and modal, and generates the structural matrices (McNeal 1984). FORTRAN programs are used to transform the structural matrices from MSC/NASTRAN into a format usable for general analysis. Then, Direct Matrix Abstraction Programming (DMAP) is used to generate the equations of equality constraint. Optimization is done by use of the ADS program (Vanderplaats, 1983).

Figure 11 shows the flow diagram for the predictor step. The finite element analysis is accomplished in two steps. First the static solution of MSC/NASTRAN, SOL 24, is run to generate the differential stiffness matrix (MacNeal, 1981). This matrix is then *checkpointed to the restart tape.* Then SOL 3 is run for the real modal analysis case (or, alternatively, SOL 28 is run for the complex eigenvalue problem). The problem is run as a restart and the differential stiffness matrix is read from the "old problem tape" (Joseph, 1984). In both the static and dynamic runs, the mass, stiffness, differential stiffness, and eigenvector matrices are written on tape in FORTRAN compatible binary via OUTPUT4. For the complex run, the Coriolis matrix is also stored. However, MSC/NASTRAN does not itself have Coriolis factors. These must be generated by a FORTRAN program. The Coriolis matrix is output by OUTPUT4 so that it can be processed by the same programs as are the other matrices. Finally, a nonrotating dynamic solution is done. This is done to generate the nonrotating eigenvalues and also to produce the global to basic system transformation matrices on an OUTPUT2 tape. These matrices are located in the KDICT table.

The following DMAP ALTER is used in SOL 24 to generate the differential stiffness matrix. Note that first the static displacment caused by the centrifugal forces is obtained

and then this is fed back into the EMG processor to get the element differential stiffness

matrices (Gockel, 1984). OUTPUT4 is then used to put on tape the matrix of the element

stiffness, differential stiffness, and mass matrices.

```
SOL 24 $STATIC ANALYSIS
CHKPNT YES
DIAG 4,8,14
ALTER 33
OUTPUT4 KELM,MELM//0/8 $
TABPT SIL// $
MATPRN CSTM// $
ALTER 30
PRTPARM ////1 $
ALTER 97
PRTPARM ////1 $
ALTER 160
EMG EST,CSTM,MPT,DIT,,UGV,ETT,EDT/KDELM,KDDICT,,,,/1/0/0/
///-1/-1//////////K6ROT $
CHKPNT KDELM,KDDICT $
OUTPUT4 KDELM//0/8 $
TABPT KDDICT,,,,// $
EMA GPECT,KDDICT,KDELM,BGPDT,SIL,CSTM/KDNN,/-1 $
CHKPNT KDNN $
EQUIV KDNN,KDFF/SINGLE $
CHKPNT KDFF $
COND LBL3D,SINGLE $
SCE1 USET,KDNN,,,/KDFF,KDFS,,,, $
CHKPNT KDFF,KDFS $
LABEL LBL3D $
EQUIV KDFF,KDAA/OMIT $
CHKPNT KDAA $
COND LBL5D,OMIT $
SMP2 USET,GO,KDFF/KDAA $
CHKPNT KDAA $
LABEL LBL5D $
ADD KDAA,KAA/KTOT/C,N,(1.0,0.0)/C,N,(1.0,0.0) $
CHKPNT KTOT $
ENDALTER
CEND
```

This following DMAP is used to modify SOL 3 to produce the real modal solution for

the rotating problem incorporating differential stiffness. The matrix of eigenvectors

created is written on tape by OUTPUT4.

```
SOL 3 $REAL MODAL ANALYSIS
DIAG 4,8,14
ALTER 395
PRTPARM ////1 $
ADD KDAA,KAA/KNEW/C,N,(1.0,0.0)/C,N,(1.0,0.0) $
EQUIV KNEW,KAA/ALWAYS $
```

```
ALTER 448
OUTPUT4 UGV,,,,//0/8 $
ENDALTER
CEND
```

For the complex case with Coriolis effects, the following is used to alter SOL 28.

The global Coriolis matrix is read via INPUTT4. Once again, OUTPUT4 is used to write

the eigenvectors on tape.

```
SOL 28 $COMPLEX MODAL ANALYSIS
DIAG 4,8,14
ALTER 66
INPUTT4 /BCOR,,,,/1/8/0 $
MATPRN BCOR// $
EQUIV BCOR,BGGX/ALWAYS $
SETVAL //V,N,NOBGGX/0 $
ALTER 392
PRTPARM ////1 $
ADD KDAA,KAA/KNEW/C,N,(1.0,0.0)/C,N,(1.0,0.0) $
EQUIV KNEW,KAA/ALWAYS $
ALTER 409
MATPRN KDXX,BDXX,MDXX// $
ALTER 456
OUTPUT4 UGV,,,,// - 1/8 $
MATPRN UGV// $
ENDALTER
CEND
```

In applying the method described above in MSC/NASTRAN, it is first necessary to

divide the structural elements in the finite element model into two elements: one with only

in-plane (membrane or rodlike) stiffness and one with only out-of-plane (bending) stiffness.

These elements are then superimposed. The element stiffness matrices, created by DMAP

module EMG, reside in triangularized form as individual columns in the matrix KELM.

Dividing up the elements results in a separate column in KELM for in-plane and bending

properties for each superimposed composite element. This permits multiplication of the

column representing membrane properties by a linear element change factor while the

column containing the bending properties can be altered by a nonlinear change factor.

These manipulations may be done by selective use of the MATMOD DMAP module.

In the MSC/NASTRAN static solution procedure, SOL 24, each element stiffness

matrix and element mass matrix has its upper triangular and diagonal components stored

as a column in the assembled system matrices KELM and MELM, respectively. To

accomplish optimal redesign it is first necessary to checkpoint these matrices and write

them to FORTRAN readable on disk using OUTPUT4. CBAR elements have element

matrices are already in the basic coordinate system; therefore, no coordinate

transformation is necessary in order to redesign. It is necessary, however, to regenerate

the full symmetric stiffness and mass matrices for each element. This is done by a

FORTRAN postprocessor.

After the initial structural problem is solved, the constants in the equation for the

frequency constraint must be obtained. First, the element matrices which are output by

MSC/NASTRAN in diagonalized form are repacked into full matrices by FORTRAN

programming. Then, these matrices are used by a DMAP sequence to obtain the equation

components. This set of DMAP steps is shown below for the case with no Coriolis forces.

```
ID GANS,BRONZ3
TIME 30
DIAG 4,14
BEGIN $
FILE EMAT=APPEND $
$ THIS DMAP COMPUTES THE COMPONENTS FOR THE PREDICTOR STEP
$ FOR THE BRONZ PROBLEM.
$ IT INVOLVES 8 CBAR ELEMENTS
PARAMR //MPY/V,N,OMEGA2/V,Y,OMEGA/V,Y,OMEGA/ $ SQUARE OMEGA
PARAMR //C,N,COMPLEX//V,N,OMEGA2/0.0/V,N,LAMA/ $ CHANGE
$ OMEGA2 TO COMPLEX
PRTPARM // $
$ THE NEXT SECTION INVOLVES THE CQUAD ELEMENTS
LABEL L2 $
INPUTT4 /K1,M1,D1,UGV1,/4/8/0 $ READ IN MATRICES
ADD K1,/K1M/1.0/ $ CUBIC APPROXIMATIONS ALREADY ACCOMPLISHED
ADD K1M,D1/K1N/ $ ADD IN DIFF STIFFNESS FOR EXTENSIONAL ELMTS
SMPYAD UGV1,K1N,UGV1,,,/A2/3/1/1/0/1/ $ GET COMPONENTS FOR REDES
SMPYAD UGV1,M1,UGV1,,,/YY2/3/1/1/0/1/ $ GET COMPONENTS FOR REDESIGN
ADD YY2,/B2/LAMA/ $ MULTIPLY YY1 BY LAMA
ADD A2,B2/C2/1.0/-1.0/ $ SUBTRACT MASS FROM STIFFNESS COMPONENTS
ADD C2,/E2/C,Y.MINV=1.0/ $ DIVIDE BY GENERALIZED MASS
$MATPRN E2// $ PRINT OUT RESULTS
APPEND E2,/EMAT/2 $
REPT L2,7 $
OUTPUT4 EMAT,,,,//-1/8 $
MATPRN EMAT// $
END $
CEND
TITLE=ASSEMBLY OF MATRICES INTO HOFF'S EQ. IV.19
```

```
SUBTITLE=FOR BRONZ PROBLEM
BEGIN BULK
PARAM*  OMEGA        2.952001E3
PARAM*  MINV         8.955021E3
ENDDATA
```

When the Coriolis case is used, there are two equations of constraint. One set

relates the real components to each other. These are the magnitude-like factors. The

other equation relates the imaginary components to each other. These are the phase-like

factors. The first set of DMAP creates the real constraint. The second set generates the

imaginary constraint.

```
ID GANS,BRONZ45A
TIME 30
DIAG 4,14
BEGIN $
FILE EMAT=APPEND $
$ THIS DMAP COMPUTES THE COMPONENTS FOR THE PREDICTOR STEP
$ FOR THE BRONZ PROBLEM 1ST EQUATION
$ IT INVOLVES 8 CBAR ELEMENTS
PARAMR //MPY/V.N,OMEGA2/V,Y,OMEGA/V,Y,OMEGA/ $ SQUARE OMEGA
PARAMR //C,N,COMPLEX//V,N,OMEGA2/0.0/V,N,LAMA/ $ CHANGE OMEGA2 TO
$COMPLEX
PARAMR //C,N,COMPLEX//V,Y,OMEGA/0.0/V,N,OMEGAC/ $CHANGE OMEGA TO
$CMPLX
PRTPARM // $
$ THE NEXT SECTION INVOLVES THE CBAR ELEMENTS
LABEL L2 $
INPUTT4 /K1,M1,D1,,/3/8/0 $ READ IN MATRICES
INPUTT4 /UGVR1,UGVI1,B1,,/3/8/0 $ READ IN MATRICES
MATPRN K1,M1,D1// $
MATPRN UGVR1,UGVI1,B1// $
ADD K1,/K1M/1.0/ $ CUBIC APPROXIMATIONS ALREADY ACCOMPLISHED
ADD K1M.D1/K1N/ $ ADD IN DIFF STIFFNESS FOR EXTENSIONAL ELMTS
SMPYAD UGVR1,K1N.UGVR1,,,/A2/3/1/1/0/1/ $ GET COMPONENTS FOR REDES
SMPYAD UGVR1.M1.UGVR1,,,/YY2/3/1/1/0/1/ $ GET COMPONENTS FOR REDESIGN
SMPYAD UGVI1.M1.UGVI1,,,/XX2/3/1/1/0/1/ $
SMPYAD UGVI1.K1N.UGVI1.,,/WW2/3/1/1/0/1/ $ GET COMPONENTS FOR
$REDESIGN
ADD YY2.XX2/Y2/1.0/-1.0 $
ADD Y2,/B2/LAMA/ $ MULTIPLY YY1 BY LAMA
ADD A2,WW2/CC2/1.0/-1.0/ $ SUBTRACT MASS FROM STIFFNESS COMPONENTS
ADD CC2,B2/E2/1.0/-1.0/ $ SUBTRACT CORIOLIS
APPEND E2,/EMAT/2 $
REPT L2,7 $
INPUTT4 /UGVR,UGVI,KGGX,,/3/8/0 $ READ IN DISPL AND CORIOLIS MATRICES
INPUTT4 /MGGX,KDNN,BCOR,,/3/8/0 $ READ IN MORE MATRICES
MATPRN MGGX// $
SMPYAD UGVI,BCOR.UGVI,,,/T1/3/1/1/0/1/ $ GET COMPONENTS FOR RHS
SMPYAD UGVR,MGGX,UGVR,,,/VV1/3/1/1/0/1/ $ GET COMPONENST
```

```
SMPYAD UGVI,MGGX,UGVI,,,/VV2/3/1/1/0/1/ $
ADD VV1,VV2/V1/1.0/-1.0 $
MATPRN T1,V1// $
OUTPUT4 EMAT,,,,//-1/8 $
MATPRN EMAT// $
END $
CEND
TITLE=ASSEMBLY OF MATRICES INTO GANS EQUATION 1
SUBTITLE=FOR BRONZ PROBLEM WITH CORIOLIS, PREDICTOR
BEGIN BULK
PARAM*  OMEGA        2.951942E3
ENDDATA

ID GANS,BRONZ45B
TIME 30
DIAG 4,14
BEGIN $
FILE EMAT=APPEND $
$ THIS DMAP COMPUTES THE COMPONENTS FOR THE PREDICTOR STEP
$ FOR THE BRONZ PROBLEM 2ND EQUATION
$ IT INVOLVES 8 CBAR ELEMENTS
PARAMR //MPY/V,N,OMEGA2/V,Y,OMEGA/V,Y,OMEGA/ $ SQUARE OMEGA
PARAMR //C,N,COMPLEX//V,N,OMEGA2/0.0/V,N,LAMA/ $ CHANGE OMEGA2 TO
$COMPLEX
PARAMR //C,N,COMPLEX//V,Y,OMEGA/0.0/V,N,OMEGAC/ $CHANGE OMEGA TO
$CMPLX
PRTPARM // $
$ THE NEXT SECTION INVOLVES THE CBAR ELEMENTS
LABEL L2 $
INPUTT4 /K1,M1,D1,,/3/8/0 $ READ IN MATRICES
INPUTT4 /UGVR1,UGVI1,B1,,/3/8/0 $ READ IN MATRICES
ADD K1,/K1M/1.0/ $ CUBIC APPROXIMATIONS ALREADY ACCOMPLISHED
ADD K1M,D1/K1N/ $ ADD IN DIFF STIFFNESS FOR EXTENSIONAL ELMTS
SMPYAD UGVR1,K1N,UGVI1,,,/A2T/3/1/1/0/1/ $ GET COMPONENTS FOR REDES
ADD A2T,/A2/2.0/ $ DOUBLE A2T
SMPYAD UGVR1,M1,UGVI1,,,/YY2T/3/1/1/0/1/ $ GET COMPONENTS FOR
$REDESIGN
ADD YY2T,/YY2/2.0/ $
SMPYAD UGVR1,B1,UGVR1,,,/ZZ2/3/1/1/0/1/ $ GET COMPONENTS FOR REDESIGN
SMPYAD UGVI1,B1,UGVI1,,,/XX2/3/1/1/0/1/ $
ADD ZZ2,XX2/ZZ3
ADD YY2,/B2/LAMA/ $ MULTIPLY YY1 BY LAMA
ADD ZZ3,/Z2/OMEGAC/ $ MULTIPLY ZZ3 BY OMEGAC
ADD A2,B2/CC2/1.0/-1.0/ $ SUBTRACT MASS FROM STIFFNESS COMPONENTS
ADD CC2,Z2/E2/1.0/1.0/ $ ADD CORIOLIS
$MATPRN A2,B2,Z2// $ PRINT OUT RESULTS
APPEND E2,/EMAT/2 $
REPT L2,7 $
INPUTT4 /UGVR,UGVI,KGGX,,/3/8/0 $ READ IN DISPL AND CORIOLIS MATRICES
INPUTT4 /MGGX,KDNN,BCOR,,/3/8/0 $ READ IN MORE MATRICES
SMPYAD UGVR,BCOR,UGVR,,,/TT1/3/1/1/0/1/ $ GET COMPONENTS FOR RHS
SMPYAD UGVI,BCOR,UGVI,,,/TT2/3/1/1/0/1/ $
ADD TT1,TT2/T1 $
SMPYAD UGVR,MGGX,UGVI,,,/VV1/3/1/1/0/1/ $
```

```
ADD VV1,/V1/2.0 $
MATPRN T1,V1// $ OUTPUT RESULT
OUTPUT4 EMAT,,,,//-1/8 $
MATPRN EMAT// $
END $
CEND
TITLE=ASSEMBLY OF MATRICES INTO GANS EQUATION 2
SUBTITLE=FOR BRONZ PROBLEM WITH CORIOLIS, PREDICTOR
BEGIN BULK
PARAM*  OMEGA       2.951942E3
ENDDATA
```

Once the equations of constraint are obtained, the problem in optimization is ready

to be run. This is done by the use of a FORTRAN program that calls the ADS program,

which is the optimizer (Vanderplaats 1985). The objective function can be either minimum

weight or minimum change. This produces the values for the element change factors α_e

and hence the thicknesses of the predictor system. An intermediate finite element analysis

is then done to generate new system matrices and eigenvectors. This is the conclusion of

the predictor step. As stated in Chapter 6, the predictor results represent a linear solution

of the problem in optimization.

In the corrector, the MSC/NASTRAN finite element analysis represented by the

last step of the predictor becomes the first step of the corrector. The structural matrices so

created are used in a corrector DMAP to produce the energy balance constraint equation.

For the case involving no Coriolis forces, there is one constraint equation. When Coriolis

effects are included, there are two equations. The following DMAP represent the steps

necessary for the real case.

```
ID GANS.BRONZ7
TIME 30
DIAG 4,14
BEGIN $
FILE EMAT=APPEND $
$ THIS DMAP COMPUTES THE COMPONENTS FOR THE CORRECTOR STEP
$ FOR THE BRONZ PROBLEM. IT INVOLVES
$ 8 CBAR ELEMENTS.
PARAMR //MPY/V,N,OMEGA2/V,Y,OMEGA/V,Y,OMEGA/ $ SQUARE OMEGA
PARAMR //C,N,COMPLEX//V,N,OMEGA2/0.0/V,N,LAMA/ $ CHANGE OMEGA2|
$ TO COMPLEX
PRTPARM // $
$ THE NEXT SECTION INVOLVES THE CQUAD ELEMENTS
LABEL L2 $
```

```
INPUTT4 /K1,M1,D1,UGV1,/4/8/0 $ READ IN MATRICES
$MATPRN K1,M1,D1,UGV1// $
ADD K1,/K1M/1.0/ $ CUBIC APPROXIMATION ALREADY ACCOMPLISHED
ADD K1M,D1/K1N/ $ ADD IN DIFF STIFFNESS FOR EXTENSIONAL ELMTS
SMPYAD UGV1,K1N,UGV1,,,/A2/3/1/1/0/1/ $ GET COMPONENTS FOR REDES
SMPYAD UGV1,M1,UGV1,,,/YY2/3/1/1/0/1/ $ GET COMPONENTS FOR REDESIGN
ADD YY2,/B2/LAMA/ $ MULTIPLY YY1 BY LAMA
ADD A2,B2/E2/1.0/-1.0/ $ SUBTRACT MASS FROM STIFFNESS COMPONENTS
$ MATPRN E2// $ PRINT OUT RESULTS
APPEND E2,/EMAT/2 $
REPT L2,7 $
$ THE NEXT SECTION COMPUTES THE RHS OF THE
$ CORRECTOR EQUATION
$ THE FOLLOWING MATRICES ARE OUTPUT FROM THE WHITE6
$ PROBLEM AND STUCK ON THE END OF THE RESULTS OF REPAK.FOR
INPUTT4 /UGV,KGGX,MGGX,KDNN,/4/8/0 $
$MATPRN UGV,KGGX,MGGX,KDNN// $
MATMOD UGV,,,,,/UGV1,/1/C,Y,COLNUM=1 $
$MATPRN UGV1// $
SMPYAD UGV1,MGGX,UGV1,,,/E3/3/////1 $
ADD KGGX,KDNN/KNEW/1.0/1.0 $
EQUIV KNEW,KGGX/ALWAYS $
$MATPRN KGGX// $
SMPYAD UGV1,KGGX,UGV1,,,/F/3/////1 $
ADD E3,/E/LAMA $
ADD E,F/G/1.0/-1.0 $
OUTPUT4 EMAT,,,,//-1/8 $
MATPRN E,F,G,EMAT// $
END $
CEND
TITLE=ASSEMBLY OF MATRICES INTO CORRECTOR
SUBTITLE=FOR GRAY PROBLEM, 2ND 10% CHANGE
BEGIN BULK
PARAM*  OMEGA          3.247201E3
ENDDATA
```

This next DMAP is the program for running the problem involving Coriolis forces.

```
ID GANS,BRONZ49A
TIME 30
DIAG 4,14
BEGIN $
FILE EMAT=APPEND $
$ THIS DMAP COMPUTES THE COMPONENTS FOR THE CORRECTOR STEP
$ FOR THE BRONZ PROBLEM. IT INVOLVES
$ 8 CBAR ELEMENTS.
PARAMR //MPY/V,N,OMEGA2/V,Y,OMEGA/V,Y,OMEGA/ $ SQUARE OMEGA
PARAMR //C,N,COMPLEX//V,N,OMEGA2/0.0/V,N,LAMA/ $ CHANGE OMEGA2 TO
$COMPLEX
PARAMR //C,N,COMPLEX//V,Y,OMEGA/0.0/V,N,OMEGAC/ $ CHANGE OMEGA
PRTPARM // $
$ THE NEXT SECTION INVOLVES THE CQUAD ELEMENTS
LABEL L2 $
INPUTT4 /K1,M1,D1,,/3/8/0 $ READ IN MATRICES
```

```
INPUTT4 /UGVR1,UGVI1,B1,,/3/8/0 $ READ IN MATRICES
$MATPRN K1,M1,D1// $
$MATPRN UGVR1,UGVI1,B1// $
ADD K1,/K1M/1.0/ $ CUBIC APPROXIMATION ALREADY ACCOMPLISHED
ADD K1M,D1/K1N/ $ ADD IN DIFF STIFFNESS FOR EXTENSIONAL ELMTS
SMPYAD UGVR1,K1N,UGVR1,,,/A2A/3/1/1/0/1/ $ GET COMPONENTS FOR REDES
SMPYAD UGVI1,K1N,UGVI1,,,/A2B/3/1/1/0/1/ $
ADD A2A,A2B/A2/1.0/-1.0 $
SMPYAD UGVR1,M1,UGVR1,,,/YY2A/3/1/1/0/1/ $ GET COMPONENTS FOR
$REDESIGN
SMPYAD UGVI1,M1,UGVI1,,,/YY2B/3/1/1/0/1/ $
ADD YY2A,YY2B/YY2/1.0/-1.0 $
ADD YY2,/B2/LAMA/ $ MULTIPLY YY1 BY LAMA
ADD A2,B2/E2/1.0/-1.0/ $ SUBTRACT MASS FROM STIFFNESS COMPONENTS
$MATPRN A2,B2,Z2// $ PRINT OUT RESULTS
APPEND E2,/EMAT/2 $
REPT L2,7 $
$ THE NEXT SECTION COMPUTES THE RHS OF THE
$ CORRECTOR EQUATION
$ THE FOLLOWING MATRICES ARE OUTPUT FROM THE WHITE6
$ PROBLEM AND STUCK ON THE END OF THE RESULTS OF REPAK.FOR
INPUTT4 /UGVR,UGVI,BCOR,,/3/8/0 $
INPUTT4 /KGGX,MGGX,KDNN,,/3/8/0 $
$MATPRN KGGX,MGGX,KDNN,BCOR// $
$MATPRN UGV1// $
SMPYAD UGVR,MGGX,UGVR,,,/E3A/3/1/1/0/1 $
SMPYAD UGVI,MGGX,UGVI,,,/E3B/3/1/1/0/1 $
ADD E3A,E3B/E3/1.0/-1.0 $
ADD KGGX,KDNN/KNEW/1.0/1.0 $
EQUIV KNEW,KGGX/ALWAYS $
$MATPRN KGGX// $
SMPYAD UGVR,KGGX,UGVR,,,/FA/3/1/1/0/1 $
SMPYAD UGVI,KGGX,UGVI,,,/FB/3/1/1/0/1 $
ADD FA,FB/F/1.0/-1.0 $
ADD E3,/E/LAMA $
ADD E,F/I/1.0/-1.0 $
OUTPUT4 EMAT,,,,//-1/8 $
MATPRN E,F,I,EMAT// $
END $
CEND
TITLE=ASSEMBLY OF MATRICES INTO CORRECTOR EQUATION 1
SUBTITLE=FOR BRONZ PROBLEM, MIN STRUCT CHANGE, CORIOLIS
BEGIN BULK
PARAM*  OMEGA           3.247136E3
ENDDATA

ID GANS,BRONZ49B
TIME 30
DIAG 4,14
BEGIN $
FILE FMAT=APPEND $
$ THIS DMAP COMPUTES THE COMPONENTS FOR THE CORRECTOR STEP
$ FOR THE BRONZ PROBLEM. IT INVOLVES
$ 8 CBAR ELEMENTS.
```

```
PARAMR //MPY/V,N,OMEGA2/V,Y,OMEGA/V,Y,OMEGA/ $ SQUARE OMEGA
PARAMR //C,N,COMPLEX//V,N,OMEGA2/0.0/V,N,LAMA/ $ CHANGE OMEGA2 TO
$COMPLEX
PARAMR //C,N,COMPLEX//V,Y,OMEGA/0.0/V,N,OMEGAC/ $ CHANGE OMEGA
PRTPARM // $
$ THE NEXT SECTION INVOLVES THE CQUAD ELEMENTS
LABEL L2 $
INPUTT4 /K1,M1,D1,,/3/8/0 $ READ IN MATRICES
INPUTT4 /UGVR1,UGVI1,B1,,/3/8/0 $ READ IN MATRICES
$MATPRN K1,M1,D1// $
$MATPRN UGVR1,UGVI1,B1// $
ADD K1,/K1M/1.0/ $ CUBIC APPROXIMATION ALREADY ACCOMPLISHED
ADD K1M,D1/K1N/ $ ADD IN DIFF STIFFNESS FOR EXTENSIONAL ELMTS
SMPYAD UGVR1,K1N,UGVI1,,,/A2T/3/1/1/0/1/ $ GET COMPONENTS FOR REDES
ADD A2T,/A2/2.0 $
SMPYAD UGVR1,M1,UGVI1,,,/YY2T/3/1/1/0/1/ $ GET COMPONENTS FOR
$REDESIGN
ADD YY2T,/YY2/2.0 $
SMPYAD UGVR1,B1,UGVR1,,,/ZZ2A/3/1/1/0/1/ $ GET COMPONENTS FOR REDES
SMPYAD UGVI1,B1,UGVI1,,,/ZZ2B/3/1/1/0/1/ $
ADD ZZ2A,ZZ2B/ZZ2/ $
ADD YY2,/B2/LAMA/ $ MULTIPLY YY1 BY LAMA
ADD ZZ2,/Z2/OMEGAC/ $ MULTIPLY ZZ2 BY OMEGAC
ADD A2,B2/C2/1.0/-1.0/ $ SUBTRACT MASS FROM STIFFNESS COMPONENTS
ADD C2,Z2/E2/1.0/1.0/ $ ADD CORIOLIS TERMS
$MATPRN A2,B2,C2,Z2// $ PRINT OUT RESULTS
APPEND E2,/FMAT/2 $
REPT L2,7 $
$ THE NEXT SECTION COMPUTES THE RHS OF THE
$ CORRECTOR EQUATION
$ THE FOLLOWING MATRICES ARE OUTPUT FROM THE WHITE6
$ PROBLEM AND STUCK ON THE END OF THE RESULTS OF REPAK.FOR
INPUTT4 /UGVR,UGVI,BCOR,,/3/8/0 $
INPUTT4 /KGGX,MGGX,KDNN,,/3/8/0 $
MATPRN KGGX,MGGX,KDNN,BCOR// $
$MATPRN UGV1// $
SMPYAD UGVR,MGGX,UGVI,,,/E3T/3/1/1/0/1 $
ADD E3T,/E3/2.0 $
ADD KGGX,KDNN/KNEW/1.0/1.0 $
EQUIV KNEW,KGGX/ALWAYS $
$MATPRN KGGX// $
SMPYAD UGVR,KGGX,UGVI,,,/FT/3/1/1/0/1 $
ADD FT,/F/2.0 $
ADD E3,/E/LAMA $
SMPYAD UGVR,BCOR,UGVR,,,/H3A/3/1/1/0/1 $
SMPYAD UGVI,BCOR,UGVI,,,/H3B/3/1/1/0/1 $
ADD H3A,H3B/H3/ $
ADD H3,/H/OMEGAC $
ADD E,F/I/1.0/-1.0 $
ADD I,H/G/1.0/-1.0 $
OUTPUT4 FMAT,,,,//-1/8 $
MATPRN E,F,H,G,FMAT// $
END $
CEND
```

```
TITLE=ASSEMBLY OF MATRICES INTO CORRECTOR EQUATION 1
SUBTITLE=FOR BRONZ PROBLEM, MIN STRUCT CHANGE, CORIOLIS
BEGIN BULK
PARAM*  OMEGA          3.247136E3
ENDDATA
```

Next, the optimization step for the corrector is run. The objective function in this part is either minimum change or minimum weight.

Once the corrected values of α_e are obtained, the element thicknesses for the system can be calculated. Then, another finite element analysis is run. This is required for the intermediate iterative or incremental steps, but otherwise it is only used to check the final, optimized solution.

APPENDIX B

BEAM SOLUTIONS

Derivation of Exact Solution for Beam Vibration

In this Appendix, the exact solution for the nonrotating beam problem posed in Chapter 4 will be obtained. Figure 29 illustrates the problem being considered: it is the planar problem of a (nonrotating) beam of constant section with one end clamped and the other end mounted on a roller that permits only vertical (y-axis) displacements and no rotations. The beam has modulus of elasticity E, moment of inertia I, length L, linear mass density m, density ρ, and cross-sectional area A. Let ω be the eigenfrequency of the structure and Y(x) denote the vertical displacement as a function of beamwise distance x.
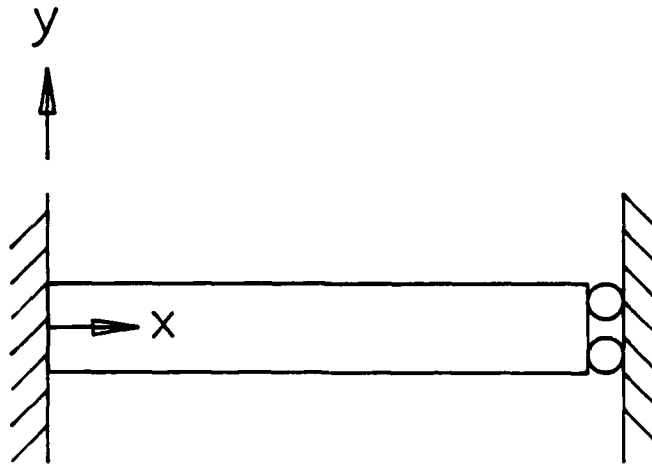

Figure 29. Rotating Beam

The governing differential equation for this problem is:

$$\frac{d^2}{dx^2}\left[EI\frac{d^2Y(x)}{dx^2}\right] = \omega^2 mY(x) \tag{B.1}$$

The boundary conditions are:

$$Y(0) = 0$$

$$Y'(0) = 0$$

$$Y'(L) = 0$$

$$Y''(L) = 0$$

Defining:

$$\beta^4 = \frac{\omega^2 m}{EI} \tag{B.2}$$

and noting that both E and I are constant in this problem obtains a new version of the differential equation:

$$\frac{d^4Y(x)}{dx^4} - \beta^4 Y(x) = 0 \tag{B.3}$$

The solution to the above equation may be assumed to be of the form:

$$Y(x) = C_1 \sin\beta x + C_2 \cos\beta x + C_3 \sinh\beta x + C_4 \cosh\beta x \tag{B.4}$$

Taking derivatives of Equation (B.4) and applying the boundary conditions results in the following matrix equation where the unknowns are the C_i constants.

$$\begin{bmatrix} 0 & 1 & 0 & 1 \\ 1 & 0 & 1 & 0 \\ \cos\beta L & -\sin\beta L & \cosh\beta L & \sinh\beta L \\ -\cos\beta L & \sin\beta L & \cosh\beta L & \sinh\beta L \end{bmatrix} \begin{bmatrix} C_1 \\ C_2 \\ C_3 \\ C_4 \end{bmatrix} = \{0\} \tag{B.5}$$

For Equation (B.5) to have a nontrivial solution, the matrix on the left-hand side of the equation must have zero determinant. Solving for the first mode one obtains:

$$\beta L = 2.4259 \tag{B.6}$$

Substituting for β, one obtains the following expression for ω:

$$\omega = 5.8850 \left[\frac{EI}{mL^4} \right]^{(1/2)} \tag{B.7}$$

For this problem, the beam is made of IN-718 steel, with E of 73.77E3 MPa, I equal to 3.2252E4 mm^4, A equal to 625 mm^2, ρ of 2.774E-9 Mg/mm^3, L equal to 250 mm, and m calculated to be 1.73375E-6 Mg/mm. Using these values, the fundamental eigenfrequency ω_1 is given as:

$$\omega_1 = 3.5043\text{E3 rad/sec}$$
$$= \omega_1(\text{theoretical})$$

This is the value used to calibrate the finite element model for the rotating beam. Convergence of ω_1 as determined by MSC/NASTRAN finite element analysis to the theoretical value, as the model is refined, is shown in Chapter 6, Table 1.

Derivation of Tangent Stiffness Matrix

The nonlinear problem under consideration in this dissertation is called *geometric nonlinearity* and the equations of equilibrium must be reformulated for the deformed configuration. An incremental procedure can then be used to obtain a tangent stiffness matrix (Przemieniecki, 1985).

For a linear elastic material, the relationship between stress $\{\sigma\}$ and strain $\{\epsilon\}$ is given by:

$$\{\sigma\} = [G]\{\epsilon\} \tag{B.8}$$

where [G] is the matrix that relates strain to stress. Since the material is linear, the same matrix [G] relates the change in strain $\{\Delta\epsilon\}$ to the change in stress $\{\Delta\sigma\}$:

$$\{\Delta\sigma\} = [G]\{\Delta\epsilon\} \tag{B.9}$$

Since the problem is geometrically nonlinear, one matrix $[B^s]$ is needed to relate displacement $\{u\}$ to strain $\{\epsilon\}$ and another matrix $[B^t]$ is required to related the change in displacement $\{\Delta u\}$ to the change in strain $\{\Delta\epsilon\}$ (Anderson, 1985):

$$\{\epsilon\} = [B^s]\{u\} \tag{B.10}$$

$$\{\Delta\epsilon\} = [B^t]\{\Delta u\} \tag{B.11}$$

The matrix $[B^t]$ is at most linear and can be taken to be the sum of the matrix that relates displacements to strains for infinitesimally small displacements $[B_0^t]$ and a transformation matrix linearly dependent on displacements:

$$[B^t] = [B_0^t] + [B_1^t(u)] \tag{B.12}$$

The tangent stiffness matrix $[K^t]$ can be found by incrementing the applied load f and the displacement u such that the equation of equilibrium for the structure becomes:

$$\Delta(\textstyle\int_V [B^t]^T \{\sigma\} dV) = \Delta\{f\} \tag{B.13}$$

Expanding the left-hand side of the above equation one obtains:

$$\textstyle\int_V [\Delta B^t]^T \{\sigma\} dV + \int_V [B^t]^T \{\Delta\sigma\} dV = \{\Delta f\} \tag{B.14}$$

The first integral gives the differential stiffness matrix:

$$[K_D]\{\Delta u\} = \textstyle\int_V [\Delta B^t]^T \{\sigma\} dV \tag{B.15}$$

An alternative definition for the differential stiffness matrix is given by Cook (1974) and is shown in Equation (5.1).

Equations (B.9), (B.11), and (B.12) are applied to the second integral of Equation (B.14) so that Equation (B.14) may be expressed as:

$$[K_T]\{\Delta u\} = \{\Delta f\} \tag{B.16}$$

where

$$[K_T] = [K_D] + \overbrace{\textstyle\int_V [B_0^t]^T [G][B_0^t] dV}^{[K_0]}$$
$$+ \underbrace{\textstyle\int_V [B_0^t]^T [G][B_1^t] dV + \int_V [B_1^t]^T [G][B_0^t] dV + \int_V [B_1^t]^T [G][B_1^t] dV}_{[K_L]} \tag{B.17}$$

The first integral on the right hand side of Equation (B.17) is the conventional, infinitesimally small displacement stiffness matrix, $[K_0]$. The other three integrals together comprise the large displacement stiffness matrix $[K_L]$. Therefore, Equation (B.17) can be rewritten as:

$$[K_T] = [K_0] + [K_D] + [K_L] \tag{B.18}$$

The above equation is identical to Equation (4.1). In this dissertation, it will be assumed that $[K_L]$ can be neglected in comparison to $[K_0]$ and $[K_D]$.

As an example of a differential stiffness matrix, let us examine the rotating bar shown in Figure 6 in Chapter 4, taken as a single element. First, define three degrees of freedom at each end: x-displacement, z-displacement, and y-rotation. The applied stress due to centrifugal loading is σ_x and is given by:

$$\sigma_x = P/A \tag{B.19}$$

where A is the cross-sectional area of the bar and P is the centrifugal loading and is shown in Equation (4.19) to be $4\pi^2\Omega^2 mL$. Therefore, the differential matrix can be shown to be:

$$[K_D] = \frac{P}{L} \times$$

$$\begin{bmatrix} 0 & 0 & 0 & 0 & 0 & 0 \\ 0 & 6/5 & L/10 & 0 & -6/5 & L/10 \\ 0 & L/10 & 2L^2/15 & 0 & -L/10 & -L^2/30 \\ 0 & 0 & 0 & 0 & 0 & 0 \\ 0 & -6/5 & -L/10 & 0 & 6/5 & -L/10 \\ 0 & L/10 & -L^2/30 & 0 & -L/10 & 2L^2/15 \end{bmatrix} \tag{B.20}$$

APPENDIX C

DEGRADED SOLUTIONS FOR BLADE AND BEAM

In this section, the problems of the rotating blade and beam presented in Chapter 7 will be degraded (simplified by omitting certain features). This will permit the examination of the results when centrifugal effects are neglected in the optimization and in the structural analysis.

Results of Degraded Cases

Table 9 shows the results in optimization for the degraded problems. This table is similar to Table 3. Case 12 is the rotating blade shown in Figure 16 with no centrifugal effects in the optimization constraints. Minimum change is used both in the predictor and corrector. Case 13 is similar to Case 12 with the hybrid objective function employed; that is, minimum weight is used in the predictor and minimum change is used in the corrector. In Case 14, centrifugal effects are neglected both in the optimization and in the structural analysis. Minimum change is used in both the predictor and the corrector. Case 15 also neglects the centrifugal forces, but the hybrid optimization routine is used. In Case 16 and Case 17, the beam problem shown in Figure 10 is reanalyzed with centrifugal effects negelected in the optimization but included in the structural analysis. Case 16 uses minimum structural change while Case 17 uses the hybrid optimization.

Table 10 contains the results of the parameters in the optimization routines. This table is similar to Table 6.

Observations

In the blade optimization, the change-change objective function obtains satisfactory results for the frequency change even if centrifugal effects are completely ignored. However, there is a slight amount of overshoot on the linear predictor step. The hybrid objective function obtains good results at the end of a complete cycle when centrifugal effects are retained in the structural analysis (Case 13), though the linear predictor does not provide a good solution. When centrifugal effects are completely ignored (Cases 14 and

Table 9. Degraded Optimization Results for Blade and Beam
10% Change

Case	Opt.	$\omega_1 \, (\times 10^3)$	$\omega_1^d \, (\times 10^3)$	$\omega_1^p \, (\times 10^3)$	$\% \, \Delta_p$	$\% \Delta W_p$	$\omega_1^c \, (\times 10^3)$	$\% \, \Delta_c$	$\% \Delta W_c$
12	C/C	8.38025	9.21828	9.24806	103.55	3.66	9.21947	100.14	3.51
13	W/C	8.38025	9.21828	9.01088	75.252	−13.26	9.20613	98.551	−12.42
14	C/C	7.66559	8.43215	8.48493	106.88	3.84	8.43240	100.03	3.54
15	W/C	7.66559	8.43215	39272	94.856	−13.67	8.42872	99.494	−13.49
16	C/C	2.95200	3.24720	3.23328	91.897	0.00	3.24435	99.034	0.14
17	W/C	2.95200	3.24720	3.09322	47.838	−15.33	3.14057	63.878	−14.13

**Table 10. Optimizer Parameters during Degraded Solutions
Blade and Beam**

Case	i (pred.)	f (pred.)	λ (pred.)	t	i (cor.)	f (cor.)	λ (cor.)	t
12	4	1.197E0	1.737E-1	1	4	1.058E-3	1.840E-2	1
13	3	−3.454E2	−2.878E-7	2	4	6.155E-2	−3.070E-2	1
14	4	9.411E-1	−1.549E0	2	5	3.242E-3	4.317E-2	1
15	4	−4.234E2	−2.003E-6	2	5	1.885E-3	−3.454E-1	1
16	4	2.388E-2	−1.416E-2	1	4	1.060E-4	−5.764E-3	1
17	5	−6.131E-1	−2.328E-9	1	4	5.915E-3	4.078E-4	1

15), satisfactory solutions are still obtained.

In the beam optimization, good results are observed in Case 16. However. Case 17 exhibits the worst results. Not even the corrector can obtain the frequency goal without a significant error.

The results shown in Table 10 are similar to those shown in the cases where centrifugal effects are included (see Tables 6 and 8). Once again. the optimizer gives a value of the objective function close to zero for minimum change but a negative number for minimum weight objective function. Values of the constraint close to zero imply that the constraint is satisfied.

BIBLIOGRAPHY

BIBLIOGRAPHY

Anarsi, K.A. (1986), "On the Importance of Shear Deformation, Rotary Inertia, and Coriolis Forces in Turbine Blade Vibrations", Journal of Engineering for Gas Turbines and Power, Vol. 108, April 1985, pp. 319–324.

Anderson, W.J. (1984), Finite Elements in Mechanical and Structural Design: Study Guide, Video Lecture Series 1001, Linear Static Analysis, Automated Analysis Corporation, Ann Arbor MI, for the MacNeal-Schwendler Corporation, Los Angeles CA, January 1984.

Anderson, W.J. (1985), Finite Elements in Mechanical and Structural Design: Study Guide, Video Lecture Series 1002, Dynamic and Nonlinear Analysis, Automated Analysis Corporation, Ann Arbor MI, for the MacNeal-Schwendler Corporation, Los Angeles CA, May 1985.

Armand, J.L. (1971), "Minimum-Mass Design of a Plate-Like Structure for Specified Fundamental Frequency", AIAA Journal, Vol. 9, No. 9, pp. 1739–1745

Baldwin, J.F. and Hutton, S.G. (1985), "Natural Modes of Modified Structures", AIAA Journal, Vol. 23, No. 11, pp. 1737–1743.

Bellagamba, L. and Yang, T.Y. (1981), "Minimum-Mass Truss Structures with Constraints on Fundamental Natural Frequency", AIAA Journal, Vol. 19, No. 11, pp. 1452–1458.

Bennet, R. (1983), "Application of Optimization Methods to Rotor Design Problems", Vertica, Vol. 7, No. 3, pp. 210–208.

Boyce, W.E., Di Prima, R.C., and Handelman, G.H. (1954), "Vibrations of Rotating Beams of Constant Section", Proceedings of the Second National Congress of Applied Mechanics, Ann Arbor MI, 1954, pp. 165–173.

Carlson, R.M., Wong, J.T. (1978), "An Exact Solution for the Static Bending of Uniform Rotating Beams", Journal of the American Helicopter Society, October 1978, pp. 36–38.

Carnegie, W. (1959), Vibrations of Pretwisted Cantilever Blading", Proceedings, Institution of Mechanical Engineers, Vol. 173, No. 12, pp. 343–374.

Carnegie, W. (1966), "The Application of the Variational Method to Derive the Equations of Motion of Vibrating Cantilever Blading Under Rotating", Bulletin of Mechanical Engineering Education, Vol. 6, pp. 29–38.

Carnegie, W. and Dawson, B. (1969), "Vibration Characteristics of Straight Blades of Asymmetrical Aerofoil Cross-Section", The Aeronautical Quarterly, May 1969, pp. 178–190.

Carnegie, W. and Dawson, B. (1971), "Vibration Characteristics of Pre-twisted Blades of Asymmetrical Aerofoil Cross-Section", The Aeronautical Quarterly, August 1971, pp. 257–273.

Cook, R. (1974), Concepts and Applications of Finite Element Analysis, John Wiley and Sons, New York NY, 1974.

Dokainish, M.A. and Rawtani, S. (1971), "Vibration Analysis of Rotating Cantilever Plates", International Journal for Numerical Methods in Engineering, Vol. 3, pp. 233–248.

Fiacco, A.V. and McCormick, G.P. (1968), Nonlinear Programming: Sequential Unconstrained Minimization Techniques, John Wiley and Sons Inc., New York NY, 1968.

Fletcher, R. and Reeves, C.M. (1964), "Function Minimization by Conjugate Gradients", The Computer Journal, Vol. 7., pp. 149–160.

Fox, R.L. (1965), "Constraint Surface Normals for Structural Synthesis Techniques", AIAA Journal, Vol. 3, No. 8, pp. 1517–1518.

Garstecki, A. (1984), "Optimal Redesign of Elastic Structures in the State of Initial Loading", Journal of Structural Mechanics, Vol. 12, No. 3, pp. 279–301.

Giurgiutiu, V. and Stafford, R.O. (1977), "Semi-Analytic Methods for Frequency and Mode Shapes of Rotor Blades", Vertica, Vol. 1. No. 4, pp. 291–306.

Gockel, M.A., ed., MSC/NASTRAN Handbook for Dynamic Analysis, MSC/NASTRAN Version 63, The MacNeal-Schwendler Corporation, June 1983.

Greenwood, D.T. (1965), Principals of Dynamics, Prentice-Hall Inc., Englewood Cliffs NJ, 1965.

Greenwood, D.T. (1977), Classical Dynamics, Prentice-Hall Inc., Englewood Cliffs NJ, 1977.

Hoa, S.V. (1979), "Vibration of a Rotating Beam With Tip Mass", Journal of Sound and Vibration, Vol. 67, No. 3, pp. 369–381.

Hodges, D.H. and Rutkowski, M.J. (1981), "Free-Vibration Analysis of Rotating Beams by a Variable-Order Finite-Element Method", AIAA Journal, Vol. 19, No. 11, pp. 1459–1466.

Hoff, C.J., Bernitsas, M.M., Sandström, R.E., and Anderson, W.J. (1984), "Inverse Perturbation Method for Structural Redesign with Frequency and Mode Shape Constraints", AIAA Journal, Vol. 22, No. 9, pp. 1304–1309.

Hoff, C.J. (1985), "Static/Dymanic Redesign of Marine Structures", Ph. D. Thesis, The University of Michigan, Ann Arbor MI, 1985.

Houbolt, J.C. and Brooks, G.W. (1958), "Differential Equations of Motion for Combined Flapwise Bending, Chordwise Bending, and Torsion of Twisted Nonuniform Rotor Blades", NACA Report 1346, 1958.

Hunter, W.F. (1970), "Integrating Matrix Methods for Determining the Natural Vibration Characteristics of Propeller Blades", NASA-TN-D-6064, Langley Research Center, Hampton VA, December 1970.

Isakson, G. and Eisley, J.G. (1960), "Natural Frequencies in Bending of Twisted Rotating and Nonrotating Blades", NASA-TN D-371, March 1960.

Isakson, G. and Eisley, J.G. (1964), "Natural Frequencies in Coupled Bending and Torsion of Twsisted Rotating and Nonrotating Blades", NASA-CR-65, July 1964.

Joseph, J.A. (1984), MSC/NASTRAN Applications Manual, IBM Edition, The MacNeal-Schwendler Corporation, Los Angeles CA, December 1984.

Karihaloo, B.L. and Niordson F.I. (1973), "Optimum Design of Vibrating Cantilevers", Journal of Optimization Theory and Applications, Vol. 11, No. 6, pp. 638–654.

Kavanagh, K. (1972), "An Approximate Algorithm for the Reanalysis of Structures by the Finite Element Method", Computers and Structures, Vol. 2, pp. 713–722.

Kengtung, C. and Gu, Y. (1984), "Sequential Quadratic Programming and Dynamic Optimal Design of Rotating Blades", Journal of Structural Mechanics, Vol. 11, No. 4, pp. 451–464.

Kim, K., Anderson, W.J., and Sandström, R.E. (1983), "Nonlinear Inverse Perturbation Method in Dynamic Analysis", AIAA Journal, Vol. 21, No. 9, pp. 1310–1316.

Kim, K. and Anderson, W.J. (1984), "Generalized Dynamic Reduction in Finite Element Dynamic Optimization", AIAA Journal, Vol. 22, No. 11, pp. 1616–1828

Kim, K. (1985), "Dynamic Condensation for Structural Redesign", AIAA Journal, Vol. 23, No. 11, pp 1830–1832.

Kirsch, U. (1981), Optimum Structural Design, McGraw-Hill Book Company, New York NY, 1981.

Kiusalaas, J. (1972), "Minimum Weight Design of Structures via Optimality Criteria", NASA-TN-D-7115, December 1972.

Kounadis, A.N. (1985), "Bending Eigenfrequencies of a Two-Bar Frame Including the Effect of Axial Inertia", AIAA Journal, Vol. 23, No. 12, pp. 2000–2002.

Lang, K.W. and Nemat-Nasser, S. (1979), "An Approach for Estimating Vibration Characteristics of Nonuniform Rotor Blades", AIAA Journal, Vol. 17, No. 9, pp. 995–1002.

Lo, H. and Renbarger, J.L. (1951), "Bending Vibrations of a Rotating Beam", Proceedings of the First National Congress of Applied Mechanics, Chicago IL, 1951, pp. 75–79.

Luenberger, D.G. (1984), Linear and Nonlinear Programming, 2nd Edition, Addison-Wesley Publishing Company, Menlo Park CA, 1984.

MacNeal, R.H., ed. (1972), The NASTRAN Theoretical Manual, Level 15.5, The MacNeal-Schwendler Corporation, Los Angeles CA, December 1972.

MacNeal, R.H. (1973), The Dynamics of Rotating Bodies, The MacNeal-Schwendler Corporation, Los Angeles CA, 1973.

MacNeal, R.H., ed. (1981), MSC/NASTRAN Handbook for Linear Static Analysis, MSC/ NASTRAN Version 63, The MacNeal-Schwendler Corporation, Los Angeles CA, 1981.

MacNeal, R.H., ed. (1984), MSC/NASTRAN User's Manual, Vol. 1 and 2, MSC/ NASTRAN Version 64, The MacNeal-Schwendler Corporation, Los Angeles CA, July 1984.

McCart, B.R., Haug, E.J., and Streeter, T.D. (1970), "Optimal Design of Structures with Constraints on Natural Frequency", AIAA Journal, Vol. 8, No. 6, pp. 1012-1019.

McDaniel, T.J. and Murthy, V.R. (1977), "Bounds on the Dynamic Characteristics of Rotating Beams", AIAA Journal, Vol. 15, No. 3, pp. 439-442.

McLean, D.M., ed., MSC/NASTRAN Programmers Manual, MSC/NASTRAN Version 63, The MacNeal-Schwendler Corporation, Los Angeles CA, September 1982.

Meirovitch, Leonard (1967), Analytical Methods in Vibrations, MacMillan Book Company, London, United Kingdom, 1967.

Meirovitch, Leonard (1970), Methods of Analytical Dynamics, McGraw-Hill Book Company, New York NY, 1970.

Meirovitch, Leonard (1980), Computational Methods in Structural Dynamics, Sijthoff & Noordhoff International Publishers B.V., Alphen aan den Rijn, The Netherlands, 1980.

Moses, F. (1964), "Optimum Structural Design Using Linear Programming", Journal of the Structural Division, Proceedings of the American Society of Civil Engineers, December 1964, pp. 89-106.

Nagaraj, V.T. and Shanthakumar, P. (1975), "Rotor Blade Vibrations by the Galerkin Finite Element Method", Journal of Sound and Vibration, Vol. 43, No. 3, 1975, pp. 575-577.

Olhoff, N. (1976), "Optimization of Vibrating Beams with Respect to Higher Order Natural Frequencies", Journal of Structural Mechanics, Vol. 4, No. 1, pp. 87-122.

Olhoff, N. (1977), "Maximizing Higher Order Eigenfrequencies of Beams with Constraints on the Design Geometry", Journal of Structural Mechanics, Vol. 5, No. 2, pp. 107-134.

Olhoff, N. and Parbery, R. (1984), "Designing Vibrating Beams and Rotating Shafts for Maximum Difference Between Adjacent Natural Frequencies", International Journal of Solids and Structures, Vol. 20, No. 1, pp. 63-75.

Prager, W. and Taylor, J.E. (1968), "Problems of Optimal Structural Design", Journal of Applied Mechanics, March 1968, pp. 102-106.

Przemieniecki, J.S. (1985), Theory of Matrix Structural Analysis, Dover Publications Inc., New York NY, 1985.

Putter, S. and Manor, H. (1978), "Natural Frequencies of Radial Rotating Beams", Journal of Sound and Vibration, Vol. 56, No. 2, pp. 175–185.

Queau, J.P., Trompette, P. (1981), "Optimal Shape Design of Turbine Blades", ASME Paper 81-DET-128, submitted for presentation at the Design Engineering Technical Conference, September 20–23, 1981, Hartford, Connecticut.

Rao, J.S. and Carnegie, W. (1970), "Non-Linear Vibrations of Rotating Cantilever Beams", The Aeronautical Journal of the Royal Aeronautical Society, Vol. 74, February 1970, pp. 161–165.

Rayleigh, J.W.S (1894), The Theory of Sound. 2nd Edition, MacMillan and Company, Ltd., London, United Kingdom, 1926.

Rubin, C. (1970), "Minimum Weight Design of Complex Structures Subject to a Frequency Constraint", AIAA Journal, Vol. 8, No. 5, pp. 923–927.

Sabuncu, M., "Coupled Vibration Analysis of Blades with Angular Pretwist of Cubic Distribution" (1985), AIAA Journal, Vol. 23, No. 9, pp. 1424–1430.

Sandström, R.E., and Anderson, W.J. (1982), "Modal Perturbation Methods for Marine Structures", Transactions of the Society of Naval Architects and Marine Engineers", Vol. 90, pp. 41–54.

Sheu, C.Y. (1968), "Elastic Minimum-Weight Design for Specified Fundamental Frequency", International Journal of Solids and Structures, Vol. 4, pp. 953–958.

Sheu, C.Y. and Prager, W. (1968), "Recent Developments in Optimal Structural Design", Applied Mechanics Reviews, Vol. 21, No. 10., pp. 985–992.

Sippel, D.L. and Warner, W.H. (1973), "Minimum-Mass Design of Multielement Structures under a Frequency Constraint", AIAA Journal, Vol. 11, No. 4, pp. 483–489.

Sisto, F., Chang, A., and Sutcu. M. (1983), "The Influence of Coriolis Forces on Gyroscopic Motion of Spinning Blades". Journal of Engineering for Power, Vol. 105, April 1983, pp. 342–347.

Stetson, K.A. (1975), "Perturbation Method of Structural Design Relevant to Holographic Analysis", AIAA Journal, Vol. 13, No. 4, pp. 457–459.

Stetson, K.A. and Palma, G.E. (1976), "Inversion of First-Order Perturbation Theory and Its Application to Structural Design", AIAA Journal, Vol. 14, No. 4, pp. 454–460.

Stetson, K.A., Harrison, I.R., and Palma, G.E (1978), "Redesgning Structural vibration Modes by Inverse Perturbation Subject to Minimal Change Theory", Computer Methods in Applied Mechanics and Engineering, Vol. 16, pp. 151–175.

Stetson, K.A. and Harrison, I.R. (1981), "Redesign of Structural Vibration Modes by Finite-Element Inverse Perturbation", Journal of Engineering for Power, April 1981, Vol. 103, pp. 319–325.

Subrahmanyam, K.B. and Kaza. K.R.V. (1984), "Improved Methods of Vibration Analysis of Pretwisted, Airfoil Blades". NASA-TM-83735, August 1984.

Subrahmanyam, K.B. and Kaza, K.R.V. (1985), "Vibration and Buckling of Rotating, Prtwisted, Preconed Beams Including Coriolis Effects", NASA-TM-87004, May 1985.

Subrahmanyam, K.B., Kaza, K.R.V., Brown, G.V., and Lawrence, C. (1987), "Nonlinear Vibration and Stability of Rotating, Pretwisted, Preconed Blades Including Coriolis Effects", Journal of Aircraft, Vol. 24, No. 5, pp. 342-352.

Taylor, J.E. (1967), "Minimum Mass Bar for Axial Vibration as Specified Natural Frequency", AIAA Journal, Vol.5, No. 10, pp. 1911-1913.

Taylor, J.E. (1968), "Optimum Design of a Vibrating Bar with Specified Minimum Cross Section", AIAA Journal, Vol. 6, No. 7, pp. 1379-1381.

Taylor, J.E. (1969), "Optimal Design of Structural Systems: An Energy Formulation", AIAA Journal, Vol. 7, No. 7, pp. 1404-1406.

Taylor, J.E. (1977), "Scaling a Discrete Structural Model to Match Measured Modal Frequencies", AIAA Journal, Vol. 15, No. 11, pp. 1647-1649.

Thomas, J. and Sabuncu, M. (1974), "Finite Element Analysis of Rotating Pretwisted Asymmetric Cross-Section Blades", ASME Paper 79-DET-95, submitted for presentation at the Design Engineering Technical Conference, St. Louis MO, September 10-12, 1979.

Tomar, J.S. and Dhole, A. (1976) "Coupled Vibrations of a Pretwisted Slender Beam in a Centrifugal Force Field", Journal of the Aeronautical Society of India, Vol. 28 No. 1, pp. 97-107.

Turner M.J. (1967), "Design Of Minimum Mass Structures with Specified Natural Frequencies", AIAA Journal, Vol. 5, No. 3, pp. 406-412.

Vanderplaats, G.N., Sugimoto, H., and Sprague, C.M. (1983), "ADS-1: A New General-Purpose Optimization Program", AIAA Paper 83-0831, presented at 24th Structures, Structural Dynamics and Materials Conference. May 2-4, 1983, Lake Tahoe, NV.

Vanderplaats, G.N. (1984), Numerical Optimization Techniques for Engineering Design with Applications, McGraw-Hill Book Comapny, New York NY, 1984.

Vanderplaats, G.N. (1985), ADS − A Fortran Program for Automated Design Synthesis (Version 1.10), Engineering Design Optimization Inc., Santa Barbara CA, 1985.

Venkayya, V.B., Khot, N.S., and Berke, L. (1973), "Application of Optimality Criteria to Automated Design of Large Practical Structures", Proceedings of the Second Symposium on Structural Optimization, AGARD-CP-123, Milan, Italy, pp. 3.1-3.19.

Wadsworth, W. and Wilde, E. (1968), "Differential Eigenvalue Problems with Particular Reference to Rotor Blade Bending", The Aeronautical Quarterly, May 1968, pp. 192-204.

Washizu, K. (1982), Variational Methods in Elasticity and Plasticity, Third Edition. Pergamon Press Ltd, Oxford, United Kingdom, 1982.

White, W.F. and Malatino, R.E. (1975), "A Numerical Method for Determining the Natural Vibration Characteristics of Rotating Nonuniform Cantilever Blades", NASA-TM-X-72.751, November 1975.

Zienkiewicz, O.C. (1977), The Finite Element Method, Third Edition. McGraw Hill Book Company Ltd., London, United Kingdom, 1977.